

DISSERTATION

INVESTIGATING THE INTERACTION BETWEEN SPOILAGE BACTERIAL GROWTH
AND BEEF STEAK COLOR STABILITY OF BEEF LONGISSIMUS LUMBORUM AND
PSOAS MAJOR STEAKS IN AEROBIC RETAIL DISPLAY USING A MULTI-OMIC
APPROACH

Submitted by

Colton L. Smith

Department of Animal Sciences

In partial fulfillment of the requirements

For the Degree of Doctor of Philosophy

Colorado State University

Fort Collins, Colorado

Fall 2025

Doctoral Committee:

Advisor: Mahesh N. Nair

Gina Geornaras
Robert J. Delmore
Jessica L. Metcalf
Jessica E. Prenni

Copyright by Colton L. Smith 2025

All Rights Reserved

ABSTRACT

INVESTIGATING THE INTERACTION BETWEEN SPOILAGE BACTERIAL GROWTH AND BEEF STEAK COLOR STABILITY OF BEEF LONGISSIMUS LUMBORUM AND PSOAS MAJOR STEAKS IN AEROBIC RETAIL DISPLAY USING A MULTI-OMIC APPROACH

One of the primary drivers of fresh red meat wastage is discoloration at the retail and consumer levels of distribution. Although discoloration is not necessarily an indicator of meat freshness, discolored meat is often reduced in price or discarded as it is viewed by consumers as spoiled. In other words, a meat product is spoiled once it is no longer desirable to the consumer. Research evaluating meat spoilage dates back nearly a century and these studies have yielded tremendous improvements to extending meat shelf-life, especially from a microbial and meat color standpoint. The intrinsic and extrinsic factors contributing to muscle-specific discoloration in beef have been investigated extensively. However, the impact of microbial growth on meat discoloration remains unclear. Previous studies have indicated that the growth of spoilage bacteria during retail display decreases the color stability of aerobically packaged beef. Therefore, the objective of Chapter 2 was to investigate the impact of the growth of common meat spoilage bacteria on the color stability of color-stable (*longissimus lumborum*; LL) and color-labile (*psoas major*; PM) beef muscles. Beef striploins (LL) and tenderloins (PM) (USDA Choice, n = 8) were wet aged (14 d), after which they were

decontaminated and fabricated into 1.27-cm thick steaks. Steaks were randomly assigned as decontaminated (DCON) or inoculated (INOC). The surface of INOC steaks was inoculated (ca. 4 log CFU/cm²) with a mixture of five spoilage bacteria, while an equivalent volume of phosphate-buffered saline was applied to the surface of DCON steaks. Steaks were aerobically retail displayed for up to 9 d. Each day, objective and subjective color evaluation and microbiological analyses were conducted. Aerobic plate counts on INOC steaks were 8.9 (LL) and 9.3 (PM) log CFU/cm² at the end of retail display. Corresponding counts on DCON steaks were <2.7 (LL) and <3.4 (PM) log CFU/cm². For LL steaks, there was a treatment by display day interaction ($P < 0.05$) for lightness (L^*), redness (a^*), yellowness (b^*), lean color scores, surface discoloration, and bacterial levels. On days 6–8, redness was lower ($P < 0.05$) for INOC compared to DCON LL steaks, while lean color scores and surface discoloration were lower ($P < 0.05$) for DCON compared to INOC LL steaks. For PM, there was a treatment by display day interaction ($P < 0.05$) for a^* values, surface discoloration, and bacterial levels. Surface discoloration was greater ($P < 0.05$) for INOC steaks compared with DCON steaks on days 4 and 5. The results indicate a connection between surface discoloration and microbial growth on beef LL and PM steaks, and differences in bacterial growth kinetics could explain some of the differential color stabilities between these muscles. Based on the data obtained in Chapter 2 and the lack of previous studies that have evaluated bacterial function during meat spoilage, the objective of Chapter 3 was to explore the functional role of spoilage bacteria on fresh beef LL steak discoloration during retail display using a multi-omic approach. Beef LL were wet-aged, decontaminated, and cut into steaks. Half of the steaks were then assigned as

inoculated (INOC; inoculated with a mixture of spoilage bacteria), and the other half remained uninoculated (DCON). The aerobically packaged steaks were placed into a retail display and analyzed daily for objective and subjective color, microbial load, lipid oxidation (TBARS), pH, 16S rRNA gene sequencing, metatranscriptomics, and surface metabolomics. The a^* (redness) and b^* (yellowness) values of the treatments were similar ($P \geq 0.05$) from days 0-4 but were lower ($P < 0.05$) in INOC compared to DCON on days 5-7. The INOC had a higher ($P < 0.05$) microbial population throughout the display period. The metabolomic analysis indicated that there were 10 metabolites that had treatment-by-day interactions ($P < 0.05$). Results from 16S rRNA gene sequencing of INOC samples indicated beta diversity was influenced ($P < 0.05$) by display day. Metatranscriptomics revealed 785 transcript changes ($P < 0.05$) between days 3 and 6. In general, glucose mediated carbohydrate metabolism associated gene transcripts did not change throughout the display period. However, there was a steady increase in alternative pathways of generating citrate cycle intermediates, derived from amino and fatty acids. Results from this study indicated that spoilage bacteria can influence color stability, and changes occurring in microbial metabolism align with changes in the steak discoloration. Further research is needed to investigate pathway intermediates and metabolites to better elucidate the microbial function in discoloration in aerobically packaged fresh beef LL steaks. Similar to Chapter 3, an identical experiment was conducted with color labile beef PM to determine bacterial function on color labile muscles. The objective of Chapter 4 was to characterize the bacterial functional changes during the discoloration of beef PM steaks. Ten beef PM muscles ($n = 10$) were aged for 14 days, decontaminated, and fabricated into steaks. Steaks from each

PM were divided into treatments: decontaminated (DCON) and inoculated (INOC; with six spoilage bacteria). They were then aerobically packaged and placed in a retail display case for 7 days. Each day, one steak per treatment per replicate per trial was sampled for instrumental and visual color analysis, microbial enumeration, lipid oxidation, pH, 16S rRNA gene sequencing, surface metabolomics, and metatranscriptomics. There was a treatment by display day interaction for ($P < 0.05$) a^* values and percentage discoloration, with DCON remaining redder with less discoloration compared to INOC until day 3. Metabolomic analysis showed a treatment by display day interaction ($P < 0.05$) for glucose, galactose, phenylalanine, and tyrosine. The metatranscriptomic data analysis revealed 32 Kyoto Encyclopedia of Genes and Genomes Orthologs (KO) with changes ($P < 0.05$) from bacteria on PM INOC steaks. The KO abundance changes were between days 2 and 3 and days 3 and 4 of display. The most pronounced changes in KO between days 3 and 4 (30 changes) coincided with the largest decreases in a^* values and increases in percentage discoloration for INOC steaks. The results suggest that bacteria on PM steaks may be decreasing reliance on glucose metabolism early in the display period and simultaneously increasing usage of aromatic amino acids. These changes in bacterial metabolism might be contributing to the relatively quick discoloration in PM, along with other muscle-specific factors.

ACKNOWLEDGEMENTS

I would like to thank everyone who has been helpful along my PhD journey. This endeavor spurred so much personal growth, maturity, and stamina in myself. I certainly would like to acknowledge key individuals who were more memorable to me, including the faculty who gave a lot of personal attention to my development at CSU: Gina, Dr. Bob, and Mahesh. Of course, none of my work would have been completed without the major assistance of fellow graduate students, and I honestly cannot thank them enough for slogging through these research trials. Lastly, I want to acknowledge my collaborators on the numerous projects I participated in. These people were the most helpful at providing support when needed, technical knowledge, and a helping hand. I am grateful for the help, support, opportunities, and time that was afforded to me at CSU, and will almost certainly look back with a keen memory, for all the fun times, the busy times, and the downright grueling times.

TABLE OF CONTENTS

ABSTRACT.....	ii
ACKNOWLEDGEMENTS.....	vi
LIST OF TABLES.....	viii
LIST OF FIGURES.....	xi
CHAPTER 1: REVIEW OF LITERATURE	1
INTRODUCTION.....	1
SECTION 1: DRIVERS OF FRESH MEAT SPOILAGE	2
SECTION 2: FRESH MEAT SPOILAGE	6
SECTION 3: METHODS TO MEASURE SHELF-LIFE OF FRESH MEATS.....	19
CHAPTER 2: IMPACT OF SPOILAGE BACTERIAL POPULATIONS ON DISCOLORATION OF BEEF STEAKS	27
CHAPTER 3: INVESTIGATING THE FUNCTION OF SPOILAGE BACTERIA ON FRESH BEEF LONGISSIMUS LUMBORUM STEAK DISCOLORATION DURING AEROBIC RETAIL DISPLAY THROUGH A MULTI-OMIC APPROACH	57
CHAPTER 4: INVESTIGATING THE FUNCTION OF SPOILAGE BACTERIA ON FRESH BEEF PSOAS MAJOR STEAK DISCOLORATION DURING AEROBIC RETAIL DISPLAY THROUGH A MULTI-OMIC APPROACH	100
REFERENCES.....	134
SUPPLEMENTAL TABLE 1. List of Kyoto Encyclopedia of Genes and Genomes Orthologs (KO) with changes ($P < 0.05$) collected from bacteria grown on beef psoas major in aerobic simulated retail display between display days 2 to 5.....	149

LIST OF TABLES

TABLE 2.1. MARGINAL MEANS \pm STANDARD ERROR OF CIE L^* (LIGHTNESS), a^* (REDNESS), AND b^* (YELLOWNESS) OF DECONTAMINATED (DCON) AND INOCULATED (INOC) TREATMENT GROUPS OF BEEF *LONGISSIMUS LUMBORUM* STEAKS DURING SIMULATED RETAIL DISPLAY (3°C).

TABLE 2.2. MARGINAL MEANS \pm STANDARD ERROR OF CIE A^* (REDNESS) OF DECONTAMINATED (DCON) AND INOCULATED (INOC) TREATMENT GROUPS OF BEEF *PSOAS MAJOR* STEAKS DURING SIMULATED RETAIL DISPLAY (3°C).

TABLE 2.3. MARGINAL MEANS \pm STANDARD ERROR OF CIE B^* (YELLOWNESS) OF DECONTAMINATED (DCON) AND INOCULATED (INOC) TREATMENT GROUPS OF BEEF *PSOAS MAJOR* STEAKS DURING SIMULATED RETAIL DISPLAY (3°C).

TABLE 2.4. MARGINAL MEANS \pm STANDARD ERROR OF PANELIST LEAN COLOR AND PERCENTAGE DISCOLORATION OF DECONTAMINATED (DCON) AND INOCULATED (INOC) TREATMENT GROUPS OF BEEF *LONGISSIMUS LUMBORUM* STEAKS DURING SIMULATED RETAIL DISPLAY (3°C).

TABLE 2.5. MARGINAL MEANS \pm STANDARD ERROR OF PANELIST LEAN COLOR AND PERCENTAGE DISCOLORATION OF DECONTAMINATED (DCON) AND INOCULATED (INOC) TREATMENT GROUPS OF BEEF *PSOAS MAJOR* STEAKS DURING RETAIL DISPLAY (3°C).

TABLE 2.6. MARGINAL MEAN \pm STANDARD DEVIATION (LOG CFU/CM²) OF AEROBIC PLATE COUNTS (APC), LACTIC ACID BACTERIA COUNTS (LABC), AND *PSEUDOMONAS* SPP. COUNTS RECOVERED FROM DECONTAMINATED (DCON) AND INOCULATED (INOC) TREATMENT GROUPS OF BEEF *LONGISSIMUS LUMBORUM* STEAKS DURING SIMULATED RETAIL DISPLAY (3°C).

TABLE 2.7. MARGINAL MEAN \pm STANDARD DEVIATION (LOG CFU/CM²) OF AEROBIC PLATE COUNTS (APC), LACTIC ACID BACTERIA COUNTS (LABC), AND *PSEUDOMONAS* SPP. COUNTS RECOVERED FROM DECONTAMINATED (DCON) AND INOCULATED (INOC) TREATMENT GROUPS OF BEEF *PSOAS MAJOR* STEAKS DURING SIMULATED RETAIL DISPLAY (3°C).

TABLE 2.8. ESTIMATED GROWTH KINETIC PARAMETERS, DERIVED FROM THE BARANYI AND ROBERTS (1994) MODEL, OF BACTERIAL POPULATIONS RECOVERED FROM INOCULATED BEEF *LONGISSIMUS LUMBORUM* (LL) AND *PSOAS MAJOR* (PM) STEAKS DURING SIMULATED RETAIL DISPLAY (3°C).

TABLE 3.1. MARGINAL MEANS \pm STANDARD ERROR OF CIE L^* (LIGHTNESS), a^* (REDNESS), AND b^* (YELLOWNESS) OF DECONTAMINATED (DCON) AND

INOCULATED (INOC) TREATMENT GROUPS OF BEEF *LONGISSIMUS LUMBORUM* STEAKS DURING SIMULATED RETAIL DISPLAY (3°C).

TABLE 3.2. MARGINAL MEANS ± STANDARD ERROR OF PANELIST LEAN COLOR AND PERCENTAGE DISCOLORATION OF DECONTAMINATED (DCON) AND INOCULATED (INOC) TREATMENT GROUPS OF BEEF *LONGISSIMUS LUMBORUM* STEAKS DURING SIMULATED RETAIL DISPLAY (3°C).

TABLE 3.3. MARGINAL MEAN ± STANDARD DEVIATION (LOG CFU/CM²) OF AEROBIC PLATE COUNTS (APC), LACTIC ACID BACTERIA COUNTS (LABC), AND *PSEUDOMONAS* SPP. COUNTS RECOVERED FROM DECONTAMINATED (DCON) AND INOCULATED (INOC) TREATMENT GROUPS OF BEEF *LONGISSIMUS LUMBORUM* STEAKS DURING SIMULATED RETAIL DISPLAY (3°C).

TABLE 3.4. MARGINAL MEANS ± STANDARD ERROR OF MUSCLE PH OF BEEF *LONGISSIMUS LUMBORUM* STEAKS DURING SIMULATED RETAIL DISPLAY (3°C).

TABLE 3.5. MARGINAL MEANS OF RELATIVE ABUNDANCE OF METABOLITES DETECTED FROM DECONTAMINATED (DCON) AND INOCULATED (INOC) TREATMENT GROUPS OF BEEF *LONGISSIMUS LUMBORUM* STEAKS DURING SIMULATED RETAIL DISPLAY (3°C) WITH TREATMENT BY DISPLAY DAY INTERACTIONS ($P < 0.05$).

TABLE 3.6. MARGINAL MEANS OF RELATIVE ABUNDANCE OF METABOLITES DETECTED FROM DECONTAMINATED (DCON) AND INOCULATED (INOC) TREATMENT GROUPS OF BEEF *LONGISSIMUS LUMBORUM* STEAKS DURING SIMULATED RETAIL DISPLAY (3°C) WITH TREATMENT MAIN EFFECTS ($P < 0.05$).

TABLE 3.7. MARGINAL MEANS OF RELATIVE ABUNDANCE OF METABOLITES DETECTED FROM BEEF *LONGISSIMUS LUMBORUM* STEAKS DURING SIMULATED RETAIL DISPLAY (3°C) WITH DISPLAY DAY MAIN EFFECTS ($P < 0.05$).

TABLE 4.1. MARGINAL MEANS ± STANDARD ERROR OF CIE a^* (REDNESS), AND b^* (YELLOWNESS) OF DECONTAMINATED (DCON) AND INOCULATED (INOC) TREATMENT GROUPS OF BEEF *PSOAS MAJOR* STEAKS DURING SIMULATED RETAIL DISPLAY (3°C).

TABLE 4.2. MARGINAL MEANS ± STANDARD ERROR OF PERCENTAGE DISCOLORATION OF DECONTAMINATED (DCON) AND INOCULATED (INOC) TREATMENT GROUPS OF BEEF *PSOAS MAJOR* STEAKS DURING SIMULATED RETAIL DISPLAY (3°C).

TABLE 4.3. MARGINAL MEAN ± STANDARD DEVIATION (LOG CFU/CM²) OF AEROBIC PLATE COUNTS (APC), LACTIC ACID BACTERIA COUNTS (LABC), AND *PSEUDOMONAS* SPP. COUNTS RECOVERED FROM DECONTAMINATED (DCON)

AND INOCULATED (INOC) TREATMENT GROUPS OF BEEF *PSOAS MAJOR* STEAKS DURING SIMULATED RETAIL DISPLAY (3°C).

TABLE 4.4. BACTERIAL GROWTH KINETICS FOR INOC TREATMENT CALCULATED FROM THE BACTERIAL POPULATION COUNTS RECOVERED FROM BEEF *LONGISSIMUS LUMBORUM* (LL) AND *PSOAS MAJOR* (PM) STEAKS IN AEROBIC PACKAGING DAY SIMULATED RETAIL DISPLAY AT 3°C UP TO 8 DAYS.

TABLE 4.5. MARGINAL MEANS OF RELATIVE ABUNDANCE OF METABOLITES WITH TREATMENT BY DISPLAY DAY INTERACTIONS ($P < 0.05$) DETECTED FROM DECONTAMINATED (DCON) AND INOCULATED (INOC) TREATMENT GROUPS OF BEEF *PSOAS MAJOR* STEAKS DURING SIMULATED RETAIL DISPLAY (3°C).

LIST OF FIGURES

FIGURE 2.1. MARGINAL MEANS \pm STANDARD ERROR OF CIE L^* (LIGHTNESS) OF BEEF *PSOAS MAJOR* STEAKS FROM BOTH DECONTAMINATED AND INOCULATED TREATMENTS AVERAGED BY DISPLAY DAY DURING SIMULATED RETAIL DISPLAY (3°C).

FIGURE 2.2. REPRESENTATIVE IMAGES OF BEEF *LONGISSIMUS LUMBORUM* STEAKS FABRICATED FROM THE SAME STRIPLOIN OVER A 3 DAY RETAIL DISPLAY PERIOD (DAYS 4 TO 6) SHOWING THE IMPACT OF MICROBIAL GROWTH ON COLOR STABILITY. DECONTAMINATED CONTROLS (DCON; TOP ROW), AND STEAKS INOCULATED WITH A FIVE-ISOLATE SPOILAGE BACTERIA MIXTURE AT CA. 4 LOG CFU/CM² (INOC; BOTTOM ROW) ARE FROM THE SAME TIME POINTS DURING SIMULATED RETAIL DISPLAY AT 3°C.

FIGURE 2.3. REPRESENTATIVE IMAGES OF BEEF *PSOAS MAJOR* STEAKS FABRICATED FROM THE SAME TENDERLOIN OVER A 3 DAY RETAIL DISPLAY PERIOD (DAYS 3 TO 5) SHOWING THE IMPACT OF MICROBIAL GROWTH ON COLOR STABILITY. DECONTAMINATED CONTROLS (DCON; TOP ROW), AND STEAKS INOCULATED WITH A FIVE-ISOLATE SPOILAGE BACTERIA MIXTURE AT CA. 4 LOG CFU/CM² (INOC; BOTTOM ROW) ARE FROM THE SAME TIME POINTS DURING SIMULATED RETAIL DISPLAY AT 3°C.

FIGURE 3.1. ALPHA DIVERSITY METRICS OF SHANNON, SIMPSON, AND INVERSE SIMPSON INDICES AS PLOTTED FOR BEEF *LONGISSIMUS LUMBORUM* STEAKS INOCULATED WITH A 6-ISOLATE SPOILAGE BACTERIA MIXTURE AND SUBSEQUENTLY PLACED INTO SIMULATED RETAIL DISPLAY (3°C).

FIGURE 3.2. BETA DIVERSITY SHOWN AS A WEIGHTED UNIFRAC PRINCIPLE COORDINATES ANALYSIS (PCOA) FOR BEEF *LONGISSIMUS LUMBORUM* STEAKS INOCULATED WITH A 6-ISOLATE SPOILAGE BACTERIA MIXTURE AND SUBSEQUENTLY PLACED INTO SIMULATED RETAIL DISPLAY (3°C).

FIGURE 3.3. RELATIVE ABUNDANCE TAXA BAR PLOT ORGANIZED AT THE FAMILY LEVEL FOR BEEF *LONGISSIMUS LUMBORUM* (LL) STEAKS INOCULATED WITH A 6-ISOLATE SPOILAGE BACTERIA MIXTURE AND SUBSEQUENTLY PLACED INTO SIMULATED RETAIL DISPLAY (3°C).

FIGURE 3.4. NUMBER OF KYOTO ENCYCLOPEDIA OF GENES AND GENOMES PROTEIN FAMILIES THAT WERE (A) INCREASED IN RELATIVE ABUNDANCE OR (B) DECREASED IN RELATIVE ABUNDANCE FROM BACTERIA ON *LONGISSIMUS LUMBORUM* BEEF STEAKS DURING AEROBIC RETAIL DISPLAY.

FIGURE 4.1. MARGINAL MEANS \pm STANDARD ERROR OF CIE L^* (LIGHTNESS) OF DECONTAMINATED (DCON) AND INOCULATED (INOC) TREATMENT GROUPS OF BEEF *PSOAS MAJOR* STEAKS DURING SIMULATED RETAIL DISPLAY (3°C).

FIGURE 4.2. MARGINAL MEANS \pm STANDARD ERROR OF VISUAL LEAN COLOR SCORES OF DECONTAMINATED (DCON) AND INOCULATED (INOC) TREATMENT GROUPS OF BEEF *PSOAS MAJOR* STEAKS DURING SIMULATED RETAIL DISPLAY (3°C). PANELISTS SCORED EACH STEAK TO ASSESS LEAN COLOR USING A CONTINUOUS 8-POINT SCALE (1 = EXTREMELY BRIGHT CHERRY-RED, 2 = BRIGHT CHERRY-RED, 3 = MODERATELY BRIGHT CHERRY-RED, 4 = SLIGHTLY BRIGHT CHERRY-RED, 5 = SLIGHTLY DARK CHERRY-RED, 6 = MODERATELY DARK RED, 7 = DARK RED, 8 = EXTREMELY DARK RED).

FIGURE 4.3. MARGINAL MEANS \pm STANDARD ERROR OF THIOBARBITURIC REACTIVE SUBSTANCES (TBARS) OF DECONTAMINATED (DCON) AND INOCULATED (INOC) TREATMENT GROUPS AVERAGED ACROSS DAY OF BEEF *PSOAS MAJOR* STEAKS DURING SIMULATED RETAIL DISPLAY (3°C).

FIGURE 4.4. ALPHA DIVERSITY METRICS OF SHANNON, SIMPSON, AND INVERSE SIMPSON INDICES AS PLOTTED FOR BEEF *PSOAS MAJOR* STEAKS INOCULATED WITH A 6-ISOLATE SPOILAGE BACTERIA MIXTURE AND SUBSEQUENTLY PLACED INTO AEROBIC RETAIL DISPLAY (3°C).

FIGURE 4.5. BETA DIVERSITY SHOWN AS A WEIGHTED UNIFRAC PRINCIPLE COORDINATES ANALYSIS (PCOA) FOR BEEF *PSOAS MAJOR* STEAKS INOCULATED WITH A 6-ISOLATE SPOILAGE BACTERIA MIXTURE AND SUBSEQUENTLY PLACED INTO AEROBIC RETAIL DISPLAY (3°C).

FIGURE 4.6. RELATIVE ABUNDANCE TAXA BAR PLOT ORGANIZED AT THE FAMILY LEVEL FOR BEEF *PSOAS MAJOR* (PM) STEAKS INOCULATED WITH A 6-ISOLATE SPOILAGE BACTERIA MIXTURE AND SUBSEQUENTLY PLACED INTO AEROBIC RETAIL DISPLAY (3°C).

FIGURE 4.7. TOTAL NUMBER OF PROTEIN FAMILIES DETECTED IN THE METATRANSCRIPTOMIC DATASET COLLECTED FROM BACTERIA GROWN ON BEEF *PSOAS MAJOR* DURING RETAIL DISPLAY IN AEROBIC PACKAGING.

CHAPTER 1: REVIEW OF LITERATURE

INTRODUCTION

Spoilage of fresh red meats is one of the greatest contributors to meat wastage and economic loss in the animal protein sector (Lipinski, 2020). Preservation of fresh meat is hardly a new concept. In fact, meat preservation has been documented as early as 10,000 years ago in the Stone Age, with technology in food preservation ever increasing until present day (Cassens, 2008). In modern times, meat preservation takes many forms, including chemical and physical preservation methods. In scientific literature, there are over 100 years of documented efforts to improve fresh meat shelf-life. This body of work and the advent of mechanical refrigeration, use of alternative packaging atmospheres, and usage of antimicrobials have vastly improved the shelf-life of meat.

Major advancements in the understanding of microbial presence and growth have contributed greatly to improving the shelf-life of meats and other highly perishable fresh foods. In a system with adequate hygiene and proper handling techniques, fresh meat spoilage is primarily dictated by bacterial growth (Nychas et al., 2008; Doulgeraki et al., 2012; Odeyemi et al., 2020). Although intact internal muscles are supposed to be sterile, bacteria can be introduced to carcasses via cross-contamination through knives, work surfaces, air flow, and employees (Stellato et al., 2016). Further cross-contaminations results in bacterial presence on all cut surfaces of fresh meat. As a result, it would be nearly impossible to create a meat harvesting and processing system that avoids any contamination with bacteria, as they are ubiquitous. Bacteria and other

microbial organisms find meat a suitable substrate for growth due to its nutrient-rich and high water activity matrix.

Understanding the underlying mechanisms of meat spoilage is paramount to extending fresh meat shelf-life. In the past, most research has focused on spoilage specific organisms (SSO) and has resulted in a plethora of knowledge contributing to our understanding of spoilage. Yet, advancements in scientific knowledge have determined symbiotic and amensal relationships between microbial organisms, and the term “metabiotic spoilage association” has been used to describe microbial communities and their interactions contributing to spoilage (Jørgensen et al., 2000; Comi, 2017).

Properties intrinsic and extrinsic to meat and microbial growth interact resulting in spoilage. Many of these characteristics have been described and some remain partially or fully unexplored, such as bacterial functional changes. The objective of this review is to characterize the physical and chemical changes that are induced by the spoilage process and to describe methods to measure and monitor the spoilage process in fresh meats.

SECTION 1: DRIVERS OF FRESH MEAT SPOILAGE

Meat spoilage is a complex set of biochemical reactions that create physical changes to the product. Intrinsic to meat are endogenous enzyme systems that often have very desirable effects, such as increased tenderness and flavor development (Bhat et al., 2018). The intrinsic factors are not directly responsible for rapid spoilage of fresh meat. When properly stored at a temperature below 5°C and at a normal ultimate pH between 5.4 and 5.8, microbial growth drives fresh meat spoilage (Gill, 1996; Casaburi et al., 2015). Additionally, in aerobically packaged fresh meat, *Pseudomonas* spp. have been implicated as the main spoilage bacteria; lactic acid bacteria (LAB) are

considered the drivers of spoilage in vacuum packaged fresh and processed meats (Gill, 1983; Nychas et al., 2008; Doulgeraki et al., 2012; Odeyemi et al., 2020).

1.1. Packaging

Packaging type is a major determinant of fresh meat shelf-life, as it selects which type of microorganisms will predominate during storage. For example, packaging systems that eliminate oxygen [i.e., vacuum or low oxygen modified atmosphere packaging (MAP)] favor the growth of lactic acid bacteria over other spoilage organisms such as *Pseudomonas* spp. In the United States, a vast majority of fresh red meat is vacuum packed as wholesale cuts for distribution before being fabricated into retail cuts and repackaged. This practice allows for extended storage of these cuts and promotes other quality benefits such as increased tenderness through endogenous enzymatic proteolysis and flavor development. Further, case-ready facilities are packaging retail cuts in low oxygen MAP environments, further enhancing conditions that promote LAB growth over other species in these environments (Wang et al., 2018; Mansur et al., 2019). In general, three main packaging types prevail in the US: vacuum packaging, carbon monoxide MAP, and aerobic packaging. It is not uncommon for retail cuts of meat to be subjected to all three types of packaging before reaching an end consumer (Mills, 2021).

1.2. Temperature and pH

Temperature and pH have a significant impact on fresh meat shelf-life. Maintaining a temperature below 5°C helps to prevent rapid growth of microorganisms. Elevated temperatures can also impact meat color stability and increase oxidation rates for lipids and proteins, thereby affecting shelf-life independent of microbes (Hammond

et al., 2015; Luong et al., 2020; Fu et al., 2022). Often, temperature abuse is most prevalent during the distribution and transport phases of the lifecycle of fresh meat, with temperatures frequently exceeding 10°C during these phases (Lulietto et al., 2015). Cold temperatures play an important role in reducing diversity of spoilage organisms, as only primarily psychrotrophic bacteria will grow at temperatures less than 5°C (Koutsoumanis et al., 2006; Nychas et al., 2008). When temperatures increase, even nominally, genera not always implicated in meat spoilage may proliferate and achieve greater population levels. Moreover, meat is slightly acidic with a normal ultimate pH between 5.4-5.8 (Matarneh et al., 2017). Meat pH below 5.4 can slow growth of spoilage bacteria; however, as pH becomes more neutral, bacterial growth rates may increase, hastening spoilage (Gill, 1983).

1.3. Microorganisms

Several microorganisms, such as bacteria, fungi, and yeasts, can play a role in meat spoilage. This review will focus on bacteria associated with meat spoilage, while the impacts of other microbes, such as fungi, including molds and yeasts, have been reviewed previously by Odeyemi et al. (2020) and Fung et al. (1990). Briefly, fungi can multiply in fresh meat, however, their growth is limited by low temperatures, and their impacts are minimal in most fresh meat spoilage. Fungi's slow growth rate and the short duration of fresh meat shelf-life limit their impact during meat spoilage. Therefore, much less attention has been given to fungi and their role in meat spoilage.

1.3.1. Pseudomonas spp.

Aerobically packaged fresh meat spoilage microbiota is predominated by *Pseudomonas* spp. *Pseudomonas* spp. bacteria are motile, non-spore forming, Gram-

negative bacilli that are well known to cause spoilage in food products (Wickramasinghe et al., 2019). Further, these bacteria are often associated with soil and water microbiomes and have shown symbiotic relationships with plants (Wickramasinghe et al., 2019). In fresh meats, *P. fragi*, *P. lundensis*, *P. putida*, and *P. fluorescens* are common species found during spoilage (Nychas et al., 2008; Papadopoulou et al., 2020). These bacteria proliferate well at refrigeration temperatures and have developed competitive advantages such as proteases, lipases, extracellular polymeric substances (EPS; slime), biosurfactants, and the ability to form biofilms, which aid in outcompeting other bacteria present (Wickramasinghe et al., 2019; Chen et al., 2023). These adaptations suggest that meat may be an ecological niche for these bacteria.

1.3.2. *Lactic acid bacteria*

Lactic acid bacteria are a large contingent of bacteria consisting of hundreds of genera. Lactic acid bacteria are Gram-positive, facultative anaerobes, non-spore forming, and non-motile (Savijoki et al., 2006). This class of bacteria is generally recognized as safe, are routinely used as starter cultures in fermented products, but can be deleterious to the quality of fresh meats (Leroy and De Vuyst, 2004; Signorini et al., 2006). Despite the desired impacts of select species of LAB in fermented foods, these bacteria also contribute to the deterioration of meat, ultimately leading to meat spoilage. Lactic acid bacteria commonly associated with fresh meat spoilage include *Carnobacterium*, *Lactobacillus*, and *Leuconostoc* spp. (Pothakos et al., 2015). Environments with low oxygen levels and cold temperatures, such as vacuum packaging and low oxygen MAP, favor LAB growth compared with other genera of bacteria (Paramithiotis et al., 2009; Pothakos et al., 2015).

SECTION 2: FRESH MEAT SPOILAGE

2.1. Defining meat spoilage

Comprehensively, fresh meat spoilage can be defined as the deteriorative changes to fresh meat that impact the organoleptic qualities, appearance, texture, odor, or nutritional content of fresh meat that leave it undesirable for human or animal consumption (Nychas et al., 2008; Hammond et al., 2015; Mansur et al., 2019; Luong et al., 2020; Odeyemi et al., 2020; Chen et al., 2024). The changes in meat include discoloration, slime formation, putrid or rancid off-odors and flavors, potential changes to texture, and nutritional profile. While these changes result in an undesirable eating experience, safety of the product may not be compromised.

Predicting shelf-life of fresh meat is a complicated process due to the multitude of factors impacting shelf-life. Yet, date labeling (e.g., “best if used by” or “best by”) is a standard practice of fresh meats in the US. There is considerable debate concerning date labeling of products because these labels tend to be conservative in their estimates to ensure product has not become spoiled or declined in quality by the time of consumption. Further, the initial microbial population levels and composition on meat can shorten or lengthen the actual shelf-life (Ramírez et al., 2018). While this practice has roots in helping to protect consumers and companies, it contributes to considerable food wastage and is not a reliable predictor of spoilage of food products (Newsome et al., 2014).

In red meats, product discoloration – the formation of brown discoloration on the meat surface – leads to considerable red meat wastage as it is considered undesirable by consumers, thus is effectively considered spoiled (Ramanathan et al., 2022). Other authors have determined that meat shelf-life is controlled by the formation of

malodorous compounds and have evaluated shelf-life on the basis of odor (Clark and Lentz, 1969; Casaburi et al., 2015). Effectively, products that are viewed as undesirable are spoiled, even if eating satisfaction or safety would not have been impacted.

Moreover, determining spoilage in fresh meat can be subjective and is not easily determined in the early stages (Nychas et al., 2008). While spoilage produces chemical and physical changes to meat products and can be objectively defined in laboratory settings, in practical applications, spoilage is nuanced.

2.2. Changes in color

2.2.1. Meat color chemistry

Meat color chemistry has been extensively reviewed (Mancini and Hunt, 2005; Ramanathan et al., 2019; King et al., 2023). In summary, the color pigment protein myoglobin and its redox form are responsible for meat color. When the iron in myoglobin is reduced and bound with oxygen or carbon monoxide, it is a bright cherry red color. When the iron in myoglobin has been oxidized, it is brown and known as metmyoglobin. Multiple factors contribute to the oxidation status and ligand attachment to the heme iron in myoglobin, thus influencing color.

Color stability can indicate freshness of products if biochemical changes in meat are considered. Color stability is a muscle specific property of red meat cuts, and microbial growth or population levels may not indicate spoilage. Still, meat color chemistry is controlled by oxidation reactions and increased oxidation of lipids or other proteins can result in increased oxidation of myoglobin, creating discoloration on fresh meats (Faustman et al., 2010). McKenna et al. (2005) measured the color stability of common beef muscle cuts and showed that color is not always a predictor of shelf-life,

as some cuts have very minimal color stability, intrinsically. Nonetheless, meat color is most frequently used by consumers to discern products' perceived freshness (Font-i-Furnols and Guerrero, 2014; Thies et al., 2024).

2.2.2. *Bacteria and meat color*

Bacterial growth has been implicated in causing fresh beef discoloration in both aerobically packaged and vacuum packaged products (Doulgeraki et al., 2012; Smith et al., 2024a). Previously, Robach and Costilow (1961) reported that high levels of *Pseudomonas* spp. consume high quantities of oxygen during the logarithmic and stationary phases of growth. They hypothesized that competition for oxygen creates low partial O₂ pressures on the surface of meat, which favor metmyoglobin formation, resulting in brown discoloration. In muscles with non-exhausted metmyoglobin reducing activity (MRA), metmyoglobin formed under low partial O₂ pressures should be reduced to deoxymyoglobin. For example, Cross et al. (1986) reported that during aerobic display, beef muscles' MRA could reduce metmyoglobin to deoxymyoglobin, forming a purple color even when *Pseudomonas* spp. population levels were sufficiently high. However, according to the authors, the deoxymyoglobin would remain reduced without a ligand bound, and remain purple because the bacteria were still competing with myoglobin for oxygen. The theory presented by Cross and others (1986) is plausible when considering conditions such as dark cutting beef where higher muscle pH results in more physiologically active mitochondria that also compete with myoglobin for oxygen. In the case of dark cutting, mitochondria are competing with myoglobin for oxygen and help to produce a deoxymyoglobin color instead of bacteria as Cross and others (1986) suggested might occur (McKeith et al., 2016).

The conversion of metmyoglobin to oxymyoglobin, or at least a bright red color, in aerobically packaged beef towards the end of retail display has been documented a handful of times (Chan et al., 1998; Motoyama et al., 2010; Smith et al., 2024a). However, the mechanism of this 'reversion in meat color' has not been well explained. The likelihood of intrinsic MRA pathways reducing metmyoglobin in meat exhibiting this process is unlikely as endogenous MRA systems are likely exhausted by day 7 or 8 of retail display, especially in color labile muscles (Seyfert et al., 2006; Joseph et al., 2012; Smith et al., 2024b). Other authors have reported similar findings in aerobically stored beef with >7 log CFU levels of *Pseudomonas* spp. present (Chan et al., 1998; Motoyama et al., 2010; Smith et al., 2024a). However, in the latter studies (Chan et al., 1998; Motoyama et al., 2010; Smith et al., 2024a), meat product returned to a bright red color after metmyoglobin formation during extended display at $<4^{\circ}$ C.

Bacterial growth has also been implicated in creating a green color on the surface of meat. Originally, the greening of meat was observed in low oxygen environments ($<1\%$ O_2) coinciding with meat that had an ultimate pH of >6.0 (Nicol et al., 1970). These authors determined that color pigment for these conditions was created by sulfmyoglobin. Sulfmyoglobin is formed when reduced deoxymyoglobin binds to hydrogen sulfide (H_2S), potentially generated by bacterial growth, and results in a green color in anoxic environments. However, exposure to oxygen generated an oxidized red colored metsulfmyoglobin. In addition to sulfmyoglobin, reactions between myoglobin and peroxides, namely hydrogen peroxide (H_2O_2), can result in the formation of another green pigment known as choleglobin (Ledward, 1992). Hydrogen peroxide

production can occur through auto-oxidation of lipids or microbial oxidation processes, and its formation is favorable at atmospheric oxygen levels (Ledward, 1992).

2.3. Changes in odor

Meat odor is determined by volatile organic compounds (VOCs). There is limited knowledge of raw meat VOCs compared with cooked meat VOCs, but Casaburi et al. (2015) reported 13 compounds that were associated with raw meat odor that could comprise the base of unspoiled raw meat. During the spoilage process, physicochemical changes in the meat caused by the microbial growth affect the VOCs released as gases, which in turn influence the odors perceived. Limited research has been conducted to identify specific VOCs and their concentrations during spoilage, and these studies often focus on single bacterial species under highly controlled conditions, reducing the broader applicability of their findings.

Nonetheless, several classes of VOCs have been associated with the odor changes in fresh meat as it becomes spoiled. Varieties of alcohols, ketones, aldehydes, esters, and volatile fatty acids have been implicated in comprising the volatilome of spoiled meat. Alcohols can be derived from oxidation of lipids or amino acids and can result in a myriad of off odors, including whiskey, earthy, fruity, and cheesy. Additionally, the fermentation of glucose or other carbohydrates can result in alcohol production. Ketones are another class of compounds impacting odor sensory of fresh meat. Ketone production could be happening through several pathways, including microbial oxidation and alcohol dehydrogenation, as well as LAB that produce ketones when utilizing glucose (Ardö, 2006). Dainty et al. (1985) reported “cheesy” as the main off odor in spoiled meat, and later reported that acetoin was the main contributor to this odor

(Dainty et al., 1989). Further, acetoin is reported as one of the most detectable and common compounds found in both aerobic and vacuum packaged beef (Casaburi et al., 2015). Aldehydes play an important role in meat sensory because of their low detection threshold (Muriel et al., 2004). Aldehydes are derivatives of lipid oxidation and amino acid deamination and are routinely used as markers of oxidation of meat products. Aldehydes are routinely produced through microbial interactions and through lipid auto-oxidation pathways. Esters are most commonly associated with *P. fragi* and are the result of esterification of alcohols (Ercolini et al., 2010; Wickramasinghe et al., 2019). Ester compounds are associated with fruity off-odors (Dainty and Mackey, 1992). Another class of compounds are volatile fatty acids (VFA), or short chain fatty acids. These VFAs are associated with both aerobic and vacuum packaged meat but are mainly associated with LAB growth (Jones, 2004). The major VFA associated with meat spoilage is butanoic acid, which can produce rancid, vomit, and cheesy odors. Butanoic acid is mostly produced by the catalysis of amino acids via the Strickland reaction (Martín et al., 2010). For a more in-depth review of how packaging, meat species, and bacterial interactions influence VOC production, see the comprehensive reviews conducted by Casaburi et al. (2015) and Ercolini et al. (2010). It is also worth mentioning that aroma constitutes approximately 80% of the sensory experience of taste (Spence, 2015). Therefore, the impacts of VOC on sensory attributes should be underscored. Moreover, VOCs that have similar off-odor notes can compound and intensify the unpleasant odor (Casaburi et al., 2015).

2.4. Changes in texture

Postmortem muscle becomes meat through a series of pathways upon an animal's death (Matarneh et al., 2017). Many of the physical changes that occur in muscle tissue after slaughter, as it transforms into meat, are uncontrollable but can be managed using techniques such as electrical stimulation and proper, species-appropriate chilling procedures (Matarneh et al., 2017). Soon after death, endogenous systems within meat, such as the calpain/calpastatin and cathepsin enzymatic systems begin to break down proteins. The proteolysis by these enzymes produces a desirable effect of increasing meat tenderness (Bhat et al., 2018).

Research involving the change in texture of meat due to spoilage is scarce. Investigators have researched changes in texture within packaging type during retail display, such as decreased tenderness in high oxygen (80% O₂) MAP (Senaratne, 2012). However, investigating actual changes in texture from spoilage is difficult to perform as there are no well-developed chemical assays for texture analysis, and conducting consumer panel surveys using raw spoiled meat poses safety and ethical risks. The literature does report that increased days in display increases tenderness, however, this is most often attributed to extended aging times and the activity of endogenous proteolytic systems. One study investigated texture changes in beef packaged in vacuum or aerobically, and reported that texture change depends on packaging, temperature of storage, and length of storage, with interactions between all conditions (Olivera et al., 2013). The effects of spoilage on meat texture are not well understood; however, this knowledge may have limited practical relevance.

Some bacterial proteases have demonstrated strong capabilities to cleave myosin, as demonstrated by Alanís et al. (1999). Unlike muscle endogenous enzymes,

which are present throughout the meat, bacterial enzymes are limited to a superficial layer of the surface (Gill and Penney, 1977). Despite this, it is reasonable to conclude that other changes in the superficial layer of the surface of meat cuts during spoilage could be recognized and contribute to minor texture changes. This impact could be more visible in ground products where surface area is substantial.

2.5. Slime formation

Certain bacteria, including *Leuconostoc*, *Lactobacillus*, and pseudomonads are known slime formers when bacterial levels reach >7 log CFU (Iulietto et al., 2015; Wickramasinghe et al., 2019). In dairy products, for example, the formation of slime contributes to rheology of the food and is desirable (Degeest et al., 2001). Conversely, in fresh meat products slime formation is an indicator of advanced spoilage. Slime functions to entrap moisture, provide toxin and antimicrobial defense, aid in biofilm formation, and cell communications (Iulietto et al., 2015; Wickramasinghe et al., 2019). Slime produced from the LAB genera *Leuconostoc* spp. and *Lactobacillus* spp. (which are the main slime forming LAB found on meat during spoilage) is comprised of extracellular polysaccharides (EPS; Iulietto et al., 2015) and is created within the cell by glucosyltransferases from sugar nucleotide precursors and is excreted extracellularly (Ullrich, 2009). There are two forms of EPS created by these bacteria, capsular polysaccharides and unattached polysaccharides, in which the latter does not remain attached to the excreting cell (Ullrich, 2009). Another characteristic of slime is the degree of ropiness, or the extent to which the slime will form “ropes” if stretched. Both ropy and non-ropy slime production is possible on meat products and is influenced by microbial genetics and the saccharides that comprise the EPS (Degeest et al., 2001;

Iulietto et al., 2015). In vacuum packaged cooked beef, LAB EPS was comprised of glucose and galactose polymers (Iulietto et al., 2015). Slime formation on fresh raw meats has been briefly studied (Ayres, 1960), but to our knowledge has not been thoroughly mechanistically explored in the recent years.

2.6. Carbohydrate changes

Fresh meat composition is less than 1% carbohydrate (Cabos and Diaz, 2015). Comprising these carbohydrates are glycogen, which are polymers of glucose, free glucose, and glucose intermediates involved in glycolysis such as glucose-6-phosphate and pyruvate (Cabos and Diaz, 2015). It has been reported that glucose is a main driver of meat spoilage, as it is a preferential energy source for bacteria when it is available (Shelef, 1977; Paramithiotis et al., 2009). In aerobically packaged meat, *Pseudomonas* spp. will sequentially consume D-glucose, then L- and D-lactic acid. *Pseudomonas* spp. frequently lack the enzymes necessary to conduct glycolysis. Therefore, these organisms will convert glucose to D-gluconate and gluconate-6-phosphate (Lambropoulou et al., 1996). These glucose derivatives are not available for use by other metabiotic spoilage organisms giving pseudomonads a competitive advantage. Further, the authors (Paramithiotis et al., 2009), reported that addition of glucose to aerobically packaged ground beef did not impact the rate of growth for the microbial populations or final population counts compared with the control samples. Gill and Newton (1979) reported that additions of glucose to dark, firm, and dry beef meat increased shelf-life of the product, which, when combined with the previously mentioned study, suggests that the addition of glucose in aerobically packaged meat could delay

the accumulation of spoilage compounds but does not reduce or significantly alter bacterial population levels.

Pseudomonas spp. have been classified as obligate aerobes but survive in anaerobic environments via glucose and pyruvate fermentation to ethanol among other pathways (Kolbeck et al., 2021). For LAB, the presence of glucose or other fermentable carbohydrates in anoxic environments leads to the production of lactic and/or acetic acid. However, in the presence of oxygen and heme iron, which aerobically packaged meat has an abundance of, LAB favor respiration over fermentation due to iron acting as a proton acceptor and aiding in co-factor regeneration. When this is the case, increased metabolites of acetate and acetoin are favored compared with lactate (Gänzle, 2015).

Excessive fermentation of glucose, which can occur in vacuum packaging, can result in high levels of lactic acid accumulation, dropping bacterial environmental pH from ~5.6 to ~5.1 (Gill and Newton, 1977). Decreases in pH can promote amino acid catalysis by bacteria (Jones, 2004; Gänzle, 2015). Increased amino acid catabolism results in increased ammonia levels which can help to increase pH to more favorable levels for bacterial growth (Pessione et al., 2010). Coincidentally, the decrease in pH serves to slow growth of other spoilage species and can effectively increase shelf-life (Shelef, 1977). However, utilization of amino acids as a carbon energy source is frequently implicated in the spoilage process because it contributes to faster meat deterioration and malodorous metabolite build-up.

Lactate is another product of glycolysis that can be utilized by bacteria. A bacterial lactate dehydrogenase can convert lactate to pyruvate which can be utilized

for energy via external respiration or within the endogenous systems. Lactate metabolism is less favorable than glucose metabolism for bacteria because it nets less ATP in the process (Gänzle, 2015). Additionally, microbial usage of pyruvate promotes homofermentation in LAB, resulting in production of lactic and acetic acid or ethanol.

2.7. Protein changes

Degradation and utilization of proteins for energy and carbon by bacteria occurs after the glucose availability becomes scarce (Nychas et al., 1988; Nychas et al., 2008). Environmental conditions, oxygen availability, temperature, and pH also play a role in determining when bacteria utilize amino acids for their energy needs. Knowledge of the role metabolic spoilage organisms have in amino acid degradation is limited, especially in fresh red meats. As mentioned in the textural changes section above, breakdown of proteins postmortem occurs through intrinsic pathways, which can confound some findings with the roles of bacteria and amino acids during spoilage. Nonetheless, in seafood and poultry, evidence of nitrogenous molecule breakdown, such as ammonia and methyl amines, have been shown to increase as bacterial population levels increase for both super chilled beef and chicken meat (Lu et al., 2020; Saenz-García et al., 2020). These findings suggest that bacteria have a part in generating these nitrogenous products.

Frequently, the initial indicators of meat spoilage are derivatives of amino acids (Pellissery et al., 2020). Microbial breakdown of leucine in bovine dairy products can produce the aldehyde 3-methyl-butanal, which can undergo further chemical reactions to become alcohols, ketones, and the VFA butanoic acid (Smit et al., 2009). Butanoic acid is one of the primary metabolites responsible for a cheesy odor during spoilage.

Further, degradation of arginine can result in production of putrescine and spermidine (Pothakos et al., 2015), which are potent malodorous compounds associated with decomposition. Microbial catalysis of arginine, methionine, and cysteine can lead to production of hydrogen sulfide gas and other sulfides which can form rotten egg smells and potentially lead to surface greening of both aerobic and vacuum packaged meat (Casaburi et al., 2015). Upon microbial cell death, internal peptidases are released and continue to cleave peptides (Signorini et al., 2006). This function serves to increase free amino acid concentrations in meat during spoilage and promote growth of other bacteria by increasing usable carbon sources for growth. More research into the specific microbial protein metabolism on fresh red meats is needed to better understand their impacts.

2.8. Lipid changes

Lipids have crucial roles in the development of rancidity and propagating oxidation within meat products that can have important deleterious impacts on shelf-life of fresh meats (Wood et al., 2004). The lipid composition of fresh red meats is variable, ranging from 2-5% of total dry mass in typical red meats (Cabos & Diaz, 2015). Lipids in meat are present in a few forms: phospholipids, triglycerides, cholesterol, lipoproteins, lipid-soluble vitamins and free fatty acids (Fu et al., 2022). Phospholipids make up about 5% of lipid in meat yet contain most of the easily oxidized polyunsaturated fatty acids and are more readily propagated during oxidation (Fu et al., 2022). Due to this, phospholipids have been indicated as the main source of lipid oxidation in fresh beef and pork (Domínguez et al., 2019; Fu et al., 2022). Triglycerides are found stored in adipose tissue present mostly as subcutaneous and inter- and intramuscular fat. Lipids

are prone to oxidation via auto-oxidation, photo-oxidation, and enzymatic oxidation (Domínguez et al., 2019). While some oxidation products are desirable for flavor development in meat products, excessive accumulation of oxidation products results in off-odors and flavors that are undesirable. Aldehydes are the most common stable end product of lipid oxidation and can be detected in low quantities, resulting in consumer rejection (Domínguez et al., 2019; Fu et al., 2022).

Bacteria belonging to both LAB and *Pseudomonas* spp. have demonstrated capabilities to have lipolytic potential (Stead, 1986; Signorini et al., 2006; Wickramasinghe et al., 2019). Papon and Talon (1988) reported that in LAB, lipolytic activity increases during the logarithmic phase of growth, when glucose levels have decreased. The role of lipolytic activity of spoilage organisms is greatly understudied in fresh meat spoilage. In fermented sausages, LAB lipases result in an increase in free fatty acid concentration and in acetate production (Hierro et al., 1997) and can lead to signature flavor development. Molly et al. (1996) reported that polyunsaturated fatty acids are liberated more frequently compared with monounsaturated and saturated fatty acids, and that greater lipolysis occurs in fermented sausages made with pork compared to beef. Moreover, lipases are excreted as extracellular enzymes by spoilage bacteria and function to cleave fatty acids from triglycerides and phosphorus heads, which can ultimately lead to increased lipid oxidation and VFA production, contributing to the spoilage volatilome.

In chicken meat, *Pseudomonas* spp. can use biosurfactants created with lipids which help to liberate nutrients from the chicken meat (Mellor et al., 2011). These biosurfactants increased the rate of breast meat spoilage. Contrarily, Chen et al. (2023)

reported that biosurfactants promoted *Pseudomonas fragi* growth but inhibited other members of the metabiotic spoilage association, thus slowing spoilage in fresh meats. In whole milk, *Pseudomonas* spp. lipase activity was greatest during the stationary phase of growth (Stead, 1987). It may be reasonable to conclude based on evidence from processed meats and the dairy industries that lipases are deployed at later phases of growth when spoilage has already progressed to noticeable degrees. Aside from lipase activity, bacterial metabolism can generate pro-oxidants such as hydrogen peroxide that can initiate lipid oxidation, leading to quality deterioration (Kanner, 1994).

SECTION 3: METHODS TO MEASURE SHELF-LIFE OF FRESH MEATS

3.1. Traditional methods to evaluate fresh meat shelf-life

Meat spoilage has long been evaluated through basic sensory and microbiological testing (Nychas et al., 2008). For the average consumer, color and odor are the main indicators of meat spoilage. In meat color research, panelists are often considered the gold standard, and when evaluating spoilage, much the same could be said (Giménez et al., 2012; King et al., 2023). As early stages of spoilage have fewer outward indicators, identifying sensorial impacts early would require trained panelists and thorough experimental design (Nychas et al., 2008; Giménez et al., 2012). In a well-designed sensory study for shelf-life of fresh meats, criteria for failure of freshness must be established before the study, and sensory data are best combined with physicochemical analyses (Giménez et al., 2012). This allows for determination of thresholds that can be measured by chemical analyses in future work and correlate panel data with biochemical changes during spoilage.

Traditional microbiology methods (e.g., plating, broth incubation) have been used for a century to evaluate fresh meat spoilage (Lepper and Martin, 1930). Only about 2%

of known bacteria can be cultured, and even further, meat microbiota require multiple media and culturing techniques to successfully capture and grow in an in vitro setting (Overmann et al., 2017). These techniques have provided a plethora of data concerning organisms responsible for meat spoilage, but they can also implicate organisms that are present but not contributing to meat spoilage (Nychas et al., 2008). Moreover, traditional microbiological analyses have elucidated much information concerning bacterial growth rates, and how temperature, pH, and packaging type affect spoilage; but they have primarily focused on external factors.

Spectroscopy is another traditional method used to evaluate meat during spoilage. These tests can determine compound presence and quantity, evaluate color reflectance, and determine microbial concentrations. Several different types of spectroscopies exist: photo, near infrared, spectral, and electromagnetic, to name a few (Vitha, 2018). In simple terms, during spectroscopy, light with specific wavelength or energy source is emitted to an object, and the reflectance, absorbance, or transmittance of that light or energy is determined (Vitha, 2018).

Measuring color reflectance to determine objective color values is still a routine practice in fresh meat research and is currently considered a best practice (King et al., 2023). Enzymatic assays and fluorescent detector kits have also been employed in the past for detecting compounds and their concentrations (Nychas et al., 2008). The foundations of fresh meat spoilage knowledge rests on the tenets of these methods but newer analytical methods, such as the methods included in the following sections, are providing new insights to meat spoilage.

3.2. Mass spectrometry approaches

The basic principle of mass spectrometry is separation and detection of charged molecule fragments (Downard, 2007). The core components of mass spectrometry are ion source, mass analyzer, and ion detector (Downard, 2007). The ion source serves to create a charged molecule that can then be passed to the mass analyzer which organizes compounds based on mass. Finally, compounds are passed to the ion detector which imputes the electrical signal that can be translated into a compound. In modern practices, mass spectrometry is paired with other forms of molecular separation such as gas chromatography (GC) or liquid chromatography (LC) or matrix assisted laser desorption ionization mass spectrometry (MALDI; Downard, 2007). For higher resolution and confidence in compound detection, two ion detectors can be coupled and is known as mass spectrometry-mass spectrometry (MS-MS). Mass spectrometry methods can be targeted or non-targeted. With targeted MS methods, steps are taken to bias samples towards a particular class of compounds (such as organic acids or phenolics) and can provide more detailed data for a target compared to non-targeted MS, but may lose resolution of other classes of compounds. For non-targeted MS, no purposeful bias is included and can be used for more general purposes and hypothesis generation.

Mass spectrometry has been used in several meat science related experiments ranging from tenderness, drug compound identification, flavor chemistry, and shelf-life studies (Shishani et al., 2003; Legako et al., 2015; Malheiros et al., 2019; Frank et al., 2020). In shelf-life studies, a common approach is gas chromatography mass spectrometry to measure VOCs. For example, Ercolini et al. (2009) employed headspace micro extraction (SPME) with GC-MS to detect VOC changes in inoculated

beef samples under vacuum during extended storage. One advantage of the MS approach is its ability to identify compounds that can serve as indicators of another condition, often referred to as biomarkers. In vacuum packaged raw pork loin chops, Yi et al. (2024) reported finding nine potential metabolite biomarkers associated with spoilage in raw fresh pork. These authors used untargeted ultra-high performance liquid chromatography MS data and machine learning to identify potential metabolites that could indicate spoilage. Mansur et al. (2019) correlated spoilage bacteria metabolites with spoilage in beef in vacuum and aerobic packaging, using head space SPME GC-MS. The authors reported that in aerobic packaging, 3-methylbutan-1-ol and its subsequent products could indicate spoilage, but acetic and butanic acid were culprits in vacuum packaged beef spoilage.

3.3. Next generation sequencing approaches

Next generation sequencing (NGS) has emerged as one of the technologies of importance over the past three decades in genomics research. The use of NGS allows for rapid and parallel sequencing of DNA molecules and fragments from multiple samples simultaneously (Grada and Weinbrecht, 2013). Before NGS, technologies such as Sanger sequencing allowed for sequencing of long chains of DNA, however, Sanger sequences were error prone, required high levels of genomic materials, and slow. New NGS platforms such as Illumina are cost-effective, quick, and accessible to researchers and clinicians alike (Grada and Weinbrecht, 2013). Use of short-read, NGS platforms allow for high throughput, deep sequencing of samples, and multiple data analysis pipelines have been constructed to allow for computational processing of sequencing data. For the purpose of this review, the next sections will focus on use of 16S rRNA

DNA gene sequencing (microbiome), shotgun metagenomics, and RNA-sequencing transcriptomics.

Classic microbiome, 16S rRNA DNA gene sequencing, is one of the most routinely utilized capabilities of NGS. Through collaborations of large projects such as the Human Microbiome Project, the workflow and applicability of the data are refined. The simplified workflow of 16S gene sequencing is as follows: collect samples > extract DNA > amplify 16S genes using PCR > sequence DNA copies > data analysis (Galloway-Peña and Hanson, 2020). Ultimately, 16S rRNA DNA gene sequencing allows for a snapshot of the bacteria present at the time of sampling. One of the key advantages to this technology is that it is not limited to the 2% of organisms that can be cultured in a laboratory (Overmann et al., 2017). 16S rRNA gene sequencing has opened the door to discovering the microbial diversity previously unknown on both meat and the environment at large. Contrarily, there are drawbacks that must be acknowledged when evaluating microbiome data. First, DNA extraction of hard to lyse organisms can impact the diversity of the resulting sample because less DNA from those organisms will be amplified and sequenced. Second, computational analysis introduces bias into the results and must be considered when making comparisons and conclusions based on 16S rRNA gene data. Lastly, DNA from unviable cells could also be sequenced but there is not currently a way to differentiate viable from nonviable cells with these techniques.

In meat science research, 16S gene sequencing has been vital to showing the previously unknown diversity of microbes present on meat. Although researchers have known for a century of the impacts of culturable bacteria, this method has provided

insights into novel species. One such bacterium is *Photobacterium*, which has been further studied and classified by Hilgarth et al. (2018). This bacterium has since been found in several other microbiome studies and classified into the metabiotic spoilage association and is known to contribute to total volatile basic nitrogen in fresh meat products and may produce biogenic amines (Nieminen et al., 2016; Fuertes-Perez et al., 2019; Dourou et al., 2023). The microbiome approach has worked to confirm spoilage associations with traditional culture based techniques showing the patterns of bacterial growth during routine spoilage (Hultman et al., 2020; Hwang et al., 2020; Johansson et al., 2020). Further yet, utilizing 16S NGS technology for meat science research has provided information on routes of contamination of fresh meat through processing and distribution (Stellato et al., 2016). The microbiome approach has also been used to assess microbial differences within separate dry aged facilities to determine location impacts on dry-aged meat development (Capouya et al., 2020).

Another NGS technology takes microbiome a step further and allows for predicted genomic function and is known as shotgun metagenomics. Shotgun metagenomics collects all the microbial DNA in a sample and sequences it to allow for more genomic coverage of species present. This approach then allows researchers to predict functions of bacteria based on genes and habitat. To date, this approach has been used for relatively few fresh meat shelf-life studies (Hwang et al., 2020; Poirier et al., 2020) but can provide insights into the behaviors of bacteria on meat. On the other hand, shotgun metagenomics has been applied in meat microbiota related antimicrobial activity and meat safety research (Yang et al., 2016; Doster et al., 2020; Flint et al., 2023; Indio et al., 2024). Two major hindrances to shotgun metagenomics are the cost

and that conclusions based on shotgun metagenomics are predictions of function based on gene presence in the genome and habitat.

RNA-seq is similar to the two previously mentioned NGS technologies, but instead of focusing on the genome, this technique focuses on the transcriptome. The transcriptome is the collection of RNA molecules within the cell or collections of cells (Lowe et al., 2017). Here, RNA molecules are captured and copied as cDNA and then sequenced. The benefits of this approach are that it can give insights as to which genes are being transcribed and provide indications as to which proteins will be created (Lowe et al., 2017).

RNA-seq has been utilized for fresh meat spoilage research in a limited capacity. Hauschild et al. (2022) investigated the impacts of *P. fragi* and *Brochothrix thermosphacta* co-contaminants on two strains of *Photobacterium* grown on chicken breast meat. These authors reported that *Photobacterium* increased oxidative stress responses and cellular division genes. Another approach, which may be more applicable in shelf-life research, is meta-transcriptomics, as it can evaluate the transcriptomes of multiple organisms at once. To the author's knowledge, metatranscriptomics has only been employed in meat science shelf-life studies a couple of times. Using chicken meat, Höll et al. (2020) evaluated the transcriptomes of co-contaminants *B. thermosphacta* and *C. divergens* in two different MAP environments only at the end of display. Further, Hultman et al. (2020) performed longitudinal metatranscriptomics on MAP beef to better understand meat spoilage. These authors reported increases in stress response genes and carbohydrate metabolism genes.

Conclusions

Fresh meat spoilage can occur due to the biochemical and physical changes caused by microbial succession. These organisms can impact the odor, appearance, texture, and taste of the product. Cold chain management, facility hygiene, and packaging type, can all contribute to extending shelf-life by controlling microbial growth.

Volatile organic compounds are one of the early and key indicators of meat spoilage, yet the thresholds and routes of production are relatively unexplored. Bacterial induced proteolysis in meat is most likely contributing to production of total volatile basic nitrogen products, yet the mechanisms remain to be elucidated. Impacts of lipids and lipid oxidation on meat eating quality is well documented, but the interaction between lipids and microbial growth during spoilage is not well established. Future work investigating microbial genomics can provide key insights to bacteria succession and production of spoilage compounds on fresh meat.

Methods of detecting, evaluating, and quantifying fresh meat spoilage have evolved with the advances in technology. Combinations of traditional methods and newer techniques can provide the greatest insights to meat spoilage. Next-generation sequencing and omics-based approaches will also contribute to a more in-depth analysis of bacterial-induced meat spoilage.

CHAPTER 2: IMPACT OF SPOILAGE BACTERIAL POPULATIONS ON DISCOLORATION OF BEEF STEAKS

Citation:

Smith, C. L., Geornaras, I. & Nair, M. N., (2024) "Impact of Spoilage Bacterial Populations on Discoloration of Beef Steaks", *Meat and Muscle Biology* 8(1): 17796, 1-13. doi: <https://doi.org/10.22175/mmb.17796>

Introduction

The demand for fresh meat is expected to increase drastically over the next three decades with global economic growth leading to increased demands on the natural resources needed to produce it (Godfray et al., 2018). At the same time, food wastage, especially wastage of perishable animal proteins, is increasing. In high-income countries, animal protein availability exceeds population needs (Ederer et al., 2023) and results in food waste. For example, approximately 26% of fresh meat produced in the U.S. is wasted annually at the retail and consumer levels (Gunders, 2012). The U.S. produced an estimated retail equivalent of 8.94 billion kg of beef in 2022 (USDA ERS - Statistics & Information, 2023), and approximately 194.7 million kg of that is wasted annually (Ramanathan et al., 2022), with one primary cause of fresh beef wastage being surface discoloration. Moreover, recent studies have indicated that 2.55% of beef produced in the U.S. is discarded due to discoloration, leading to an economic loss of \$3.7 billion/year to the beef industry (Ramanathan et al., 2022). The wastage is partially attributed to consumers' preference for fresh beef that is bright cherry-red colored and their reluctance to purchase meat products that do not meet these color expectations (Viana et al., 2005; Grebitus et al., 2013a; Feuz et al., 2020). The importance of fresh beef color on consumer perceptions of quality has been reported previously (Glitsch, 2000; Carpenter et al., 2001;

Robbins et al., 2003; Killinger et al., 2004) as consumers commonly associate beef color with freshness and product safety (Grebitus et al., 2013b).

King et al. (2011) reported that muscle variation within carcass explained more differences in observed a^* (redness) values than animal variation, suggesting that muscle-specific factors could be driving the meat color stability differences. For example, tenderloin (*psoas major*; PM) steaks are considered color-labile as they discolor rapidly during retail display (within 2-3 days), whereas striploin (*longissimus lumborum*; LL) steaks are considered color-stable as they can retain a bright cherry-red color for longer than 5 days (McKenna et al., 2005; Najar-Villarreal et al., 2021). Although factors such as muscle fiber type differences, myoglobin concentrations, oxygen consumption rates, proteome differences, and microbiome diversities have been examined, none of them fully explain the muscle specificity in discoloration (Atkinson and Follett, 1973; Hood, 1980; Klont et al., 1998; McKenna et al., 2005; Mancini et al., 2018; Smith et al., 2024).

The initial bacterial load on fresh meat depends on a multitude of factors such as the use of antimicrobial interventions during harvest and processing, harvest facility hygiene, fabrication facility cleanliness, temperature during transport and display, as well as retail store sanitation standard operating procedures (De Filippis et al., 2013). Preventing bacterial growth on fresh meat during retail display is nearly impossible as meat provides a nutrient-dense medium for microbial growth (Labadie, 1999). The changes in meat associated with bacterial growth during storage can lead to spoilage (Nychas et al., 2008; Argyri et al., 2015). Fresh beef is typically considered microbially spoiled when it reaches 7-8 log CFU of bacteria and is often characterized by slime formation, surface greening, and malodorous volatile compounds (Nychas et al., 2008).

However, there is limited evidence on the impact of spoilage bacteria on surface discoloration in fresh meat. Previously, Robach and Costilow (1961) reported that the genus *Pseudomonas* can contribute to metmyoglobin formation in beef but failed to observe similar results with lactic acid bacteria. Moreover, Chan et al. (1998) demonstrated that the common meat spoilage organism, *Pseudomonas fluorescens*, may cause a more rapid formation of metmyoglobin, resulting in brown discoloration. *Pseudomonas fragi*, another predominant spoilage microorganism associated with aerobically stored fresh beef, may contribute to surface discoloration by increasing lipid and protein oxidation, thus instigating metmyoglobin formation (Bala et al., 1977). However, bacteria are rarely present in fresh beef as a monoculture; they exist as a community (Nychas et al., 2008; Hwang et al., 2020). To the authors' knowledge, the community effects of spoilage bacteria on fresh beef steak color stability during retail display have not been examined previously. Therefore, the objective of this study was to examine the effect of a mixture of common meat spoilage microorganisms on beef discoloration during aerobic retail display using color stable (LL) and color labile (PM) beef muscles.

Materials and Methods

Experimental design

Beef striploins and tenderloins obtained from a processing facility were wet-aged and then subjected to a surface decontamination process. The goal of the decontamination process was to reduce the existing microbial load on the surface of the loins, which, based on various beef slaughter, processing, and storage practices, can be highly variable. Standardization of the initial microbial contamination level amongst the

LL and PM loins and subsequently fabricated steaks allowed us to have two treatment groups, namely, (1) steaks with a low initial contamination level of the natural microflora (DCON treatment) and (2) steaks that were surface inoculated to a target initial concentration of ca. 4 log CFU/cm² with a 5-isolate mixture of common spoilage bacteria (INOC treatment). Steaks from LL and PM of both treatments were overwrapped and placed in a retail display case for up to 9 days. To determine the effects of microbial growth during retail display on surface discoloration, steaks were analyzed daily for microbial counts, instrumental color, and visual color. The experimental details are provided in the sections below.

Meat collection and processing

Eight ($n = 8$) USDA Choice striploins (LL) and tenderloins (PM) were collected from a commercial beef processing facility 24 h postmortem and wet-aged in individual vacuum bags (2°C) until 14 days postmortem. Muscles were selected from carcasses of similar age and background. After aging, the muscles were cut into halves (for ease of handling) and decontaminated by submerging them into a pot of boiling water for 2 min. Due to differences in size and fat coverage between LL and PM, the decontamination process was modified for PM to ensure internal temperatures did not exceed 4°C. For PM, the muscle was placed into boiling water for 1 min, removed for 30 sec, and then submerged into the boiling water for another 1 min, while LL was submerged in boiling water for 2 min continuously. The internal temperature of the muscles was monitored by inserting a thermometer (ThermaPen One, ThermoWorks, American Fork, UT) into the center and slightly beneath the surface to ensure that temperatures did not exceed 4°C during the decontamination process. The decontaminated muscles were aseptically trimmed,

removing the entire outer heat-exposed surface of each piece. The trimmed muscles were then aseptically cut into 0.5 in (1.27 cm) thick steaks, randomly assigned as decontaminated control (DCON) or inoculated (INOC), and placed onto soaker pad-lined foam trays.

Bacterial strains and inoculum preparation

The inoculum included three isolates of *Pseudomonas* spp. and two of lactic acid bacteria from our laboratory's culture collection. The isolates, all of which had been recovered from spoiled beef steaks, included *P. fragi* (CMSQ-SB3), *P. fluorescens* (CMSQ-SB4), *P. lundensis* (CMSQ-SB5), *Carnobacterium divergens* (CMSQ-SB1), and *Leuconostoc gelidum* (CMSQ-SB2). These particular bacterial species were included in the inoculum as they are commonly associated with spoilage in aerobically packaged beef steaks (Nychas et al., 2008; Wickramasinghe et al., 2019). The isolates, which were maintained as 15% glycerol stocks at -80°C, were individually revived prior to the start of the experiment by transferring a loopful of frozen culture into 10 mL of tryptic soy broth (TSB; Difco™; Becton, Dickinson, and Company, Sparks, MD). Following 24 h of incubation at 25°C, the TSB cultures were streak-plated onto tryptic soy agar (TSA; Neogen Culture Media, Lansing, MI) and incubated at 25°C for 72 h. A subsequent streak plate from a single colony from each original TSA plate was used as the working culture for the experiment.

For the purpose of inoculum preparation, a single colony from the TSA plate of each isolate was separately inoculated into 10 mL TSB and incubated at 25°C (24 h). Each strain was then subcultured (25°C, 24 h) by transferring a 0.1 mL aliquot of the broth culture to 10 mL of fresh TSB (designated as TSB2). Based on preliminary work

conducted to determine the cell concentration of each strain following the above culturing protocol, all strains except *P. fragi* reached a concentration of ca. 9 log CFU/mL in the TSB2 culture. The concentration of *P. fragi* was ca. 8 log CFU/mL. To ensure a similar representation of all five strains in the inoculum mixture used to inoculate the LL and PM samples, TSB2 cultures of *P. fluorescens*, *P. lundensis*, *C. divergens*, and *L. gelidum* were diluted 10-fold in phosphate-buffered saline (PBS; pH 7.4, Sigma-Aldrich, St. Louis, MO) to a ca. 8 log CFU/mL concentration. This dilution, as well as the undiluted TSB2 culture of *P. fragi*, were then combined and centrifuged (Sorvall Legend X1R, Thermo Scientific, Germany) at $6,000 \times g$ for 15 min at 4°C. The resulting bacterial cell pellet was washed with 10 mL PBS and centrifuged as described above. This washing step was repeated one additional time and after the second wash, the cell pellet was resuspended in 45 mL of PBS. This cell suspension (ca. 8 log CFU/mL) was then diluted tenfold in PBS, and the resulting cell suspension (ca. 7 log CFU/mL) was used to inoculate the meat samples. To determine the actual concentration of the individual strains before centrifugation and of the mixed cell suspension used to inoculate the meat samples, cell suspensions were tenfold diluted in maximum recovery diluent (MRD; Neogen Culture Media) and were plated, in duplicate, onto TSA.

Inoculation, packaging, and retail display

The upper surface of INOC steaks was inoculated with 0.15 mL of the spoilage bacteria inoculum. The cell suspension was deposited on the meat surface with a micropipette and then spread over the entire surface with a sterile disposable spreader. The inoculated samples were left undisturbed for 15 min to allow for bacterial cell attachment. For the DCON steaks, a 0.15 mL volume of PBS was deposited and spread

over the surface and also left for 15 min before packaging. Steaks were overwrapped (O_2 transmission = 23,250 mL x m² x d⁻¹, 72 gauge: Resinite Packaging Films, Borden, Inc., North Andover, MA) and placed into a multideck retail display case with continuous lighting at $3 \pm 1^\circ\text{C}$ (2800 lx, 1810LX4000 LED fixture; Kason, Newnan, GA; color rendering index = 84, color temperature = 4,500 K) for up to 9 days. Steaks were allowed to bloom for 2 h after wrapping before day 0 color assessment and microbial analysis. Additionally, steaks were rotated in the retail display case daily to ensure minimal impacts from temperature and lighting variance. In a pre-determined random order, one steak per loin per treatment (i.e., $n = 8$ each for LL INOC and DCON, and PM INOC and DCON), at $24 \text{ h} \pm 1 \text{ h}$ intervals were used to assess instrumental color, panelist visual color evaluation, and microbial population levels.

Instrumental color evaluation

Instrumental lightness (L^*), redness (a^*), and yellowness (b^*) were measured using a HunterLab MiniScan LabScan EZ4500 colorimeter (Hunter Associates Laboratory, Reston, VA), with a 2.54-cm diameter aperture with a 12.5 mm measurement port, illuminant A, and 10° standard observer (King et al., 2023). An average was taken of three random locations on the light-exposed surface of INOC or DCON steaks. The colorimeter was calibrated with the black and white tiles prior to use daily.

Visual color evaluation

Using a randomized survey tool (Qualtrics, Provo, UT), five to eight panelists assessed lean redness and percent surface discoloration. This work was approved by the Colorado State University Institutional Review Board (IRB#2929). A continuous lean redness color lexicon was adapted from King et al. (2023) with values ranging from 1 to

8 (e.g., 1 = extremely bright cherry red, 8 = extremely dark red). Percent discoloration was evaluated using a continuous scale from 0 – 100%. Results for both were reported as estimated marginal means and standard error on a per treatment by day basis.

Microbial analyses and bacterial growth kinetics

For LL, a 4 × 4 cm (16 cm²) surface section of steak, approximately 1 mm thick, was aseptically excised using a sterile template and scalpel, with care to ensure only the lean surface was removed. The sample was placed into a filter-separated sterile sample bag (710-mL; Whirl-Pak, Pleasant Prairie, WI), and 25 mL of MRD was added. For the PM samples, a 3 × 4 cm (12 cm²) section of the surface (to adjust for the smaller muscle dimensions of PM as compared to those of LL) was excised (approximately 1 mm thick) and 19 mL of MRD was added to the sample bag. Other than this difference in dimensions of the excised sample, PM and LL samples were further processed and analyzed for microbial counts the same. Bags containing excised meat samples were mechanically pummeled (Masticator, IUL Instruments, Barcelona, Spain) for 2 min, for bacterial cell detachment. The resulting homogenate was tenfold serially diluted and appropriate dilutions were surface-plated, in duplicate, on TSA (for aerobic plate counts; APC), and *Pseudomonas* agar base (Oxoid Ltd., Wake Road, Basingstoke, Hants, UK) supplemented with *Pseudomonas* CFC supplement (comprised of cetrimide, fucidin, and cephalosporin; Oxoid Ltd.) (for *Pseudomonas* spp. counts). Additionally, a pour plate overlay method was used with Lactobacilli MRS agar (MRS; Difco™; Becton, Dickinson and Company) to obtain lactic acid bacteria counts (LABC). Plates of all three culture media were incubated at 25°C for 72 h, followed by manual counting of colonies. Colony

counts were converted to log CFU/cm². The detection limit of the microbiological analysis was 0.2 log CFU/cm².

Estimated growth kinetic parameters of the bacterial populations recovered from LL and PM INOC samples were determined. The Baranyi and Roberts (1994) growth kinetics model was used to model the bacterial population data (log CFU/cm²) as a function of time, with the Microsoft Excel predictor plug-in DMFit (version 3.5), made publicly available from ComBase (<https://www.combase.cc>). This primary model characterizes growth kinetics based on four parameters: (1) lag phase duration, (2) maximum specific growth rate (μ_{\max}), (3) the lower asymptote corresponding to initial population counts (y_0 ; log CFU/cm²), and (4) the upper asymptote corresponding to maximum population counts (y_{end} ; log CFU/cm²).

Statistical analysis

Statistical analysis for instrumental color, microbial population enumerations, and visual color data was performed in R (version 4.2.2) using the lme4 (version 1.1.33) package for mixed models. The statistical analysis was performed within muscle only since it is known that beef LL and PM differ in their biochemical properties (McKenna et al., 2005). Therefore, separate but similar factorial models were created for LL and PM. Display day and treatment type (DCON and INOC) were considered the fixed effects for both LL and PM, and the interaction between display day and treatment was analyzed. Loin was used as a random variable. The lmerTest package (version 3.1.3) in R was used, and an analysis of variance (ANOVA) with a Kenward-Roger degrees of freedom adjustment. Estimated marginal means were calculated with the emmeans package (version 1.8.5) and used to make means comparisons for both interactions and main

effects where applicable. Tukey's multiple testing correction was applied, and the significance was set at $\alpha = 0.05$.

Results

Instrumental color evaluation

There was a treatment \times display day interaction ($P < 0.05$) for L^* (lightness) values of LL steaks (Table 1). The L^* values were similar ($P \geq 0.05$) for DCON and INOC until day 7, after which DCON had greater ($P < 0.05$) lightness values compared to INOC. Additionally, there was a treatment \times display day interaction ($P < 0.05$) for a^* and b^* values of LL. Initially, both DCON and INOC had similar ($P \geq 0.05$) redness (a^* values) until day 5, but on days 6 through 8, the a^* values for INOC were lower ($P < 0.05$) than those of DCON (Table 1).

There was no interaction between display day and treatment for PM for L^* values. However, there was a display day main effect ($P < 0.05$) for L^* values in PM, but there was no treatment effect ($P \geq 0.05$) between DCON and INOC (Figure 1). A treatment \times display day interaction ($P < 0.05$) was observed for a^* values of PM steaks (Table 2). Although there was no statistical difference, the DCON steaks had numerically higher redness (15.67 ± 1.01) than INOC steaks (11.64 ± 0.46) on day 4. However, the a^* values began to increase unexpectedly for INOC steaks during the later days of retail display. There was a treatment effect ($P < 0.05$) and display day effect ($P < 0.05$) for the b^* values of PM, but there was no interaction between them (Table 3). The DCON steaks had higher ($P < 0.05$) b^* values on day 0 compared to those of INOC, but on days 1 through 6, the b^* values of both treatments were similar ($P \geq 0.05$). On the last day, day 7, PM INOC samples had a lower ($P < 0.05$) b^* value than that of DCON (Table 3).

Visual color assessment

A treatment × display day interaction ($P < 0.05$) was observed for LL steaks for both lean color and surface discoloration (Table 4). The lean color was similar ($P \geq 0.05$) between the treatments until day 5, after which the INOC steaks were darker ($P < 0.05$) than DCON steaks. Percentage surface discoloration was similar ($P \geq 0.05$) between the treatments, with less than 5% for both DCON and INOC on days 0 through 4 (Table 4; Figure 2). On day 5, surface discoloration increased to 13.7% for the INOC steaks and steadily increased each day reaching nearly 80% discoloration by the end of the study. On the other hand, the discoloration score did not increase ($P \geq 0.05$) for the LL DCON steaks during the display period (Table 4).

Like LL, there was a treatment × display day interaction ($P < 0.05$) for lean color scores and surface discoloration for PM (Table 5). The lean color became darker ($P < 0.05$) throughout display for both treatments. Initially, treatments had similar ($P \geq 0.05$) surface discoloration, however, surface discoloration substantially increased ($P < 0.05$) for INOC steaks from 24.16% on day 3 to over 70% on days 4 and 5, while DCON did not display as sharp an increase (Table 5; Figure 3). By days 6 and 7, surface discoloration was again similar ($P \geq 0.05$) for both treatments on PM steaks.

Microbial populations

For all the bacterial count types assessed (APC, LABC, *Pseudomonas* spp. counts), there was a treatment × display day interaction ($P < 0.05$) for LL steaks (Table 6). Initial (day 0) levels of APC, LABC, and *Pseudomonas* spp. counts on the inoculated (INOC) steaks were 3.9, 3.6, and 3.5 log CFU/cm², respectively, while initial bacterial levels on DCON steaks were below the analysis detection limit (<0.2 log CFU/cm²)

regardless of bacterial count type. Bacterial counts of DCON steaks remained lower ($P < 0.05$) than those of INOC samples throughout the display period. By the end of display, APC, LABC, and *Pseudomonas* spp. counts on INOC LL steaks were 8.9, 6.7, and 8.9 log CFU/cm², respectively, whereas those on DCON samples were <2.7, <1.7, and <2.3 log CFU/cm², respectively (Table 6).

A treatment × display day interaction ($P < 0.05$) for all bacterial count types was also obtained for PM steaks, and as observed for LL samples, bacterial levels on INOC samples were greater ($P < 0.05$) than those of DCON samples throughout retail display (Table 7). On day 0, APC, LABC, and *Pseudomonas* spp. counts were <0.3, 0.2, and 0.2 log CFU/cm², respectively, on DCON PM steaks, and 4.0, 3.7, and 3.7 log CFU/cm², respectively, on INOC PM steaks. At the end of the display period, DCON steak bacterial levels were <3.4, 1.0, and 2.8 log CFU/cm² for APC, LABC, and *Pseudomonas* spp., respectively (Table 7). In comparison, bacterial levels of 9.3, 8.1, and 9.2 log CFU/cm² for APC, LABC, *Pseudomonas* spp. counts, respectively, were obtained on INOC PM samples.

Bacterial growth kinetics for INOC steaks

Bacterial growth kinetics parameters (Baranyi and Roberts, 1994) were only estimated for the bacterial populations recovered from the INOC treatment of LL and PM steaks. This analysis was not performed on the DCON microbial data because of the inconsistent occurrence of detectable increases in microbial counts on these steaks during the display period. As such, an accurate estimation of lag phase duration and maximum specific growth rates, when growth did occur, could not be calculated. Starting with LL, estimated lag phase durations for APC, *Pseudomonas* spp., and LABC

populations were 2.2, 1.5, and 3.3 days, respectively (Table 8). Conversely, there was no (i.e., <1 day) observed lag phase for APC, LABC, and *Pseudomonas* spp. populations for INOC PM steaks. Growth parameters for populations of all count types recovered from LL INOC steaks did show a slightly higher μ_{\max} compared with the populations recovered from PM INOC steaks (Table 8).

Discussion

Microbial growth and color stability of beef LL steaks

Beef LL muscle has been used in a plethora of fresh beef steak color stability studies due to its color stability (Joseph et al., 2012; Yu et al., 2017; Mancini et al., 2018; Ramanathan et al., 2021), which makes it one of the ideal muscles for examining the interaction between color and microbial growth. The a^* values for DCON LL steaks remained relatively steady throughout the display period, only ever getting below 25 on day 8 of display (Table 1), demonstrating that DCON steaks remained bright cherry-red throughout the study. Conversely, the redness values for the INOC LL samples declined through the display period dropping below 25 from day 5 onwards, and were well below the consumer acceptance level (Holman et al., 2017) on the last day of display. The decreased redness of INOC compared with DCON LL steaks indicates that the presence or absence of bacteria may be playing a critical role in color stability of beef LL during aerobic retail display. These results illustrate a connection between bacterial growth and surface discoloration for beef LL steaks in aerobic packaging. Similarly, Yang et al. (2016) indicated that an increase in *Pseudomonas* spp. count corresponded with a decrease in a^* values (redness) when highly marbled beef steaks were displayed in a 50% O₂ modified atmosphere packaging. In the present study, percent surface discoloration also

indicated that LL INOC steaks had greater surface discoloration compared to DCON starting from day 6 (Table 4; Figure 2).

Bacteria rapidly catabolize substrates and excrete waste products during the exponential phase of their growth curve (Nychas et al., 2008). Six days of retail display, in the current study, could have provided enough time for bacteria to enter the exponential phase of growth, begin to catabolize the steak for nutrients, and their metabolites to accumulate resulting in surface color deterioration. Their consumption of meat proteins and lipids, and the production of microbial metabolites ultimately lead to the deterioration of a steak's surface resulting in spoilage (Nychas et al., 2008), as observed in INOC steaks. In the current study, the bacterial growth kinetics results showed that there was an estimated 1.5 day lag phase duration for the *Pseudomonas* spp. compared to a 3.3 day lag phase for lactic acid bacteria (Table 8). This suggests that these populations entered the exponential phase of growth on days 1 and 3 for *Pseudomonas* spp. and lactic acid bacteria, respectively. Since the growth and resulting production of microbial metabolites greatly controls the shelf-life of fresh meat, the longer lag phase allows for a longer shelf-life because bacteria are minimally metabolically active during the lag phase (Nychas et al., 2008).

Microbial growth and color stability of beef PM steaks

The color labile nature of PM steaks has been well documented (Seyfert et al., 2006; Joseph et al., 2012; Mancini et al., 2018; Ramanathan et al., 2021), and is routinely used as a color labile muscle model in beef color research. Alongside metmyoglobin formation on the surface of PM steaks, the redness decreases rapidly (Joseph et al., 2012; Mancini et al., 2018), which results in PM displaying a relatively short shelf-life.

Initially, the a^* values (redness) of PM steaks of both treatments were similar and remained so until day 6 of display, after which, the redness of INOC steaks increased compared to DCON (Table 2). Najjar-Villarreal et al. (2021) conducted a meta-analysis and reported that the estimated consumer acceptable a^* value for PM was 20.99. Based on this, the level of redness of the steaks of both treatments in the current study may have dropped below levels acceptable to consumers by day 2 of display. Additionally, the percentage discoloration was much higher for INOC steaks (70.40%) compared to DCON steaks (26.19%) on day 4 of the retail display (Table 5; Figure 3) indicating that the INOC steaks discolored faster than the DCON steaks. The deterioration in lean color for both treatments with time was anticipated and agrees with previously reported data for beef PM color during retail display (Seyfert et al., 2006; Nair et al., 2018). However, the faster rate of discoloration on INOC PM steaks was a new finding, as far as the authors are aware. By day 4, there was an approximate 7 log CFU difference in APCs between INOC and DCON PM steaks (Table 7), and the bacterial populations on INOC samples had been in exponential growth for more than 4 days. Further, considering the much higher a^* values and lower surface discoloration for DCON versus INOC for PM steaks, it is reasonable to suggest that bacterial growth plays a role in surface color stability and discoloration.

Although there was not a statistical difference in a^* values between the DCON and INOC PM steaks on days 4 and 5, the a^* values were numerically lower for INOC steaks during these two days. Interestingly, on days 6 and 7, the a^* value of PM INOC steaks increased compared to the previous day's INOC a^* values and to PM DCON steaks at the same time point (Table 2). It is noteworthy that the increase in a^* values during the

later portion of the retail display on INOC PM steaks coincided with slime formation on the surface of the steaks, and has been reported previously (Motoyama et al., 2010). According to a study by Ayres (1960), bacterial slime formation on beef occurs when populations reach a concentration of 7-8 log CFU, which was reached around day 4 for PM INOC steaks in the current study (Table 7). Despite the increased redness of INOC steaks, when evaluating the decline in a^* values of DCON steaks by display day, it is apparent that DCON steaks remained redder compared to INOC PM steaks until the point of slime formation. Furthermore, the surface discoloration percentage was greater for PM INOC steaks compared to PM DCON steaks on days 4 and 5 (Table 5). In summary, these data showed the PM DCON steaks decreased in redness, but had much less surface discoloration compared to PM INOC steaks.

The bacterial growth kinetics estimated using the Baranyi and Roberts (1994) primary model showed that there was not a measurable lag phase duration (i.e., <1 day) for the bacterial populations recovered from the INOC PM steaks. As previously mentioned, bacteria in the lag phase have substantially reduced metabolic activity and are not catabolizing much of their growing medium and not producing high quantities of metabolites (Nychas et al., 2008). However, with the short lag phase, bacteria on PM steaks could be rapidly catabolizing nutrients from the steak and producing metabolic waste. This is a similar finding as reported in Smith et al. (2024), where the authors reported a less than 24 h lag time for naturally occurring bacteria on aerobically packaged beef PM steaks, similar to the current study. The lack of a detectable bacterial lag phase suggests that PM is a very suitable substrate for microbial growth, and within a few days of growth, deleterious effects on color are observed, similar to the effects of growth

observed in LL. This is highly suggestive that muscle specificity, specifically the PM and its biochemical properties, are interwoven with the negative consequences of microbial growth.

Qualitative comparison of LL and PM steaks

As the purpose of this study was not to compare the color stability of beef LL and PM, which has been done previously (Seyfert et al., 2006; Ramanathan et al., 2021; Smith et al., 2024), we did not perform statistical comparisons between these two muscles. However, comparing these color stable and color labile muscle models qualitatively could provide insights into the interaction between bacterial growth and differential color stabilities of these muscles. In this study, PM was used as the color labile model and LL was the color stable model. Generally, color labile muscles have a greater percentage of type I muscle fibers resulting in higher mitochondrial density which contributes to a greater oxygen consumption rate, thus decreasing the color stability (McKenna et al., 2005). Without considering microbial influence, muscles similar to PM may be more biochemically pre-disposed to discolor rapidly compared to the color stable muscles such as LL. However, based on the results of the current study, it is reasonable to speculate that muscles more intrinsically predisposed to rapid bacterial growth (such as PM), would have a much more rapid decrease in color stability, compared to muscles that are color stable and facilitate slower microbial growth such as LL.

The bacterial growth kinetics could also have had a role in the differential shelf-life of these two muscles. Bacterial populations on INOC PM samples experienced an estimated lag phase of less than 1 day and entered the exponential phase faster than populations on INOC LL samples (Table 8). Further, INOC PM samples experienced

discoloration at a considerable percentage of the steak surface after day 3 of the retail display (Tables 5 and 8). In LL, bacterial populations had a lag phase of approximately 2-3 days, and surface discoloration began 3 days after entering the lag phase (day 6 of retail display; Tables 4 and 8, respectively).

Regardless of muscle, once bacterial growth commenced during retail display, higher levels of *Pseudomonas* spp. were recovered than those of lactic acid bacteria. The dominance of *Pseudomonas* spp. in aerobically stored meat is not a new finding (Molin and Ternström, 1982; Labadie, 1999; Koutsoumanis et al., 2006). In the current study, *Pseudomonas* spp. and lactic acid bacteria were introduced onto the meat surface at similar levels (Tables 6 and 7). The predominance of *Pseudomonas* spp. could have been a driving force in the difference in color stability between the treatments (Bala et al., 1977; Chan et al., 1998). In fact, the greater surface discoloration and lower redness for INOC steaks compared to DCON steaks observed in the current study could be attributed to the aerobic *Pseudomonas* spp. growth. Steaks with higher microbial loads could also have greater lipid and protein oxidation compared with steaks of lower microbial populations (Robach and Costilow, 1961; Bala et al., 1977), which could have resulted in the color differences due to myoglobin oxidation (Faustman et al., 2010).

Conclusions

The results of this study demonstrated the impact of microbial growth on the color stability of beef LL and PM during retail display. The differences in bacterial growth kinetics between LL and PM could be playing a role in the muscle-specific color stability discrepancy between these muscles, although more research is needed. In general, the spoilage bacteria mixture used in this study grew faster on PM, compared with LL,

indicating that PM provides a highly hospitable environment for bacterial growth, which could be contributing to its rapid discoloration. These findings demonstrated that the role of microbial growth on fresh beef color should be further investigated and must be considered in fresh beef color stability research.

Table 2.1. Marginal means \pm standard error of CIE L^* (lightness), a^* (redness), and b^* (yellowness) of decontaminated (DCON) and inoculated (INOC) treatment groups of beef *longissimus lumborum* steaks ($n = 8$) during simulated retail display (3°C).

Day	L^* value		a^* value		b^* value	
	DCON	INOC	DCON	INOC	DCON	INOC
0	39.61 \pm 0.59 ^a	39.45 \pm 0.60 ^a	28.09 \pm 0.61 ^{abcde}	27.78 \pm 0.47 ^{bcde}	21.90 \pm 0.54 ^{cd}	21.52 \pm 0.44 ^{cd}
1	38.75 \pm 0.68 ^{abc}	38.80 \pm 1.31 ^{abc}	28.97 \pm 0.50 ^{abcd}	29.50 \pm 0.57 ^{abc}	23.87 \pm 0.57 ^{cd}	24.45 \pm 0.54 ^{bc}
2	38.08 \pm 1.04 ^{abc}	39.05 \pm 0.90 ^{ab}	28.53 \pm 0.86 ^{abcde}	28.18 \pm 0.52 ^{abcde}	24.04 \pm 0.18 ^{cd}	22.93 \pm 0.65 ^{cd}
3	35.27 \pm 1.05 ^{bcd}	35.22 \pm 1.03 ^{bcde}	32.26 \pm 1.19 ^a	31.07 \pm 1.05 ^{ab}	28.82 \pm 1.27 ^a	27.63 \pm 1.05 ^{ab}
4	38.45 \pm 0.70 ^{abc}	39.14 \pm 1.01 ^a	28.14 \pm 0.52 ^{abcde}	26.74 \pm 0.64 ^{cde}	22.91 \pm 0.49 ^{cd}	22.09 \pm 0.68 ^{cd}
5	36.62 \pm 0.62 ^{abcd}	35.89 \pm 0.73 ^{abcd}	26.63 \pm 0.69 ^{cde}	24.80 \pm 0.94 ^{de}	22.25 \pm 0.72 ^{cd}	21.17 \pm 0.85 ^d
6	37.70 \pm 0.90 ^{abc}	38.12 \pm 0.94 ^{abc}	25.71 \pm 0.91 ^{cde}	15.50 \pm 1.10 ^{fg}	21.24 \pm 0.73 ^d	16.08 \pm 0.83 ^e
7	33.55 \pm 0.76 ^{de}	31.40 \pm 1.53 ^e	31.37 \pm 0.99 ^{ab}	18.04 \pm 2.16 ^f	28.94 \pm 0.83 ^a	22.77 \pm 1.12 ^{cd}
8	39.44 \pm 0.97 ^a	35.11 \pm 1.49 ^{cde}	24.66 \pm 0.75 ^e	12.38 \pm 0.63 ^g	21.00 \pm 0.75 ^d	14.77 \pm 0.53 ^e

^{a-g}Marginal means within the same measurement without a common superscript letter are different ($P < 0.05$).

Table 2.2. Marginal means \pm standard error of CIE a^* (redness) of decontaminated (DCON; $n = 8$) and inoculated (INOC; $n = 8$) treatment groups of beef *psoas major* steaks during simulated retail display (3°C).

Day	DCON	INOC
0	27.98 \pm 1.21 ^a	28.45 \pm 0.17 ^a
1	24.63 \pm 0.65 ^a	24.50 \pm 0.36 ^{ab}
2	20.41 \pm 0.61 ^{bc}	20.00 \pm 0.53 ^c
3	17.65 \pm 0.78 ^{cde}	17.16 \pm 0.78 ^{cde}
4	15.67 \pm 1.01 ^{def}	11.68 \pm 0.46 ^f
5	15.37 \pm 0.81 ^{def}	12.28 \pm 0.48 ^f
6	14.09 \pm 1.52 ^{ef}	14.45 \pm 0.93 ^{ef}
7	14.80 \pm 1.55 ^{ef}	18.97 \pm 1.35 ^{cd}

^{a-f}Marginal means without a common superscript letter are different ($P < 0.05$).

Table 2.3. Marginal means \pm standard error of CIE b^* (yellowness) of decontaminated (DCON; $n = 8$) and inoculated (INOC; $n = 8$) treatment groups of beef *psoas major* steaks during simulated retail display (3°C).

Day	DCON	INOC
0	24.77 \pm 1.08 ^{aw}	22.68 \pm 0.25 ^{bv}
1	21.30 \pm 0.36 ^{ax}	21.18 \pm 0.23 ^{awv}
2	18.88 \pm 0.65 ^{ayx}	18.87 \pm 0.55 ^{axw}
3	18.46 \pm 0.59 ^{azy}	17.76 \pm 0.56 ^{ayx}
4	16.30 \pm 0.66 ^{az}	15.59 \pm 0.38 ^{azy}
5	16.23 \pm 0.68 ^{az}	15.6 \pm 0.83 ^{azy}
6	16.22 \pm 0.64 ^{az}	15.12 \pm 0.70 ^{az}
7	19.05 \pm 0.49 ^{ayx}	17.01 \pm 0.44 ^{bzyx}

^{a-b}Within each row and within the same measurement, means without a common superscript letter are different ($P < 0.05$).

^{z-v}Marginal means in the same column without a common superscript letter are different ($P < 0.05$).

Table 2.4. Marginal means \pm standard error of panelist lean color and percentage discoloration of decontaminated (DCON; $n = 8$) and inoculated (INOC; $n = 8$) treatment groups of beef *longissimus lumborum* steaks during simulated retail display (3°C).

Day	Lean Color ¹		% Discoloration	
	DCON	INOC	DCON	INOC
0	1.67 \pm 0.05 ^j	1.67 \pm 0.03 ^j	0.00 \pm 0.00 ^c	0.02 \pm 0.02 ^c
1	1.77 \pm 0.07 ^{ij}	1.75 \pm 0.08 ^{ij}	0.00 \pm 0.00 ^c	0.16 \pm 0.16 ^c
2	2.34 \pm 0.17 ^{hij}	2.40 \pm 0.13 ^{hi}	1.39 \pm 0.24 ^c	1.29 \pm 0.10 ^c
3	2.95 \pm 0.17 ^{gh}	3.22 \pm 0.18 ^{fg}	0.51 \pm 0.27 ^c	1.04 \pm 0.74 ^c
4	3.72 \pm 0.25 ^{ef}	3.86 \pm 0.21 ^{def}	1.81 \pm 1.54 ^c	3.53 \pm 2.30 ^c
5	3.72 \pm 0.28 ^{ef}	4.16 \pm 0.21 ^{de}	1.76 \pm 0.85 ^c	13.70 \pm 2.49 ^c
6	3.88 \pm 0.23 ^{def}	4.92 \pm 0.12 ^c	1.28 \pm 0.82 ^c	38.03 \pm 3.61 ^b
7	4.31 \pm 0.22 ^{cde}	5.64 \pm 0.16 ^b	9.59 \pm 6.22 ^c	69.25 \pm 7.77 ^a
8	4.55 \pm 0.21 ^{cd}	6.60 \pm 0.26 ^a	6.11 \pm 2.69 ^c	79.74 \pm 3.60 ^a

^{a-j}Marginal means within the same measurement without a common superscript letter are different ($P < 0.05$).

¹Panelists scored each steak to assess lean color using a continuous 8-point scale (1 = extremely bright cherry-red, 2 = bright cherry-red, 3 = moderately bright cherry-red, 4 = slightly bright cherry-red, 5 = slightly dark cherry-red, 6 = moderately dark red, 7 = dark red, 8 = extremely dark red).

Table 2.5. Marginal means \pm standard error of panelist lean color and percentage discoloration of decontaminated (DCON; $n = 8$) and inoculated (INOC; $n = 8$) treatment groups of beef *psaos major* steaks during retail display (3°C).

Day	Lean Color ¹		% Discoloration	
	DCON	INOC	DCON	INOC
0	4.17 \pm 0.22 ^g	4.07 \pm 0.26 ^g	0.00 \pm 0.00 ^e	0.10 \pm 0.07 ^e
1	4.88 \pm 0.29 ^{fg}	4.91 \pm 0.17 ^{fg}	9.67 \pm 5.41 ^{de}	1.09 \pm 0.51 ^e
2	5.53 \pm 0.15 ^{ef}	5.64 \pm 0.25 ^{def}	11.82 \pm 2.39 ^{de}	16.86 \pm 4.33 ^{de}
3	5.99 \pm 0.23 ^{bcde}	5.67 \pm 0.19 ^{def}	13.96 \pm 3.60 ^{de}	24.16 \pm 7.73 ^{de}
4	5.99 \pm 0.18 ^{bcde}	5.70 \pm 0.30 ^{def}	26.19 \pm 7.07 ^{cde}	70.40 \pm 11.22 ^{ab}
5	5.88 \pm 0.23 ^{cde}	6.79 \pm 0.10 ^{abc}	39.50 \pm 7.69 ^{bcd}	82.38 \pm 6.68 ^a
6	6.53 \pm 0.22 ^{abcd}	6.90 \pm 0.17 ^{ab}	58.78 \pm 11.03 ^{abc}	68.10 \pm 8.25 ^{ab}
7	7.10 \pm 0.21 ^a	7.11 \pm 0.08 ^a	74.89 \pm 12.00 ^a	69.06 \pm 5.65 ^{ab}

^{a-g}Marginal means within the same measurement without a common superscript letter are different ($P < 0.05$).

¹Panelists scored each steak to assess lean color using a continuous 8-point scale (1 = extremely bright cherry-red, 2 = bright cherry-red, 3 = moderately bright cherry-red, 4 = slightly bright cherry-red, 5 = slightly dark cherry-red, 6 = moderately dark red, 7 = dark red, 8 = extremely dark).

Table 2.6. Marginal mean \pm standard deviation (log CFU/cm²) of aerobic plate counts (APC), lactic acid bacteria counts (LABC), and *Pseudomonas* spp. counts recovered from decontaminated (DCON; $n = 8$) and inoculated (INOC; $n = 8$) treatment groups of beef *longissimus lumborum* steaks during simulated retail display (3°C).

Day	APC		LABC		<i>Pseudomonas</i> spp.	
	DCON	INOC	DCON	INOC	DCON	INOC
0	<0.2±0.1 ^{g*}	3.9±0.1 ^{cd}	<0.2±0.0 ^e	3.6±0.2 ^c	<0.2±0.0 ^f	3.5±0.1 ^d
1	<0.2±0.0 ^g	3.9±0.1 ^{cd}	<0.2±0.1 ^e	3.5±0.1 ^c	<0.2±0.0 ^f	3.7±0.1 ^d
2	<0.3±0.2 ^g	4.4±0.4 ^c	<0.3±0.2 ^e	3.5±0.2 ^c	<0.2±0.0 ^f	4.4±0.4 ^{cd}
3	<0.9±1.2 ^{fg}	5.1±0.3 ^{bc}	<0.7±1.2 ^{de}	3.5±0.2 ^c	<0.3±0.4 ^f	5.1±0.3 ^c
4	<0.4±0.3 ^g	5.8±0.6 ^b	<0.4±0.4 ^e	4.0±0.6 ^c	<0.2±0.0 ^f	6.3±0.5 ^b
5	NA ¹	NA	NA	NA	NA	NA
6	<0.8±1.0 ^{fg}	8.3±0.6 ^a	<0.8±1.0 ^{de}	5.5±0.4 ^b	<0.2±0.0 ^f	8.3±0.6 ^a
7	<1.7±1.7 ^{ef}	8.7±0.4 ^a	<1.3±1.2 ^{de}	6.1±0.4 ^{ab}	<1.2±1.8 ^{ef}	8.7±0.4 ^a
8	<2.7±1.4 ^{de}	8.9±0.4 ^a	<1.7±1.7 ^d	6.7±0.3 ^a	<2.3±1.5 ^e	8.9±0.4 ^a

^{a-f}Marginal means within the same count type without a common superscript letter are different ($P < 0.05$).

*Marginal means with a less than symbol (<) indicate one or more of the samples within the treatment had plate counts below the analysis detection limit (0.2 log CFU/cm²).

¹Observed data for day 5 not available due to laboratory error.

²Observed data for day 5 not available due to laboratory error; values for INOC were estimated using the Biogrowth package (version 1.0.4) in R (version 4.2.2).

Table 2.7. Marginal mean \pm standard deviation (log CFU/cm²) of aerobic plate counts (APC), lactic acid bacteria counts (LABC), and *Pseudomonas* spp. counts recovered from decontaminated (DCON; $n = 8$) and inoculated (INOC; $n = 8$) treatment groups of beef *psoas major* steaks during simulated retail display (3°C).

Day	APC		LABC		<i>Pseudomonas</i> spp.	
	DCON	INOC	DCON	INOC	DCON	INOC
0	<0.3±0.3 ^{i*}	4.0±0.1 ^f	0.2±0.0 ^g	3.7±0.1 ^f	0.2±0.0 ⁱ	3.7±0.1 ^f
1	<0.2±0.0 ⁱ	4.5±0.3 ^{ef}	0.2±0.0 ^g	4.0±0.2 ^{ef}	0.2±0.0 ⁱ	4.3±0.3 ^{ef}
2	<0.3±0.4 ⁱ	5.6±0.5 ^{de}	0.2±0.0 ^g	4.8±0.5 ^{de}	0.2±0.0 ⁱ	5.6±0.4 ^{de}
3	<1.0±1.0 ^{hi}	6.9±0.5 ^{cd}	0.5±1.0 ^g	5.4±0.5 ^d	0.3±0.4 ^{hi}	6.9±0.4 ^{cd}
4	<0.6±0.8 ^{hi}	7.7±0.4 ^{bc}	0.2±0.0 ^g	5.9±0.4 ^{cd}	0.5±0.6 ^{hi}	7.7±0.4 ^{bc}
5	<1.1±1.3 ^{hi}	8.5±0.4 ^{ab}	0.2±0.0 ^g	6.7±0.5 ^{bc}	1.0±1.3 ^{hi}	8.5±0.4 ^{ab}
6	<2.1±2.1 ^{gh}	9.0±0.3 ^{ab}	0.9±1.2 ^g	7.5±0.5 ^{ab}	1.8±2.2 ^{gh}	9.0±0.3 ^{ab}
7	<3.4±2.1 ^{fg}	9.3±0.5 ^a	1.0±1.6 ^g	8.1±0.7 ^a	2.8±2.3 ^{fg}	9.2±0.4 ^a

^{a-i}Marginal means within the same measurement without a common superscript letter are different ($P < 0.05$).

*Marginal means with a less than symbol (<) indicate one or more of the samples within the treatment had plate counts below the analysis detection limit (0.2 log CFU/cm²).

Table 2.8. Estimated growth kinetic parameters, derived from the Baranyi and Roberts (1994) model, of bacterial populations recovered from inoculated beef *longissimus lumborum* (LL; $n = 8$) and *psaos major* (PM; $n = 8$) steaks during simulated retail display (3°C).

Bacterial count type	Muscle	Growth parameters				R ²
		Lag phase duration (days ± SE)	Maximum specific growth rate (μ_{\max} ; days ⁻¹ ± SE)	Y ₀ (log CFU/cm ²) ^a	Y _{end} (log CFU/cm ²) ^b	
APC	LL	2.2±0.3	1.175±0.114	3.9	8.9	0.958
	PM	- ^c	0.975±0.038	3.8	9.3	0.958
LABC	LL	3.3±0.3	0.715±0.056	3.5	- ^d	0.939
	PM	-	0.644±0.025	3.5	-	0.913
<i>Pseudomonas</i> spp.	LL	1.5±0.3	1.120±0.098	3.5	8.8	0.968
	PM	-	1.050±0.037	3.5	9.2	0.968

APC: Aerobic plate count populations; LABC: Lactic acid bacteria count populations; SE: standard error

^aLower asymptote estimated by the Baranyi and Roberts (1994) model.

^bUpper asymptote estimated by the Baranyi and Roberts (1994) model.

^cNo lag phase observed.

^dNo upper asymptote observed.

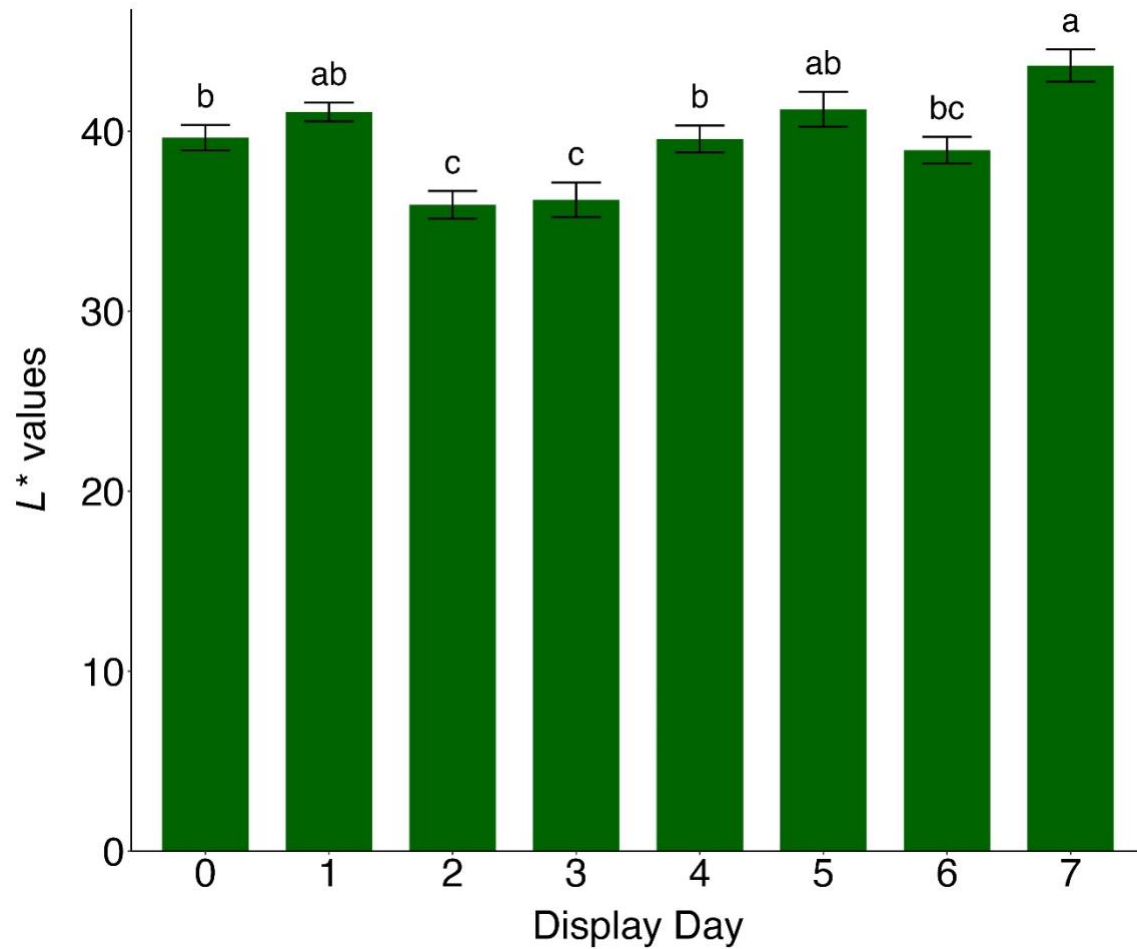


Figure 2.1. Marginal means \pm standard error of CIE L^* (lightness) of beef *psoas major* steaks ($n = 8$) from both decontaminated and inoculated treatments averaged by display day during simulated retail display (3°C).

^{a-c}Bars without a common letter are different ($P < 0.05$).

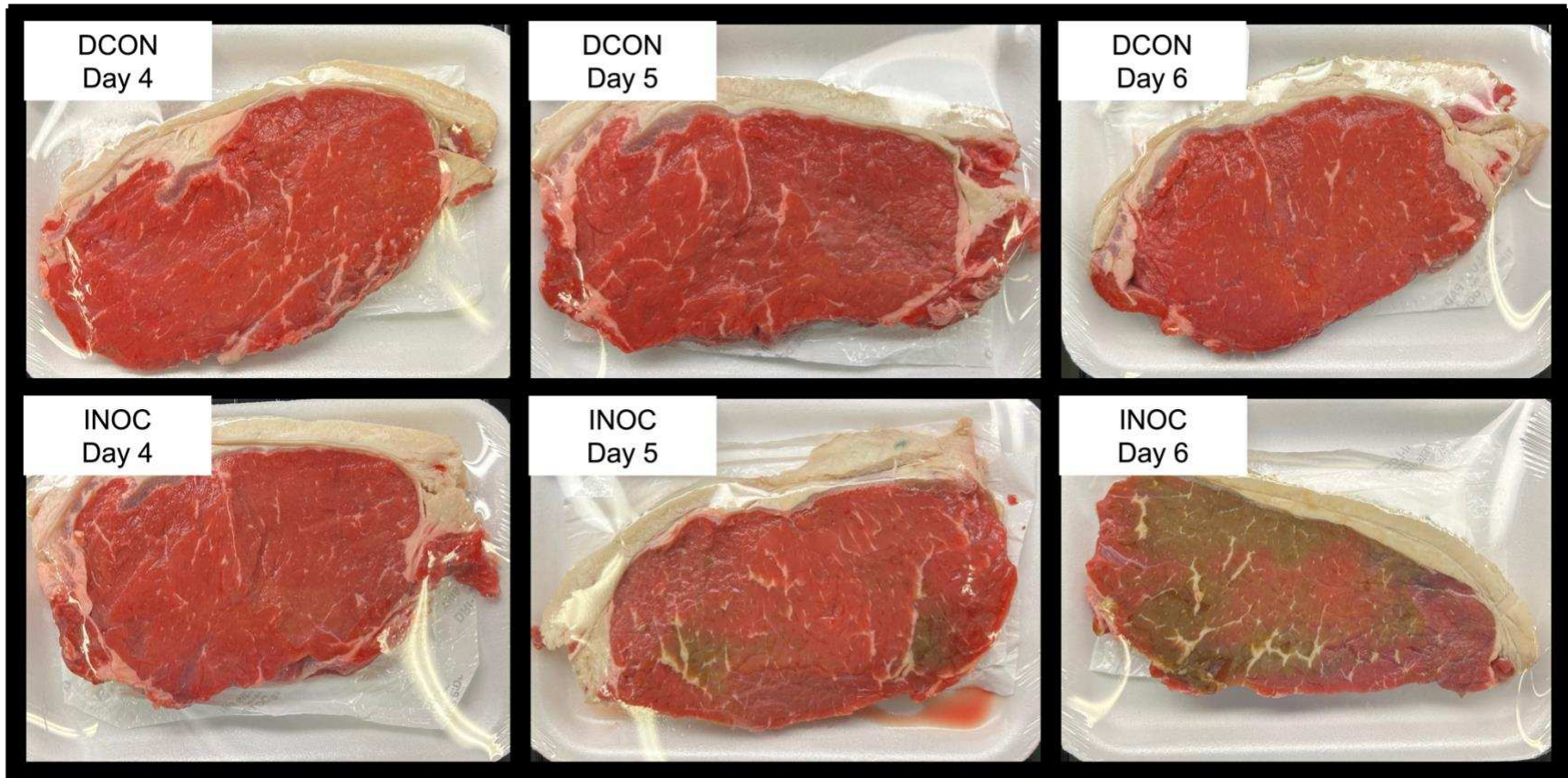


Figure 2.2. Representative images of beef *longissimus lumborum* steaks fabricated from the same striploin over a 3 day retail display period (days 4 to 6) showing the impact of microbial growth on color stability. Decontaminated controls (DCON; top row), and steaks inoculated with a five-isolate spoilage bacteria mixture at ca. 4 log CFU/cm² (INOC; bottom row) are from the same time points during simulated retail display at 3°C.

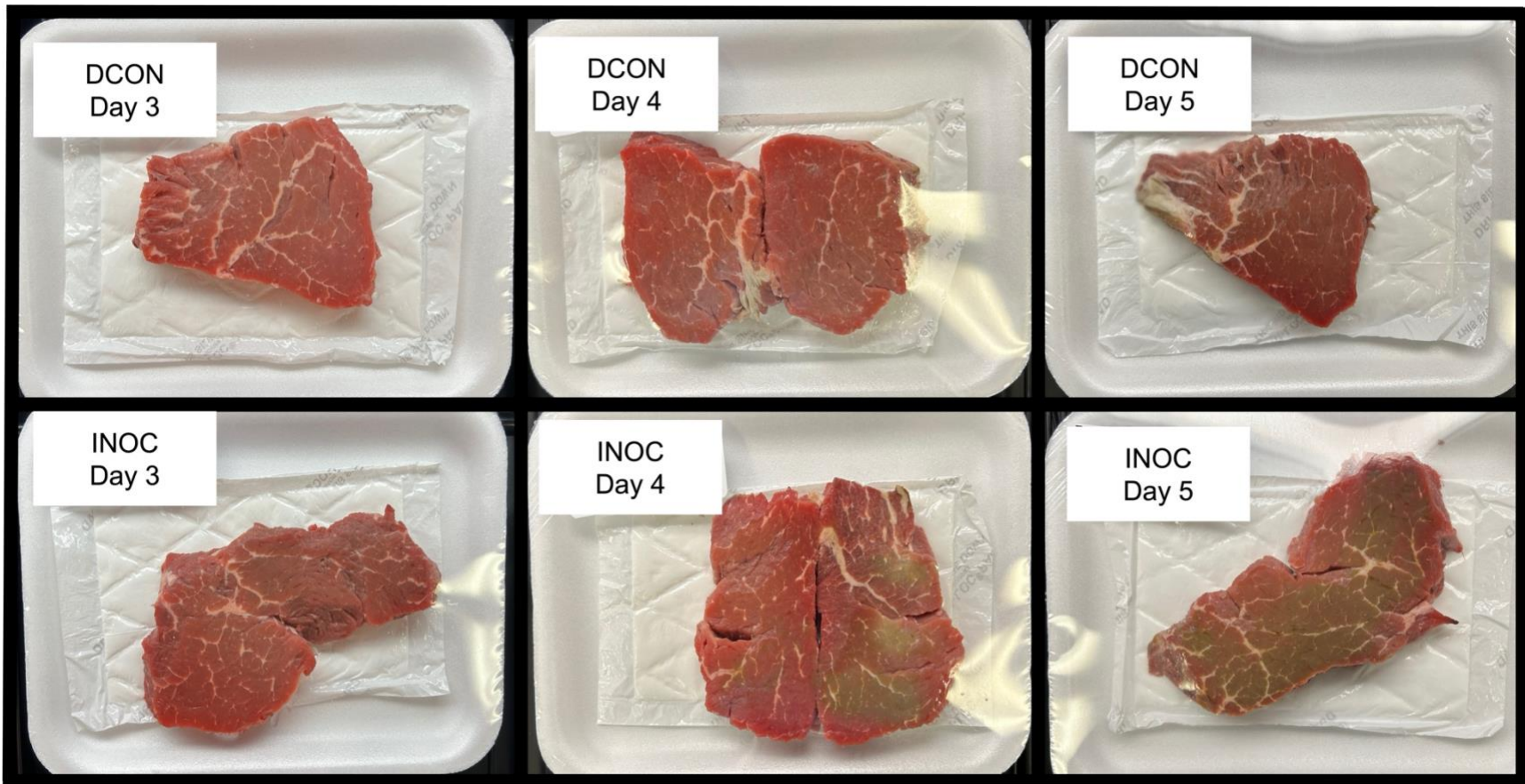


Figure 2.3. Representative images of beef *psoas major* steaks fabricated from the same tenderloin over a 3 day retail display period (days 3 to 5) showing the impact of microbial growth on color stability. Decontaminated controls (DCON; top row), and steaks inoculated with a five-isolate spoilage bacteria mixture at ca. 4 log CFU/cm² (INOC; bottom row) are from the same time points during simulated retail display at 3°C.

CHAPTER 3: INVESTIGATING THE FUNCTION OF SPOILAGE BACTERIA ON FRESH BEEF *LONGISSIMUS LUMBORUM* STEAK DISCOLORATION DURING AEROBIC RETAIL DISPLAY THROUGH A MULTI-OMIC APPROACH

Introduction

It is well regarded that meat color is the main criterion consumers use when making fresh red meat purchase decisions, and consumers often choose not to purchase discolored meat (Font-i-Furnols and Guerrero, 2014). Recently, Theis et al. (2024) reported that consumers' willingness to pay decreases with an increase in the number of days of retail display on fresh beef LL steaks. These meat color preferences result in significant economic losses to the beef industry (Ramanathan et al., 2022), estimated to be as high as \$3.7 billion annually. Therefore, improving and increasing fresh red meat color stability is a critical requirement to reduce food waste.

Bacteria are ubiquitous in the environment and are endemic on fresh meat. In fact, bacteria associated with fresh meat spoilage have evolved to grow in cold temperatures, may have developed more flexible oxygen requirements, and increased robustness to sanitation (Nychas et al., 2008; Comi, 2017). Several factors, including food animal harvest procedures, antimicrobial interventions, facility and employee hygiene, and packaging, can impact the bacterial load and composition existing on fresh meat. There are a few bacterial species that are typically associated with meat spoilage. Specifically, in fresh beef, species of *Pseudomonas*, lactic acid bacteria, and potentially *Enterobacteriaceae* have been identified as contributing to spoilage (Nychas et al., 2008). Although it is important to note that in aerobic environments (e.g., overwrap packaging and high oxygen modified atmosphere packaging) aerobic genera such as

Pseudomonas may have a competitive advantage compared to facultative anaerobes such the lactic acid bacteria, which typically predominate in vacuum packaging and other low oxygen environments (Nychas et al., 2008; Wickramasinghe et al., 2019). While bacterial growth can result in desired changes in foods such as yogurts, cheeses, and fermented sausages (Jones, 2004; Leroy and De Vuyst, 2004; Gänzle, 2015), their growth in fresh meat can produce less than desirable impacts, including malodorous compounds and changes to the meat's appearance (Casaburi et al., 2015; Bekhit et al., 2021).

Previous work has indicated an association between myoglobin oxidation state and *Pseudomonas fluorescens* in vitro (Chan et al., 1998), suggesting that *P. fluorescens* could accelerate beef discoloration. Recently, Smith et al. (2024) showed that microbial growth directly results in discoloration of fresh beef *longissimus lumborum* (LL) steaks during aerobic retail display. Despite knowledge that bacteria are involved in meat discoloration, to our knowledge, a thorough investigation into the bacterial mechanisms that may result in meat discoloration has not been conducted. Prior investigations of the functional roles of spoilage bacteria have utilized more traditional laboratory and chemical based methods such as culturing and media manipulation (Gill, 1983; Nychas et al., 1988; Papadopoulou et al., 2020). Results from these studies have indicated potential changes in bacterial metabolism during spoilage and suggested that changes in bacterial utilization of meat derived glucose could be a key driver in meat spoilage. Newer methods, including microbiome and metabolomics, have greater potential to help elucidate potential microbial mechanisms involved in meat discoloration. Therefore, the aim of this study was to investigate the functional role of

bacteria growing on fresh beef during retail display, utilizing a combination of traditional and multi-omics approaches.

Materials and Methods

Experimental design

Beef striploins were obtained from a processing facility and wet-aged for 14 d before a surface decontamination process. The decontamination process reduced the microbial load on the surface of the meat and resulted in a standardized microbial load across the striploins. Decontaminated loins were then fabricated into 1-cm thick steaks and half of the steaks were designated as (1) steaks with a low initial contamination level of the natural microbiota (DCON treatment) and (2) steaks that were surface inoculated to a target initial concentration of ca. 4 log CFU/cm² with a 6-isolate mixture of common meat spoilage bacteria (INOC treatment). Steaks from both treatments were then packaged and placed into retail display for up to 8 days. One steak per treatment per loin was analyzed on each retail display day, with $n = 10$ per treatment. The process was divided into two trials ($n = 5$ /trial).

Meat collection and processing

Ten USDA Choice striploins (LL) were collected from a commercial beef processing facility from carcasses of similar age and background, at 24 h postmortem in two trials (five LL per trial, $n = 10$ total). Individual striploins were then wet-aged for 14 days postmortem at 3°C. After aging, the LL was divided into halves and submerged in boiling water for 2 min to reduce natural microbial levels. The decontaminated pieces of LL were then drip dried and then aseptically trimmed to remove all of the heat-exposed surface. Our laboratory previously determined that the internal temperature of the whole

muscle is not affected by the 2 min exposure to boiling water. Each LL half was then cut into 1-cm thick steaks, randomized, placed onto a soaker pad-lined foam tray, and assigned a treatment group. The treatments were either DCON (decontaminated but not inoculated) or INOC (decontaminated and then inoculated).

Bacterial strains and inoculum preparation

The inoculum consisted of three *Pseudomonas* spp. and three lactic acid bacteria isolates from our laboratory's culture collection; all recovered from spoiled beef steaks. These included *P. fragi* (CMSQ-SB3), *P. fluorescens* (CMSQ-SB4), *P. lundensis* (CMSQ-SB5), *Carnobacterium divergens* (CMSQ-SB1), *Leuconostoc gelidum* (CMSQ-SB2), and *Lactobacillus sakei* (CMSQ-SB26). We selected these species because they are commonly associated with spoilage in aerobically packaged beef steaks (Nychas et al., 2008; Wickramasinghe et al., 2019). Isolates, maintained as 15% glycerol stocks at -80°C, were revived before the experiment by transferring a loopful of frozen culture into 10 mL of tryptic soy broth (TSB; Difco™, Becton, Dickinson, and Company, Sparks, MD). After 24 h at 25°C, TSB cultures were streak-plated onto tryptic soy agar (TSA; Neogen Culture Media, Lansing, MI) and incubated at 25°C for 72 h. A subsequent streak plate from a single colony of each original TSA plate served as the working culture.

To prepare the inoculum, a single colony from each isolate's TSA plate was inoculated into 10 mL TSB and incubated at 25°C for 24 h. Subsequently, each strain underwent subculturing (25°C, 24 h) by transferring a 0.1 mL aliquot of the broth culture to 10 mL of fresh TSB, which we designated as TSB2. Based on preliminary studies to determine cell concentrations, all strains except *P. fragi* achieved a concentration of

approximately 9 log CFU/mL in the TSB2 culture; *P. fragi* reached approximately 8 log CFU/mL. To ensure a consistent representation of all six strains in the final inoculum mixture for inoculation of the LL samples, TSB2 cultures of *P. fluorescens*, *P. lundensis*, *C. divergens*, *L. gelidum*, and *L. sakei* were diluted 10-fold in phosphate-buffered saline (PBS; pH 7.4, Sigma-Aldrich, St. Louis, MO) to achieve a concentration of approximately 8 log CFU/mL.

This diluted mixture, along with the undiluted *P. fragi* TSB2 culture, was then combined and centrifuged using a Sorvall Legend X1R centrifuge (Thermo Scientific, Germany) at 6,000 x g for 15 min at 4°C. The resulting bacterial cell pellet underwent two washes with 10 mL of PBS, with centrifugation performed after each wash as described above. Following the second wash, the cell pellet was resuspended in 45 mL of PBS, yielding a cell suspension of approximately 8 log CFU/mL. This suspension was then further diluted tenfold in PBS to obtain a final concentration of approximately 7 log CFU/mL, which was used to inoculate the meat samples. To verify the actual concentrations of individual strains prior to centrifugation and of the final mixed cell suspension, we performed tenfold dilutions in maximum recovery diluent (MRD; Neogen Culture Media) and plated them in duplicate onto TSA.

Inoculation, packaging, and retail display

The upper surface of INOC steaks was inoculated with 0.15 mL of the spoilage bacteria inoculum. The cell suspension was deposited on the meat surface with a micropipette and then spread over the entire surface with a sterile disposable spreader. The inoculated samples were left undisturbed for 15 min to allow for bacterial cell attachment before they were packaged. For the DCON steaks, a 0.15 mL volume of

PBS was deposited and spread over the surface and left for 15 min before packaging. Steaks were overwrapped (O_2 transmission = 23,250 mL x m² x d⁻¹, 72 gauge: Resinite Packaging Films, Borden, Inc., North Andover, MA) and placed into a multideck retail display case with continuous lighting at $3 \pm 1^\circ\text{C}$ (2800 lx, 1810LX4000 LED fixture; Kason, Newnan, GA; color rendering index = 84, color temperature = 4,500 K) for up to 8 days, with the first day of retail display designated as day 0. Steaks were allowed to bloom for 2 h after overwrapping before day 0 color assessment and microbial analysis. Additionally, steaks were rotated in the retail display case daily to ensure minimal impacts from temperature and lighting variance. In a pre-determined random order, one steak per loin per treatment (i.e., $n = 10$ each for LL INOC and DCON), at $24 \text{ h} \pm 1 \text{ h}$ intervals, was used to assess instrumental color, panelist visual color evaluation, microbial population levels, meat pH, TBARS, 16S rRNA gene sequences, metatranscriptomics, and surface metabolites.

Instrumental color evaluation

Instrumental lightness (L^*), redness (a^*), and yellowness (b^*) were measured using a HunterLab MiniScan LabScan EZ4500 colorimeter (Hunter Associates Laboratory, Reston, VA), with a 2.54-cm diameter aperture with a 12.5 mm measurement port, illuminant A, and 10° standard observer (King et al., 2023). On the light exposed surface of the LL steaks, three measurements were taken in random locations and averaged to provide color values. Black and white tiles were used to calibrate the colorimeter prior to use each day.

Visual color evaluation

Visual color scores were collected using a computerized survey tool (Qualtrics, Provo, UT). For both lean color scores and percentage discoloration, six to eight panelists assessed each steak. This work was approved by the Colorado State University Institutional Review Board (IRB#5092). A continuous lean redness color lexicon was adapted from King et al. (2023) with values ranging from 1 to 8 (e.g., 1 = extremely bright cherry red, 8 = extremely dark red). Percent discoloration was evaluated using a continuous scale from 0 to 100%. Results for both were reported as estimated marginal means and standard error on a per treatment by day basis.

Microbiological analyses

We aseptically excised from a 4 x 4 cm (16 cm³) surface section of steak, approximately 1 mm thick, using a sterile template and scalpel, ensuring only the lean surface was removed. The sample was placed into a filter-separated sterile sample bag (710 mL; Whirl-Pak, Pleasant Prairie, WI), and 25 mL of MRD was added. Bags were hand-massaged for 60 s, then vigorously shaken 60 times for bacterial detachment (Smith et al., 2024). The resulting rinsate was serially diluted tenfold, and appropriate dilutions were surface-plated in duplicate on TSA for aerobic plate counts (APC) and *Pseudomonas* agar base (Oxoid Ltd., Wake Road, Basingstoke, Hants, UK) supplemented with *Pseudomonas* CFC supplement (comprised of cetrimide, fucidin, and cephalosporin; Oxoid Ltd.) for *Pseudomonas* spp. counts. Additionally, a pour plate overlay method with Lactobacilli MRS agar (MRS; Difco™, Becton, Dickinson and Company) was used to obtain lactic acid bacteria counts (LABC). All plates were incubated at 25°C for 72 h, followed by manual colony counting. Colony counts were converted to log CFU/cm², with a detection limit of 0.2 log CFU/cm². After

microbiological analysis, 15 mL of remaining rinsate was collected into a sterile tube and centrifuged (Sorvall Legend X1R, Thermo Scientific) at 4,280 x g at 4°C for 20 min. The supernatant was discarded, and pellets were frozen at -70°C until processing for 16S rRNA sequencing and RNA extraction.

Meat pH

To measure pH, approximately 20 g of tissue, including the surface, avoiding connective tissue and external fat, from each sample was homogenized using a blender (Waring Laboratory Science, Stamford, CT). Duplicate 2.5 g portions of the meat homogenate were homogenized with 15 mL of distilled water using an immersion blender (Pro Scientific, Oxford, CT). An Orion Star A211 pH meter (Fisher Scientific, Pittsburgh, PA) fitted with an Orion 8157BNUMD Ross Ultra pH/ATC triode electrode (Fisher Scientific) was used for measuring pH.

Lipid oxidation - thiobarbituric acid reactive substances

Lipid oxidation was quantified using the following *thiobarbituric acid reactive substances* (TBARS) procedure. First, 2.5 g of homogenized sample (in duplicate) was mixed with 11.25 mL of 11% trichloroacetic acid (TCA; Sigma-Aldrich, St. Louis, MO). The mixture was then filtered through Whatman #1 filter paper (Global Life Sciences Solutions, Buckinghamshire, UK) and 2 mL of filtrate was combined with 2 mL of 20 mM thiobarbituric acid (MP Biomedicals, Solon, OH). Samples were incubated for 20 h at 25°C. After incubation, absorbance at 532 nm was measured using a spectrophotometer (UV-1800 Shimadzu, Canby, OR). A standard curve was constructed using 1,1,3,3-tetraethoxypropane (Sigma-Aldrich) to determine concentration. Experimental absorbance values were then used to calculate the

concentration of malondialdehyde (MDA) per sample. Finally, the concentration of MDA was converted to mg/kg of meat basis.

Bacterial DNA extraction, library preparation, and 16S rRNA gene sequencing and analysis

For 16S rRNA gene sequencing, the previously stored sample pellets of all INOC LL steaks were resuspended in 4 mL of PBS. From the resuspended pellet, 2 mL was frozen at -70°C for RNA extraction, and the remaining 2 mL was used for DNA extraction. Bacterial DNA was extracted using the DNeasy PowerFood Microbial Kit (Qiagen, Germantown, MD) following the manufacturer's instructions with minor modifications. Briefly, modifications included adding an additional 200 µL of lysis buffer, and samples were heated in a water bath at 65°C for 10 min to facilitate a more complete bacterial cell lysis.

Amplification and sequencing preparation were performed according to the Earth Microbiome Project (<https://earthmicrobiome.org/>) protocol. The resulting sequences were demultiplexed using QIIME2 (version 2024.2; Boylen et al., 2019) and denoised using the DADA2 pipeline. After denoising, forward reads were trimmed at 13 base pairs, and all sequences were truncated at 250 base pairs to ensure quality. QIIME2 with the SILVA taxonomical database was used to create a relative abundance feature table with taxonomy and a phylogenetic tree. Chloroplasts, eukaryota, and mitochondria were removed from the dataset prior to analysis. Further, there was no evidence of contamination in the samples, nor evidence of errors in the extraction, library preparation, and sequencing steps; therefore, the environmental and positive controls were removed from the dataset before statistical analysis. The statistical analysis for the

16S rRNA gene sequences was performed in R using the phyloseq package (version 4.4.1; McMurdie and Holmes, 2013). Alpha diversity metrics were analyzed using a pairwise Wilcoxon rank sum test, and beta diversity was analyzed using the cumulative sum squared normalization with a PERMANOVA with 9,999 permutations in the vegan and adonis packages in R (version 2.6-6.1; Oksanen et al., YEAR). For both diversity metric analyses, the Benjamini-Hochberg multiple comparisons test adjustment was used. For all 16S rRNA gene sequencing analyses, significance was set at $\alpha = 0.05$.

Mass spectrometry for metabolomic analysis

For both metabolomic and metatranscriptomic analysis, a subset of 32 samples was used, which contained samples from retail display days 3 through 6. These days represented one day before discoloration occurred on the INOC steaks and extended until discoloration was greater than 50% of the surface. The samples included four replicates from both treatments (INOC and DCON) from the same loin on the same display day. Care was taken during selection to ensure that the samples of the DCON treatment had aerobic plate counts (obtained with the culture-dependent analysis) that were below the microbial analysis detection limit ($<0.2 \log \text{CFU/cm}^2$), so that we could more accurately assess the impacts of microbial growth on discoloration.

For the metabolomic analysis, a section of the top surface of each steak, approximately 8 cm^2 and 1 mm thick, was removed and flash frozen in liquid nitrogen before being subsequently stored at -70°C until further processing. The samples were then lyophilized and subsequently homogenized into powder, filtered through a fine mesh sieve, and stored at -70°C until analysis.

To extract metabolites for gas chromatography mass spectrometry (GC-MS), 20 ± 1 mg was weighed into tubes. To each sample, 1 mL of 40% methanol in LCMS grade water was added. Samples were then shaken at 4°C for 2 h. After shaking, samples were placed at -80°C for 2 h, then centrifuged for 15 min at 4°C at 3,500 rpm. Eight hundred and fifty microliters of supernatant were then transferred to new glass vials, and 100 μ L was taken for further derivatization. Samples were again centrifuged for 2 min at 4°C at 3,500 rpm. Next, samples were dried using a nitrogen evaporator and the resulting pellet was resuspended in 100 μ L of a 4:4:2 methanol, acetonitrile, and water mixture and incubated at -20°C for 19 h. After the incubation step, samples were centrifuged for 15 min at 4°C at 3,500 rpm and 90 μ L of supernatant was transferred to a clean glass vial. To create the quality control samples, 10 μ L of each sample was placed into another clean glass vial and allowed to rest for 1 h at room temperature. Finally, all samples were placed on the nitrogen evaporator until completely dry.

The GC-MS samples were derivatized by adding 50 μ L of 25 mg/mL of methoxamine hydrochloride in pyridine solution to each sample. Samples were then centrifuged at 3,500 rpm for 2 min at room temperature, before being incubated at 60°C for 45 min, followed by another centrifugation step. Samples were then sonicated for 10 min and centrifuged at 3,500 rpm for 2 min at room temperature, followed by a 45 min 60°C incubation. Once again, samples were centrifuged at 3,500 rpm for 2 min at room temperature, and 50 μ L of MSTFA +1% TMCS was added to each sample and centrifuged the same as before. Next, samples were incubated at 60°C for 30 min, then rested at room temperature for 10 min, and centrifuged at 3,500 rpm for 2 min at room

temperature. Finally, the derivatized samples were loaded into inserts and centrifuged at 3,500 rpm for 2 min at room temperature.

One microliter of derivatized sample was injected at a 1:12 split ratio and 1.0 mL/min helium gas flow. A Clarus 690 gas chromatography system (PerkinElmer, Waltham, MA) coupled to a PerkinElmer Clarus SQ 8T mass detector was used to detect small semi-volatile and non-volatile molecules. Separation of analytes was conducted with a TG-5MS column (Thermo Scientific, 30 m × 0.25 mm × 0.25 μm). The oven profile consisted of an 80°C hold for 30 s, ramping 15°C/min to 330°C, with an 8-min hold at the end of the run. Masses between 50-620 m/z were scanned at 4 scans/s after electron impact ionization operating at 70 eV. The injector temperature was held at 285°C, the transfer line was set to 300°C, and the source was set to 260°C. A pooled QC was run every 6th sample and was used to control analytical variation.

The GC-MS files were converted to .cdf format and processed using R statistical software, as previously described (Yao et al., 2019). This process involved: (1) XCMS software defining a matrix of molecular features, (2) normalizing samples to total ion current, (3) clustering co-varying and co-eluting features into spectra using the RAMClustR package for R (Broeckling et al., 2014), and (4) annotating spectra by searching against external databases via RAMSearch software (Broeckling et al., 2016). Identification of metabolites was made by matching mass spectra and retention indices with external databases (Hummel et al., 2013). For compounds with highly similar spectra, elution order was used to determine identification.

Metatranscriptomics

From the 32 previously identified samples used in the metabolomic analysis, total RNA was extracted from the rinsate pellet collected from the INOC steaks, providing a total of 16 samples used for metatranscriptomic analysis. Total RNA was extracted using the RNeasy PowerFecal Pro Kit (Qiagen) following the manufacturer's instructions. The eluted RNA was then frozen and sent to Novogene (Novogene Corp. Inc., Sacramento, CA) for rRNA depletion, library preparation, and sequencing. For data processing, paired end sequences were evaluated for quality using FastQC (version 0.12.0; Andrews, 2010), and 14 of 16 samples produced sequences of acceptable quality. Adapter sequences were removed from each read using Trimmomatic (version 0.39; Bolger et al., 2014), and paired end sequences were merged using the bbmerge function of the BBTools package (Bushnell et al., 2017). Next, merged reads were processed using the HuMaNn2.0 pipeline and genes were converted to Kyoto Encyclopedia of Genes and Genomes (KEGG) orthologs (KO). Statistical analysis was performed in R using the MaAsLin3.0 package. For metatranscriptomics analysis, a linear model was created with display day as the main effect, and the ordered parameter was set to compare day 3 to 4, 4 to 5, and 5 to 6. Significance was set at 0.05, and a False Discovery Rate correction was applied.

Statistical analysis

Statistical analysis for instrumental color, panelist visual color evaluation, microbial population levels, meat pH, TBARS, and comparisons of relative abundance of metabolites was performed in R (version 4.2.2) using the lme4 (version 1.1.33) and lmerTest (version 3.1.3) packages for mixed models. Display day and treatment (DCON and INOC) were considered the fixed effects and trial was treated as a block, and the

interaction between display day and treatment was analyzed. Loin was used as a random variable. The relative abundance values for metabolites were normalized and log transformed prior to analysis. An analysis of variance (ANOVA) with a Kenward-Roger degrees of freedom adjustment was used to statistically separate means. Estimated marginal means were calculated with the emmeans package (version 1.8.5) and used to make means comparisons for both interactions and main effects where applicable. Tukey's multiple testing correction was applied, and the significance was set at $\alpha = 0.05$. Similarly, a False Discovery Rate correction was applied for metabolomic data and significance was set at 0.05.

Results

Instrumental color

There was a display day x treatment interaction ($P < 0.05$) for L^* , a^* , and b^* of LL steaks. The DCON and INOC L^* values were similar ($P \geq 0.05$) for days 1 through 5 of display; however, on days 6 and 7, L^* values of INOC steaks were lower ($P < 0.05$) than those of DCON steaks (Table 3.1). The a^* and b^* values were similar ($P \geq 0.05$) between the LL treatments until day 4, after which INOC had lower ($P < 0.05$) a^* and b^* values compared to those of the DCON treatment (Table 1).

Visual color evaluation

A display day x treatment interaction ($P < 0.05$) was obtained for visual lean scores and percentage surface discoloration of LL steaks. Specifically, lean color scores and surface discoloration were similar ($P \geq 0.05$) between the treatments until day 4 (Table 3.2). From days 5 to 7, panelists scored INOC LL steaks as darker red and more discolored ($P < 0.05$) as compared to DCON steaks. The INOC LL steaks were over

70% discolored by day 7 compared with less than 1% discoloration for the DCON LL steaks on the same day (Table 3.2).

Culture-based analysis of microbial population levels

There was a display day x treatment interaction ($P < 0.05$) for all three bacterial count types (APC, LABC, and *Pseudomonas* spp.) recovered from LL steaks (Table 3.3). For the INOC steaks, APC, LABC, and *Pseudomonas* spp. counts increased ($P < 0.05$) from 3.6, 3.7, and 3.4 log CFU/cm², respectively, on day 0, to 9.1, 6.7, and 9.1 log CFU/cm², respectively, by day 7 (Table 3.3). By contrast, for the DCON steaks, 90%, 100%, and 100% of the samples analyzed on day 0 had APC, LABC, and *Pseudomonas* spp. counts, respectively, that were below the analysis detection limit (0.2 log CFU/cm²; Table 3.3). On the last day of retail display, APC, LABC, and *Pseudomonas* spp. counts of DCON LL were <1.4, <0.3, and <0.2 log CFU/cm², respectively, with 50% (APC), 80% (LABC), and 60% (*Pseudomonas* spp. counts) of the samples having counts that were below the detection limit.

pH and TBARS

There was only a display day effect ($P < 0.05$) for the pH values of LL steaks, with pH values generally increasing during display (Table 3.4). Similar to pH, there was only a main effect of display day ($P < 0.05$) for TBARS, with malondialdehyde (MDA) concentration of meat increasing throughout the display period (Table 3.4).

16S rRNA sequencing

For LL INOC samples, there was an average of 24,112 ASVs per sample, ranging from 3,642 to 107,606 ASVs, and 194 unique taxa in 73 samples. Alpha diversity decreased ($P < 0.05$) each day from days 0 to 4, while from days 4 through 7

alpha diversity was similar ($P \geq 0.05$) as measured by Shannon's Index, Simpsons, and Inverse Simpson's Index (Figure 3.1). The beta diversity, as evaluated with weighted UniFrac distances, was different ($P < 0.05$) between display days, with days 0, 1, 2, 3, and 4 each having different ($P < 0.05$) beta diversity (Figure 3.2). Conversely, display days 4, 5, 6, and 7 were similar ($P \geq 0.05$) to each other, but had less diversity compared with days 0, 1, 2, and 3 (Figure 3.2). To further illustrate the change over time, Figure 3.3 shows an increase in the relative abundance of *Pseudomonadaceae* over the display period, and by day 5, *Pseudomonadaceae* made up greater than 95% of the ASVs detected.

GC-MS metabolomics

There was a display day x treatment interaction ($P < 0.05$) for the relative abundances of 10 metabolites. First, lysine and glutamic acid were detected in greater ($P < 0.05$) concentrations on days 5 and 6 for DCON LL steaks compared with INOC steaks (Table 3.5). Xylose, creatinine, hypoxanthine, and urea were greater ($P < 0.05$) in INOC LL steaks compared to DCON on day 6, and lactic acid and idose were greater ($P < 0.05$) for DCON LL steaks on day 6 compared to INOC steaks. Xanthine levels were higher on the INOC steaks on days 4, 5, and 6 compared to the DCON steaks. Pyruvic acid was detected in greater ($P < 0.05$) concentrations for INOC LL steaks compared to DCON steaks on all four days measured (Table 3.5).

There were treatment effects ($P < 0.05$) but no interaction ($P \geq 0.05$) for another four metabolites (Table 3.6). Mannose, fructose-6-phosphate, galactose-6-phosphate, and inosine-5'-phosphate were all greater ($P < 0.05$) for INOC samples compared to DCON samples. Moreover, there was a display day main effect ($P < 0.05$) without an

interaction ($P \geq 0.05$) for an additional nine metabolites. These included: beta-alanyl-histidine, mannose, fructose, fructose-6-phosphate, citric acid, tyrosine, inosine-5'-phosphate, leucine, and valine (Table 3.7).

Metatranscriptomics

There was an average of 29,190,469 reads per sample, with an average read length of 150 base pairs per sequence prior to analysis. After data processing, there were 28,167,259 average reads per sample with an average of 147 base pairs in length. There were 7,140 unique KEGG orthologs in the dataset, which corresponded to 128 complete (all enzymes to complete a metabolic process were detected) KEGG pathway modules. Statistical analysis determined there were 785 KOs with changes ($P < 0.05$) in relative abundance between days 3 and 4, 4 and 5, and/or days 5 and 6. Of these changes, the vast majority occurred between days 3 and 4, and 4 and 5, with only nine statistical changes occurring between days 5 and 6.

The statistically relevant KOs corresponded to genes in 194 different pathways, in 35 BRITE protein families, within 14 different BRITE complete pathway modules. To more thoroughly investigate the changes in microbial metabolism and functional changes, we narrowed the analysis to focus on KOs associated with metabolism. Nonetheless, significant KOs associated with cellular structures, replication, antimicrobial resistance, and other undefined modules were also observed (data not shown).

Pathway modules

Three complete carbohydrate metabolism modules were determined to increase in abundance during the display period: (1) pyruvic acid oxidation to acetyl-CoA, (2)

citrate cycle to 2-oxoglutarate, and (3) pentose phosphate pathway (PPP). Furthermore, 21 pathway modules with incomplete KEGG pathways were identified as statistically significant ($P < 0.05$) KOs in the carbohydrate metabolism modules. These included the citrate cycle, glycolysis, glucuronate pathways, glyoxylate cycle, methylcitrate cycle, and inositol phosphate metabolism.

The largest category of modules with differences ($P < 0.05$) in abundance in KOs was amino acid metabolism. In this group, serine, threonine, cysteine, methionine, branched chain amino acids, lysine, arginine, proline, histidine, aromatic amino acids (tryptophan, tyrosine, phenylalanine), glutathione, hydroxyproline, and gamma-aminobutyrate were identified as different compared with the previous day. The metabolism of cofactors and vitamins was the second most changed module category. There were 36 pathway modules with significant KOs, which included thiamine, riboflavin, NAD, coenzyme A, biotin, molybdenum, and heme.

There were 15 pathway modules with KOs assigned to energy metabolism in the categories of carbon fixation, methane metabolism, sulfur metabolism, and adenosine triphosphate synthesis. Nine additional pathway modules included fatty acid metabolism, with two modules including lipid metabolism. Moreover, six modules were detected for purine metabolism and three for pyrimidine metabolism. There were also four modules identified within biosynthesis of terpenoids and polyketides.

Carbohydrate metabolism

There were no differences ($P \geq 0.05$) found for KOs involved in extracellular glucose utilization for glycolysis throughout the display days. Additionally, no differences ($P \geq 0.05$) were detected for hexokinase or phosphofructokinase. However, the pyruvic

acid dehydrogenase and pyruvic acid kinase enzymes were increased in abundance ($P < 0.05$) between display days 3 and 4, but there was no increase ($P \geq 0.05$) afterwards. There was an increase ($P < 0.05$) in the abundance of the KOs for the citrate cycle between days 3 and 4 and days 4 and 5. The KOs for enzymes crucial to the development of extracellular polysaccharide (EPS; slime) formation were also increased in abundance ($P < 0.05$) across display days (Table 3.7).

Amino acid metabolism

Key KOs associated with enzymes for amino acid synthesis and degradation were increased in abundance ($P < 0.05$) during the testing period. Moreover, there was also an increase ($P < 0.05$) in KOs for the assembly and degradation of arginine, methionine, glycine, cysteine, isoleucine, leucine, lysine, proline, histidine, glutathione, hydroxyproline, and valine (Table 3.7).

Metabolism of cofactors

Numerous genes regulating the biosynthesis of cofactors for enzymatic processes were identified as different. Specifically, heme, siroheme, biotin, and pyridoxal-P biosynthesis were increased ($P < 0.05$) in relative abundance across display days. The non-mevalonate pathway, for constructing isoprenoids, was also increased in abundance ($P < 0.05$) over display days (Table 3.7).

Fatty acid metabolism

There were KO modules associated with fatty acid metabolism with significant changes in their expression. Specifically, there were increases ($P < 0.05$) in the fatty acid biosynthesis pathways, and beta-oxidation pathways between days 3 and 4 and 5

and 6 (Table 3.6). Further, there was an increase in the ($P < 0.05$) KOs of the methylcitrate pathway and fatty acid derived quorum sensing proteins (Table 3.7).

Discussion

Meat color

As anticipated, the redness (a^*) values of both treatments steadily decreased during display. However, the magnitude of this decrease varied significantly between the treatments. For the INOC treatment, the initial significant ($P < 0.05$) decrease was between days 4 and 5, with a sharp decline in a^* values between days 5 and 6, which resulted in an a^* value of 14.27 on day 6. However, such a sharp decline was not observed in DCON, which had an a^* value of 26.68 on day 6 (Table 3.1). There was also a notable increase in surface discoloration and panelist lean color scores for the INOC samples at the same time points (Table 3.2). The decrease in redness of INOC steaks was expected and agreed with our previous findings (Smith et al., 2024b). Of significance, the change in the a^* values occurred at similar approximate time points as major changes in the metabolic functions of bacteria, suggesting a highly likely relationship between these events.

Microbial growth

Pseudomonas spp. predominated during the display period, as shown in Table 3.3, and greatly influenced the APC results reported. It is expected that *Pseudomonas* spp. growth would outpace the LAB growth during aerobic retail display due to the more favorable atmospheric conditions. Furthermore, the decontamination process was successful in greatly reducing microbial load and resulted in DCON steaks that were mostly below the detection limit of 0.2 log CFU/cm². This step was crucial for

establishing treatment models in this study. The discoloration of INOC steaks was approximately 20% of the surface when APC counts were approximately 7 log CFU/cm², which corresponds with previous findings that suggest spoilage occurs at approximately 7 log CFU (Table 2; Chai et al., 2017).

TBARS and pH

For lipid oxidation (TBARS), there was only a day effect, but no difference ($P > 0.05$) was observed between the INOC and DCON steaks. The day effect for TBARS would be expected in aerobically packaged beef as oxidation is known to increase during retail display (Franco et al., 2012; Legako et al., 2015). Faustman et al. (2010) indicated that lipid oxidation can increase myoglobin oxidation and thus decrease the color stability of fresh beef. The sample used for TBARS analysis was taken from the steak surface and thus, should have captured oxidation caused by the bacteria. Yet, the lack of a treatment effect or a display day x treatment interaction for TBARS suggested that lipid oxidation was likely not driving the discoloration process induced by bacterial growth.

The pH of the steaks slightly increased during the display period from 5.55 to 5.60 (Table 3.4). A similar increase in meat pH during retail display has been previously reported (Gill, 1983; Smith et al., 2024b). Studies have also reported that slight changes in pH can impact microbial growth on fresh meat, and increasing to a more neutral pH is more favorable for meat spoilage bacterial growth (Gill and Newton, 1978; Koutsoumanis et al., 2006). Additionally, bacteria can create microenvironments that have differing pH values, but these are nearly impossible to measure during meat

spoilage (Gill, 1983). Similar to TBARS, pH was not influenced by the treatment, suggesting that microbial load and growth had minimal influence on pH.

16S rRNA gene sequencing

Results for the 16S rRNA gene sequencing indicated a decrease in diversity throughout the display period, which is in agreement with previous research (Smith et al., 2024a). In fresh meat, as spoilage progresses, a select few genera tend to predominate the microbial composition (Nychas, et al., 2008). In the current study, *Pseudomonas* spp. predominated the taxa recovered, and similar results have been reported previously in aerobically packaged beef steaks (Nychas et al., 2008; Wickramasinghe et al., 2019; Papadopoulou et al., 2020).

The 16S gene sequencing has a potential for bias towards Gram-negative bacteria, which could be a limitation for the analysis (Jo et al., 2016; Laursen et al., 2017). In the current study, the positive controls did not indicate quality issues with extraction or sequencing, yet there was a bias towards *Pseudomonas* spp. in the results. This could be due to differences in 16S gene copy numbers between genera, improper lysis of Gram-positive bacteria, less compatible primers during amplification or an unknown bias. Nonetheless, the culture based methods, and previous work have indicated that *Pseudomonas* spp. tends to predominate red meat spoilage in aerobic packaging.

Metabolomics

The use of metabolomics in conjunction with microbiome analysis provided an opportunity to evaluate the potential chemical changes in surface metabolites caused by bacteria, which might be responsible for the surface meat color changes during retail

display. In the current study, glutamic acid in the INOC samples showed a sharp decrease in abundance compared to DCON samples on display day 5, approximately the same time point at which the color values changed (a^* values decreased, and percentage discoloration increased) (Table 3.5). The potential mechanistic reasons behind the decline of this amino acid will be discussed in detail in the next section. In brief, these compounds can be more easily utilized by bacteria for energy production or amino acid synthesis compared to other amino acids. ≥

The increase in xylose on INOC steaks observed could be attributed to the PPP during microbial metabolism (Stincone et al., 2015). Lactic acid was similar between treatments until day 5; however, on day 6, it was lower in INOC compared to DCON. The increase in pyruvic acid was not surprising and is discussed in much greater detail in the following sections.

Changes observed in creatinine between the treatments on day 6 could be from several sources. First, as muscle breaks down, creatinine is formed, and this occurs naturally in meat samples as they decompose. Another route could be through pyrimidine synthesis. The metatranscriptomic data showed an increase in transcripts encoding for enzymes in the pyrimidine synthesis pathway during display. Creatinine could also be created through metabolism of select amino acids such as arginine or glycine (Yoshimoto et al., 1976).

The metabolomic data also captured key compounds that denote meat spoilage and nitrogen havens, including xanthine, hypoxanthine, and urea (Table 3.5). Metabolic pathways for these metabolites were also shown to be increased in abundance in the metatranscriptomic analysis, as expected. Nitrogenous compounds and total basic

volatile nitrogen have been used to assess meat spoilage in the past (Bekhit et al., 2021). Further, nitrogen and carbon metabolism are inextricably linked with one another (Bren et al., 2016).

Four metabolites only exhibited treatment effects (Table 3.6), indicating that bacteria were most likely responsible for the change in abundance. Of these, three compounds, including mannose, fructose-6-phosphate, and galactose-6-phosphate, are carbohydrate intermediates and most likely are the result of microbial energy production. The remaining compound, inosine-5'-monophosphate, can serve several functions, including purine synthesis, ATP production, and is involved in co-factor synthesis and regulation. Metabolites with only day effects (Table 3.6) suggest that these compounds changed in abundance regardless of the treatment and the endogenous breakdown of meat could be primarily responsible for the change.

Metatranscriptomics

Under aerobic conditions, the spoilage bacteria used in this study prefer aerobic respiration for the most efficient energy production (Jones, 2004; Wickramasinghe et al., 2019). For instance, glucose would be used to make pyruvic acid via glycolysis, and the pyruvic acid would be utilized through the citrate cycle. In certain circumstances, such as high oxidative stress or a limited supply of preferred nutrients, bacteria may also employ alternate routes of glucose utilization for energy production. For example, bacteria may oxidize an alcohol group on glucose to form gluconate, which can then be used in the PPP or Entner-Doudoroff pathway. The current data provide little evidence of an active Entner-Doudoroff pathway. However, the transcriptome of the rate limiting enzyme of the PPP, gluconate kinase, increased in relative abundance between days 3

and 4 and days 4 and 5 in INOC samples (Supplemental Table 1). This suggests that most gluconate is being shuttled to the PPP. Papadopoulou et al. (2020) reported that species of *Pseudomonas* (including *fragi*, *lundensis*, and *fluorescens*) can exclusively survive on gluconate. These bacteria may have been using gluconate as a competitive advantage for growth on meat substrates by limiting glucose for other bacteria. Yet, there was no change in the transcriptome of glucose phosphotransferase system enzymes, which transport extracellular glucose into the cell (Romano et al., 1970). There was also a decrease in the relative abundance of transcripts in the mannose phosphotransferase systems, suggesting bacteria were still intaking similar levels of glucose across retail display days (Supplemental Table 1).

The metatranscriptomic data provided little evidence that there were changes in the extracellular utilization of glucose in the glycolytic pathway by bacteria across days. Additionally, the metabolomic data showed no difference in the glucose concentrations between INOC and DCON treatments (Table 3.5). Previous studies have shown that bacteria do not rapidly assimilate amino acids until glucose availability has become scarce (Gill, 1983; Rood et al., 2022). In contrast, using metatranscriptomic methods, Hultman et al. (2020) reported that microbial glucose utilization pathways increased over time during a longitudinal retail display study of beef packaged in 80% oxygen modified atmosphere packaging (MAP). The current data suggest that bacteria are generating pyruvic acid at increasing rates across display days, but the uptick in pyruvic acid generation was not derived from glycolysis or increased carbohydrate intake. The excess accumulation of pyruvic acid, as observed in this study, is generally indicative that other energy pathways are being upregulated, as high pyruvic acid levels tend to

initiate regulatory feedback loops to decrease utilization of glucose as a sole carbon source (Rajpurohit and Eiteman, 2024). Further strengthening this hypothesis, there was a sharp increase in isoprenoid synthesis pathways, which produce compounds for cellular structures, cellular signaling, and electron transfer, among other functions. The isoprenoids created could be formed via the non-mevalonate pathway utilizing two pyruvic acid molecules (Eisenreich et al., 2004). The metabolomic data show that pyruvic acid concentrations increased during the display period for the INOC treatment (Table 3.5), which could be an artifact of greater numbers of bacteria, and/or that pyruvic acid production was increased. The following sections will discuss likely pathways involved in supplementing glucose as a carbon source.

Amino acid metabolism

Across display days, there was an increase in transcripts involved in the synthesis and degradation of numerous amino acids, including glutamate, lysine, arginine, and proline. The amino acid glutamate is a precursor to alpha-ketoglutarate, an important compound of the citrate cycle (Amino Acid Catabolism, 2016). Glutamate is converted to alpha-ketoglutarate and ammonium via the glutamate dehydrogenase enzyme. Glutamate dehydrogenase showed an increase in abundance over the display period, along with urea, which is formed in the presence of excess ammonium. However, too much alpha-ketoglutarate in the cell can signal for a downregulation of glucose utilization through cyclic adenosine monophosphate (cAMP) dysregulation (Huergo and Dixon, 2015; Amino Acid Catabolism, 2016).

Aromatic amino acid transaminase, which catalyzes the aromatic amino acids (phenylalanine, tyrosine, and tryptophan) to produce aromatic alpha-ketoacids and

glutamate, was also increased in abundance in INOC for the current study. The metabolomic data also showed a decrease in glutamic acid in the INOC samples compared to DCON samples, and a steady decrease in glutamic acid across display days for INOC steaks (Table 3.5). However, the metabolomic data did not show differences between the treatments for phenylalanine, tyrosine, and tryptophan. Along the same lines, there was an increase in urea, which is created via the urea cycle, from break down of primarily amino acids such as glutamate, and was supported by a marked increase in the transcripts for enzyme ornithine carbomoyltransferase, an important enzyme for collecting ammonium in cytosol (Couchet et al., 2021). In addition, proline degradation can also directly produce glutamate (Ye et al., 2022). Overall, the metabolomic and metatranscriptomic data together strongly suggest that bacteria increasingly relied on glutamate and its down pathway impacts may have been observed.

Pentose-phosphate pathway (PPP)

The PPP begins with glucose-6-phosphate in the oxidative phase and ends with ribose-6-phosphate in the non-oxidative phase. The PPP serves several functions, including producing intermediaries for the glycolysis pathway, nicotinamide adenine dinucleotide phosphate (NADPH), and producing ribose for nucleotide synthesis (Stincone et al., 2015). In the current study, there was an upregulation of the transcripts of PPP in the INOC treatment. The increase in expression of the enzymes in this pathway is not surprising during the logarithmic phase of bacterial growth, but the increase in the transcripts of enzymes transketolase and transaldolase suggests that the PPP is providing intermediates to the glycolytic pathway (Stincone et al., 2015). On

the other hand, the increase in transcripts of the enzymes ribose isomerase and xylose isomerase provides credence to the hypothesis that the PPP may have been functioning more strongly as an alternative energy production system, as these enzymes convert the 5-carbon saccharides ribose and xylose to ribulose and xylulose, respectively. Specifically, xylulose can be phosphorylated and converted to alpha-ketoglutarate or converted to glyceraldehyde 3-phosphate (Wagner et al., 2018; Zhao et al., 2020). This is a likely scenario given the abundance of xylose detected in the INOC treatment on day 6 in the metabolomic analysis (Table 3.5).

Extracellular polymeric substances

Extracellular polymeric substances (EPS) or slime formation was apparent on the INOC steaks by day 7 of retail display. Lulietto et al. (2015) reported EPS formation begins to occur at approximately 7.5 log CFU for lactic acid bacteria, and Ayers (1960) reported slime formation begins at approximately 7 log CFU for aerobic bacteria, on meat surfaces. The slime serves several functions, including increasing nutrient availability, cellular protection, community signaling, stress response, and entrapment of moisture (Lulietto et al., 2015).

The EPS is made of polymeric saccharides, or chains of sugars (Degeest et al., 2001; Lulietto et al., 2015). Although it has been previously reported that shifts in bacterial metabolism occur when glucose is exhausted, metabolic adaptations to utilizing more amino acids and fatty acids may coincide with a functional change to EPS formation. For example, in the current study, the KO for polysaccharide biosynthesis and cellulose synthase increased in abundance during retail display. Transcripts for another enzyme, glycosyltransferase, was also increased in abundance during the retail

display period, which can join sucrose molecules together to form oligosaccharides, most likely destined for EPS formation. Due to the lack of changes found on extracellular glucose uptake and the early stages of glycolysis, there is a possibility that glucose has not been exhausted but rather repurposed for EPS formation. This might have also led to the potential increase in amino acid and fatty acid degradation pathways to generate substrates for aerobic respiration.

Fatty acid metabolism

There is limited knowledge concerning the role of fatty acids in microbial metabolism during meat spoilage. The results of the current study offer further insights into this process. First, the transcripts associated with the glyoxylate pathway, which, in simple terms, convert fatty acids to carbohydrates (Ahn et al., 2016), were detected in increasing quantities in INOC during the display period. It has also been reported that the glyoxylate pathway is activated when carbohydrate availability is scarce and/or oxidative stress is increased within cells, although competing theories exist regarding its exact purpose (Ahn et al., 2016). Specifically, the transcripts for rate limiting enzymes of the glyoxylate pathway, citrate synthase and aconitate hydratase, were increased in abundance in INOC samples, suggesting fatty acids are being utilized as a carbon source for energy production.

The transcripts of several key enzymes for the methylcitrate pathway were also increased in abundance in INOC. The methylcitrate pathway converts propionyl-CoA, which is formed by beta-oxidation of odd chain fatty acids, to pyruvic acid (Upton and McKinney, 2007). The current data also provided evidence of two distinct pathways with upregulation of KOs responsible for beta-oxidation of fatty acids to form acetyl-CoA.

These mechanisms could form fatty acid radicals and promote lipid oxidation. However, the TBARS data did not indicate a difference between treatments for malondialdehyde, a secondary lipid oxidation product.

There were also several pathways with more KOs corresponding to fatty acid synthesis in the INOC. These pathways included fatty acid initiation and elongation. Interestingly, transcripts for S-malonyltransferase, an enzyme that regulates beta-oxidation, were also increased in abundance with increase in display day, suggesting bacteria are synthesizing fatty acids for purposes other than energy production, which could potentially include the synthesis of cell membrane components or quorum sensing compounds (Parsons and Rock, 2013).

Additional considerations

The metatranscriptomic data also showed numerous changes in the abundance of transcripts associated with cofactor regulation and metabolism. Metallic cofactors, such as iron, magnesium, and manganese, are essential for microbial enzyme functionality and substrate processing. For example, manganese or zinc are necessary to act as an electron stabilizer in class II aldolases typically found in bacteria (Jacques et al., 2018). Further, iron plays a critical role in bacterial metabolism, especially for *Pseudomonas* spp. *Pseudomonas* spp. require higher iron levels compared to lactic acid bacteria to form EPS, and have multiple methods of collecting iron from substrates (Cornelis, 2010). Iron in the Fe³⁺ (ferric) form is not as bioavailable to pseudomonads compared to ferrous (Fe²⁺), and the siderophore iron pathway can be utilized to collect ferric iron. Still, ferric iron will be reduced to ferrous iron in the bacterial cell (Cornelis, 2010). Several authors have suggested that bacteria's interaction with iron—through its

use and reduction—may be triggering oxidation-reduction (redox) reactions in myoglobin, and as such, potentially affecting meat color (Chan et al., 1998; Motoyama et al., 2010; Zhang et al., 2024).

The transcripts for the generation of co-factors, such as the B complex vitamins, were also increased in the INOC treatment. Complexes such as vitamins and metals act as cofactors in numerous biological processes, including fatty acid synthesis and amino acid synthesis. Additionally, the upregulation of several other vitamin cofactors that are important as antioxidants suggests high levels of oxidative stress within bacterial cells. Transcripts for cellular replication also showed a sharp increase in relative abundance during the display days in INOC. This is to be expected, and metabolic processes governing replication typically produce their own metabolites or utilize metabolites from other pathways, such as the pentose phosphate pathway. Along the same lines, transcripts for cellular components including cell walls, membranes, and genetic materials, increased in expression during the display period. Lastly, community interaction transcripts were also increased in abundance, such as antimicrobial resistance and quorum sensing transcripts.

Overall, there is no evidence in the current study to indicate that glucose exhaustion is the primary reason for microbial functional changes, as previous research has suggested (Gill, 1976). Instead, oxidative stress, bacterial efforts to form biofilms, or currently unknown conditions may trigger both meat discoloration and shifts in bacterial metabolism simultaneously. In summary, these data provide evidence that bacteria are less reliant on glucose and carbohydrate metabolism in the latter portion of the display compared to earlier days. Increases in transcripts for amino and fatty acid degradation

suggest that these biomolecules are being utilized in greater quantities at times that coincide with changes in meat color stability. These increases also support previous findings that suggest meat quality deteriorates when bacteria consume amino acids as sources of carbon and/or nitrogen.

Conclusions

The results of this study further demonstrate the impact of spoilage bacteria on the color stability of beef *longissimus lumborum*. Additionally, there was no difference in lipid oxidation or pH between the INOC and the DCON treatments, suggesting that neither could be responsible for the lower color stability in the INOC treatment compared to the DCON under the current experimental conditions. The metabolomic and metatranscriptomic data suggest that the changes in color stability coincide with the shift in bacterial metabolism away from glucose-dependent pathways. Further research exploring the specific pathways identified in this study could narrow down the links between microbial metabolism regulators and beef color stability.

Table 3.1. Marginal means \pm standard error of CIE L^* (lightness), a^* (redness), and b^* (yellowness) of decontaminated (DCON; $n = 10$) and inoculated (INOC; $n = 10$) treatment groups of beef *longissimus lumborum* steaks during simulated retail display (3°C).

Day	L^* value		a^* value		b^* value	
	DCON	INOC	DCON	INOC	DCON	INOC
0	39.05 \pm 0.94 ^{ay}	40.57 \pm 0.91 ^{bz}	29.34 \pm 0.49 ^{az}	28.93 \pm 0.64 ^{az}	24.20 \pm 0.57 ^{az}	23.50 \pm 0.59 ^{az}
1	39.76 \pm 0.79 ^{azy}	39.12 \pm 0.70 ^{azy}	28.57 \pm 0.73 ^{azy}	28.48 \pm 0.68 ^{az}	23.44 \pm 0.77 ^{azy}	23.42 \pm 0.76 ^{az}
2	37.85 \pm 0.83 ^{ay}	37.65 \pm 0.81 ^{ay}	27.51 \pm 0.38 ^{azy}	27.26 \pm 0.35 ^{azy}	23.24 \pm 0.49 ^{azy}	22.91 \pm 0.39 ^{az}
3	41.59 \pm 0.88 ^{az}	40.57 \pm 0.98 ^{az}	27.41 \pm 0.49 ^{azy}	26.96 \pm 0.69 ^{azy}	23.21 \pm 0.48 ^{azyx}	22.52 \pm 0.74 ^{azy}
4	39.00 \pm 0.89 ^{ay}	38.98 \pm 0.88 ^{azy}	26.00 \pm 0.48 ^{ayx}	24.63 \pm 0.36 ^{ay}	21.37 \pm 0.45 ^{axy}	20.42 \pm 0.44 ^{ayx}
5	38.01 \pm 0.47 ^{ay}	37.33 \pm 0.73 ^{ay}	26.34 \pm 0.49 ^{ayx}	21.86 \pm 1.34 ^{bx}	22.37 \pm 0.35 ^{azyx}	19.85 \pm 0.69 ^{by}
6	38.44 \pm 0.73 ^{ay}	34.83 \pm 0.83 ^{bx}	26.68 \pm 0.69 ^{ayx}	14.27 \pm 0.93 ^{bw}	23.22 \pm 0.57 ^{azyx}	18.26 \pm 0.66 ^{by}
7	38.15 \pm 0.82 ^{ay}	34.03 \pm 0.93 ^{bx}	24.59 \pm 0.75 ^{ax}	12.55 \pm 0.61 ^{bw}	21.01 \pm 0.60 ^{ax}	15.01 \pm 1.51 ^{bw}

^{a-b}Marginal means within a row and measurement type without a common superscript letter are different ($P < 0.05$).

^{z-w}Marginal means within a column without a common superscript letter are different ($P < 0.05$).

There was a display day x treatment interaction for all measurements ($P < 0.05$).

Table 3.2. Marginal means \pm standard error of panelist lean color and percentage discoloration of decontaminated (DCON; $n = 10$) and inoculated (INOC; $n = 10$) treatment groups of beef *longissimus lumborum* steaks during simulated retail display (3°C).

Day	Lean Color ^{1,2}		% Discoloration ²	
	DCON	INOC	DCON	INOC
0	3.2 \pm 0.1 ^{bv}	3.0 \pm 0.2 ^{bv}	0.0 \pm 0.0 ^{bz}	0.0 \pm 0.0 ^{bx}
1	3.2 \pm 0.1 ^{bvw}	3.4 \pm 0.1 ^{bvw}	0.0 \pm 0.0 ^{bz}	0.0 \pm 0.0 ^{bx}
2	3.5 \pm 0.2 ^{bxwv}	3.5 \pm 0.1 ^{bvw}	0.0 \pm 0.0 ^{bz}	0.0 \pm 0.0 ^{bx}
3	3.7 \pm 0.1 ^{byxwv}	3.6 \pm 0.1 ^{bxw}	0.0 \pm 0.0 ^{bz}	0.0 \pm 0.0 ^{bx}
4	3.7 \pm 0.1 ^{byxw}	3.9 \pm 0.2 ^{bxw}	0.0 \pm 0.0 ^{bz}	1.5 \pm 1.3 ^{bx}
5	3.8 \pm 0.1 ^{bzyx}	4.2 \pm 0.2 ^{ax}	0.8 \pm 0.8 ^{bz}	16.1 \pm 8.0 ^{ay}
6	4.2 \pm 0.1 ^{bzy}	5.4 \pm 0.2 ^{ay}	0.2 \pm 0.1 ^{bz}	58.1 \pm 5.9 ^{az}
7	4.3 \pm 0.1 ^{bz}	6.4 \pm 0.3 ^{az}	0.7 \pm 0.4 ^{bz}	70.0 \pm 6.5 ^{az}

^{a-b}Marginal means within a row and measurement type without a common superscript letter are different ($P < 0.05$).

^{z-v}Marginal means within a column without a common superscript letter are different ($P < 0.05$).

¹Panelists scored each steak to assess lean color using a continuous 8-point scale (1 = extremely bright cherry-red, 2 = bright cherry-red, 3 = moderately bright cherry-red, 4 = slightly bright cherry-red, 5 = slightly dark cherry-red, 6 = moderately dark red, 7 = dark red, 8 = extremely dark red).

²There was a display day x treatment interaction ($P < 0.05$).

Table 3.3. Marginal mean \pm standard deviation (log CFU/cm²) of aerobic plate counts (APC), lactic acid bacteria counts (LABC), and *Pseudomonas* spp. counts recovered from decontaminated (DCON; $n = 10$) and inoculated (INOC; $n = 10$) treatment groups of beef *longissimus lumborum* steaks during simulated retail display (3°C).

Day	APC		LABC		<i>Pseudomonas</i> spp.	
	DCON	INOC	DCON	INOC	DCON	INOC
0	<0.4±0.6 ^{by*}	3.6±0.6 ^{av}	<0.2±0.0 ^{bz}	3.7±0.2 ^{av}	<0.2±0.0 ^{by}	3.4±0.3 ^{au}
1	<0.2±0.0 ^{by}	4.0±0.2 ^{av}	<0.2±0.0 ^{bz}	3.6±0.2 ^{av}	<0.2±0.0 ^{by}	3.7±0.3 ^{au}
2	<0.2±0.0 ^{by}	4.3±0.3 ^{av}	<0.2±0.0 ^{bz}	3.6±0.2 ^{av}	<0.2±0.0 ^{by}	4.3±0.4 ^{av}
3	<0.2±0.2 ^{by}	5.1±0.4 ^{aw}	<0.3±0.2 ^{bz}	3.8±0.2 ^{av}	<0.2±0.0 ^{by}	5.3±0.4 ^{aw}
4	<0.7±1.0 ^{bzy}	6.2±0.6 ^{ax}	<0.5±0.9 ^{bz}	4.4±0.6 ^{aw}	<0.6±0.8 ^{by}	6.4±0.6 ^{ax}
5	<0.2±0.1 ^{by}	7.2±0.5 ^{ay}	<0.2±0.0 ^{bz}	5.1±0.4 ^{ax}	<0.2±0.0 ^{by}	7.3±0.4 ^{ay}
6	<0.2±0.0 ^{by}	8.0±0.4 ^{ay}	<0.2±0.2 ^{bz}	5.5±0.4 ^{ay}	<0.2±0.0 ^{by}	8.0±0.4 ^{ay}
7	<1.4±1.7 ^{bz}	9.1±0.4 ^{az}	<0.3±0.2 ^{bz}	6.7±0.5 ^{az}	<1.4±1.7 ^{bz}	9.1±0.4 ^{az}

^{a-b}Marginal means within a row and bacterial count type without a common superscript letter are different ($P < 0.05$).

^{z-u}Marginal means within a column without a common superscript letter are different ($P < 0.05$).

*Marginal means with a less than symbol (<) indicates one or more of the samples within the treatment had plate counts below the analysis detection limit (0.2 log CFU/cm²).

There was a display day x treatment interaction for all bacterial count types ($P < 0.05$).

Table 3.4. Marginal means \pm standard error of muscle pH of beef *longissimus lumborum* during simulated retail display (3°C).

Day	pH value	mg MDA/kg meat
0	5.55 \pm 0.02 ^b	0.02 \pm 0.00 ^e
1	5.55 \pm 0.02 ^{ab}	0.01 \pm 0.00 ^e
2	5.59 \pm 0.02 ^{ab}	0.05 \pm 0.01 ^{de}
3	5.55 \pm 0.02 ^{ab}	0.06 \pm 0.01 ^{cde}
4	5.58 \pm 0.02 ^{ab}	0.07 \pm 0.02 ^{cd}
5	5.56 \pm 0.03 ^{ab}	0.16 \pm 0.04 ^{bc}
6	5.58 \pm 0.02 ^{ab}	0.15 \pm 0.03 ^{ab}
7	5.60 \pm 0.02 ^a	0.22 \pm 0.05 ^a

^{a-e}Marginal means within a column without a common superscript letter are different ($P < 0.05$).

Table 3.5. Marginal means of relative abundance of metabolites detected from decontaminated (DCON; $n = 10$) and inoculated (INOC; $n = 10$) treatment groups of beef *longissimus lumborum* steaks during simulated retail display (3°C) with treatment by display day interactions ($P < 0.05$).

Metabolite	Display Day							
	3		4		5		6	
	DCON	INOC	DCON	INOC	DCON	INOC	DCON	INOC
Lysine	1.3×10^{7a}	1.4×10^{7a}	1.3×10^{7a}	1.3×10^{7a}	1.6×10^{7a}	1.3×10^{7b}	1.6×10^{7a}	1.4×10^{7b}
Glutamic Acid	8.6×10^{6a}	8.9×10^{6a}	9.5×10^{6a}	8.2×10^{6a}	1.0×10^{7a}	5.9×10^{6b}	9.7×10^{6a}	5.1×10^{6b}
Hypoxanthine	4.5×10^{7a}	4.1×10^{7a}	4.2×10^{7a}	4.4×10^{7a}	4.7×10^{7a}	4.7×10^{7a}	4.7×10^{7b}	5.7×10^{7a}
Xanthine	1.3×10^{7a}	1.3×10^{7a}	1.1×10^{7b}	1.4×10^{7a}	1.4×10^{7b}	2.5×10^{7a}	1.5×10^{7b}	2.8×10^{7a}
Xylose	5.1×10^{7a}	4.8×10^{7a}	5.5×10^{7a}	5.7×10^{7a}	5.8×10^{7a}	5.9×10^{7a}	5.5×10^{7b}	7.4×10^{7a}
Lactic Acid	2.9×10^{8a}	2.8×10^{8a}	3.0×10^{8a}	2.9×10^{8a}	2.7×10^{8a}	2.7×10^{8a}	2.7×10^{8a}	2.3×10^{8b}
Pyruvic Acid	2.3×10^{5b}	7.3×10^{5a}	2.0×10^{5b}	6.0×10^{6a}	2.1×10^{5b}	3.8×10^{7a}	2.8×10^{5b}	8.5×10^{7a}
Creatinine	2.8×10^{8a}	2.7×10^{8a}	3.1×10^{8a}	2.9×10^{8a}	2.7×10^{8a}	2.6×10^{8a}	2.5×10^{8b}	2.9×10^{8a}
Idose	1.9×10^{8a}	1.9×10^{8a}	1.8×10^{8a}	1.9×10^{8a}	2.0×10^{8a}	1.8×10^{8a}	2.1×10^{8a}	1.6×10^{8b}
Urea	2.5×10^{7a}	2.4×10^{7a}	2.3×10^{7a}	2.4×10^{7a}	2.4×10^{7a}	2.4×10^{7a}	2.3×10^{7b}	2.6×10^{7a}

^{a-b}Marginal means within a row and display day without a common superscript letter are different ($P < 0.05$).

Table 3.6. Marginal means of relative abundance of metabolites detected from decontaminated (DCON; $n = 10$) and inoculated (INOC; $n = 10$) treatment groups of beef *longissimus lumborum* steaks during simulated retail display (3°C) with treatment main effects ($P < 0.05$).

Metabolite	Treatment	
	DCON	INOC
Inosine-5' Monophosphate	3.6×10^{6b}	4.3×10^{6a}
Mannose	8.7×10^{7b}	1.0×10^{8a}
Fructose-6-Phosphate	3.2×10^{7b}	3.6×10^{7a}
Galactose-6-Phosphate	1.8×10^{7b}	2.0×10^{7a}

^{a-b}Marginal means within a row without a common superscript letter are different ($P < 0.05$).

Table 3.7. Marginal means of relative abundance of metabolites detected from of beef *longissimus lumborum* steaks during simulated retail display (3°C) with display day main effects ($P < 0.05$).

Metabolite	Display Day			
	3	4	5	6
Tyrosine	2.9×10^{7b}	2.8×10^{7b}	3.3×10^{7a}	3.5×10^{7a}
Leucine	9.7×10^{6b}	1.0×10^{7ab}	1.1×10^{7ab}	9.8×10^{6a}
Valine	1.0×10^{7b}	1.0×10^{7b}	1.1×10^{7ab}	1.2×10^{7a}
Beta-Alanyl-Histidine	1.1×10^{8a}	1.0×10^{8b}	1.1×10^{8ab}	1.0×10^{8ab}
Inosine-5' Monophosphate	4.7×10^{6a}	3.6×10^{6ab}	3.9×10^{6ab}	3.5×10^{6b}
Mannose	8.6×10^{7ab}	8.3×10^{7b}	9.8×10^{7ab}	1.1×10^{8a}
Fructose	7.2×10^{7b}	7.1×10^{7b}	7.9×10^{7ab}	8.5×10^{7a}
Fructose-6-Phosphate	3.6×10^{7a}	2.9×10^{7b}	3.6×10^{7a}	3.6×10^{7a}
Citric Acid	1.5×10^{5b}	1.8×10^{5ab}	2.6×10^{5ab}	3.4×10^{5b}

^{a-b}Marginal means within a row without a common superscript letter are different ($P < 0.05$).

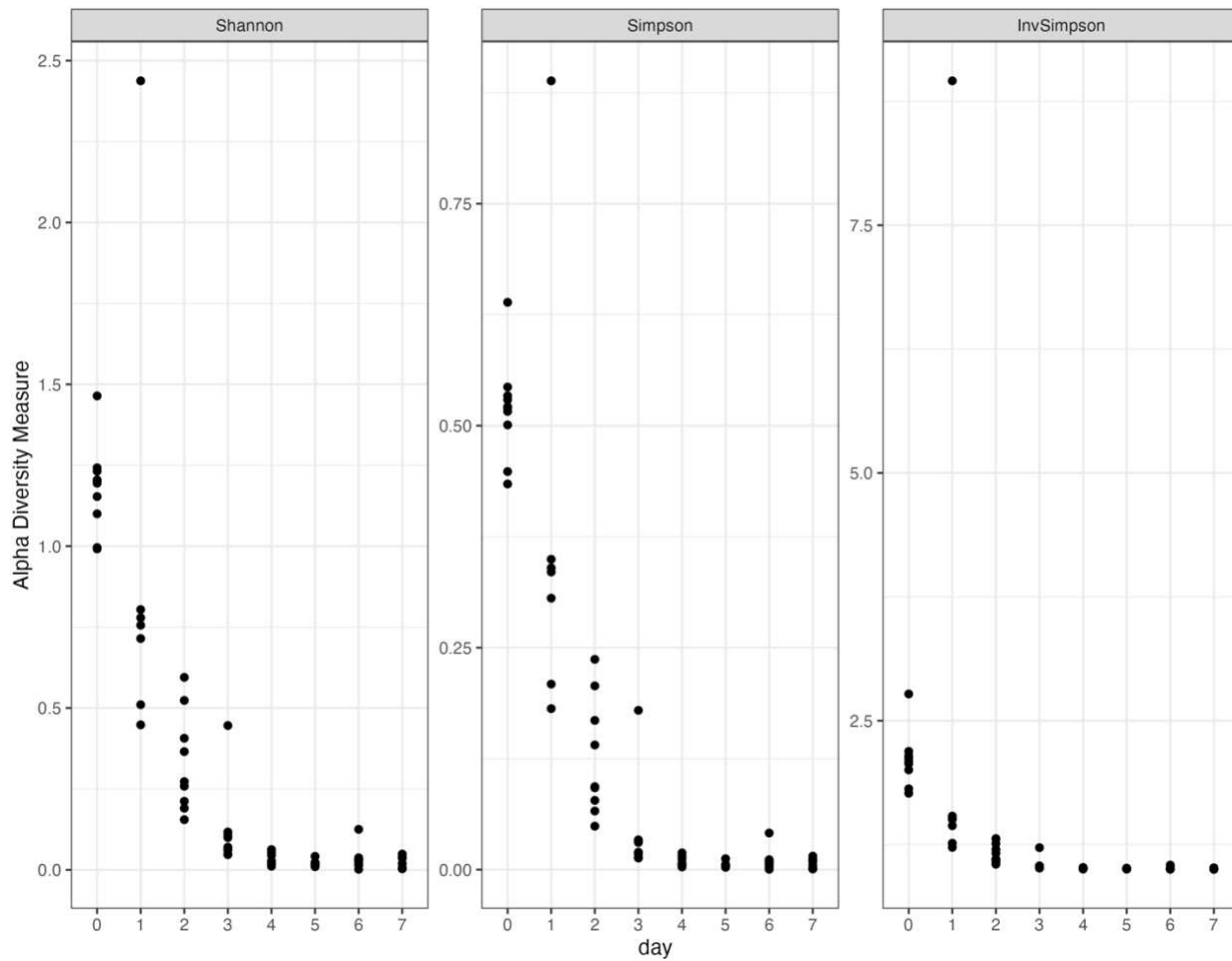


Figure 3.1. Alpha diversity metrics of Shannon, Simpson, and Inverse Simpson Indices as plotted for beef *longissimus lumborum* steaks inoculated with a 6-isolate spoilage bacteria mixture and subsequently placed into simulated retail display (3°C).

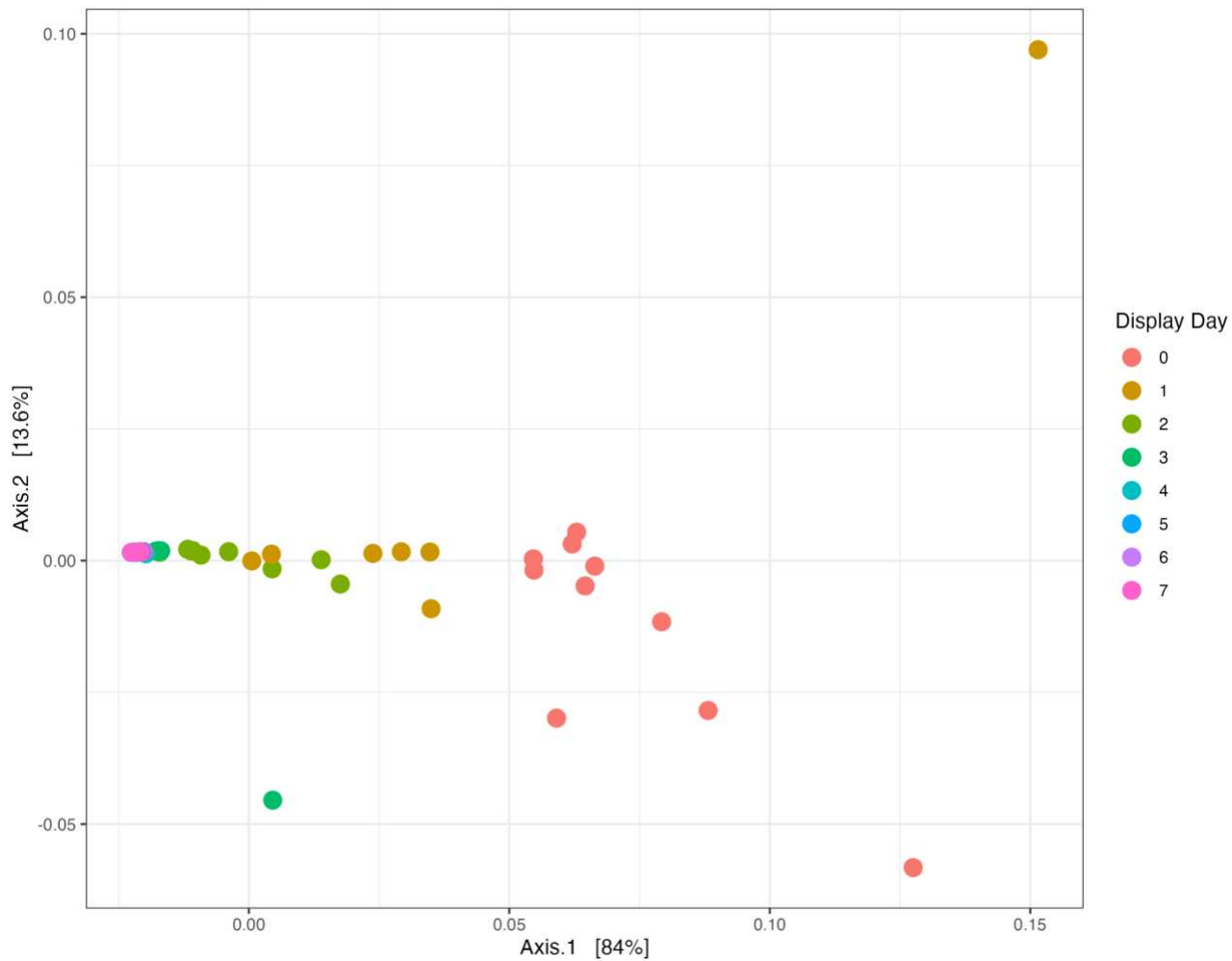


Figure 3.2. Beta diversity shown as a weighted UniFrac principle coordinates analysis (PCoA) for beef *longissimus lumborum* steaks inoculated with a 6-isolate spoilage bacteria mixture and subsequently placed into simulated retail display (3°C).

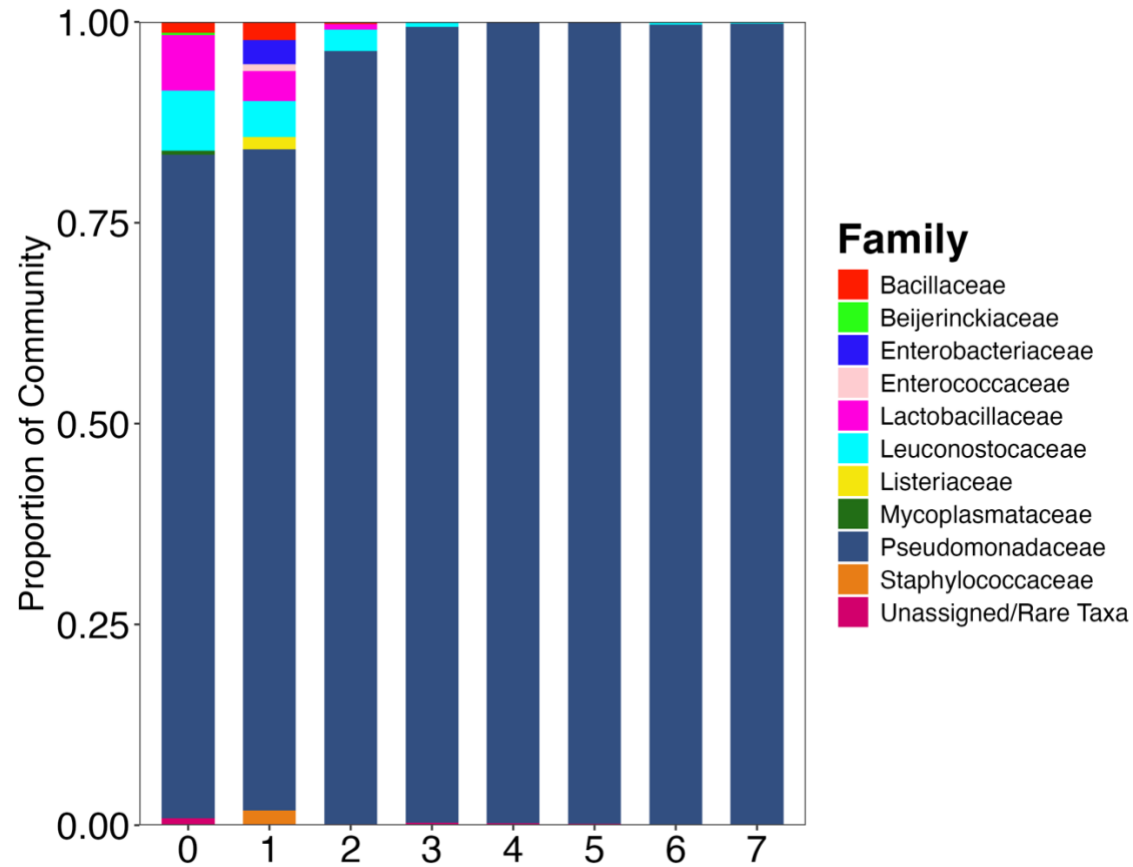


Figure 3.3. Relative abundance taxa bar plot organized at the family level for beef *longissimus lumborum* steaks inoculated with a 6-isolate spoilage bacteria mixture and subsequently placed into simulated retail display (3°C).

CHAPTER 4: INVESTIGATING THE FUNCTION OF SPOILAGE BACTERIA ON FRESH BEEF *PSOAS MAJOR* STEAK DISCOLORATION DURING AEROBIC RETAIL DISPLAY THROUGH A MULTI-OMIC APPROACH

Introduction

The beef *psoas major* (PM; tenderloin) is a high value beef muscle cut that is highly desirable to consumers due to its high eating satisfaction (O'Quinn et al., 2015). Yet, this muscle has a short shelf-life (2-3 days), primarily due to rapid discoloration (McKenna et al., 2005; Najjar-Villarreal et al., 2021; Smith et al., 2024a). Several studies have examined the biochemical basis for the PM's low color stability during retail display compared with color stable muscles (Yu et al., 2019; Najjar-Villarreal et al., 2021; Ramanathan et al., 2021, Smith et al., 2024). However, the exact mechanism behind this difference has not been clearly elucidated.

Previous findings have suggested that color stable muscles generally exhibit a lower proportion of type 1 fibers compared to color labile muscles (Hunt and Hedrick, 1977). The muscle fiber type can also influence the concentration of muscle carbohydrates, lipids, and proteins, and type 1 fibers generally exhibit increased concentrations of myoglobin as well as iron (Picard and Gagaoua, 2020). Further, type 1 fibers have a more oxidative metabolism with greater numbers of mitochondria which impacts muscle color stability (Picard and Gagaoua, 2020; Ramanathan et al., 2021).

It has been established that bacterial growth can impact the PM color stability (Smith et al., 2024a), and that in comparison to color stable *longissimus lumborum* (LL) steaks, bacterial growth kinetics may play a role in the rapid discoloration of PM steaks (Smith et al., 2024b). The muscle-specific factors might be influencing meat color

stability between different beef muscles, but it could also influence the bacterial growth and bacterial function on fresh meat.

The use of modern techniques, including metabolomics and next generation sequencing, to evaluate fresh meat shelf-life represents an opportunity to better understand bacterial function, assimilation, and metabolites that may be leading to meat spoilage or discoloration. Our previous study investigating microbial function on beef LL steaks showed changes in the bacterial function and metabolic profile of LL steaks inoculated with meat spoilage bacteria, compared to decontaminated steaks (i.e., with a low initial level of natural microbiota) (Chapter 3). More specifically, bacterial transcripts for metabolic pathways that provide alternative routes for providing carbon substrates to glucose metabolism were increased in inoculated steaks, and the resulting metabolomic changes included decreased glutamic acid concentration and increased pyruvic acid concentration, which occurred simultaneously with increased surface discoloration (Chapter 3). Therefore, the objective of this study was to investigate bacterial functional changes on inoculated and decontaminated PM steaks during discoloration during aerobic retail display. The utilization of two next generation sequencing methods (16S rRNA gene sequencing and metatranscriptomic RNA-sequencing) and metabolomics combined with chemical and sensory attributes of fresh PM steaks allows the examination of the impact of bacterial growth on meat color stability and shelf-life.

Materials and Methods

Meat collection and processing

Ten ($n = 10$) USDA Choice tenderloins (*psoas major*, PM) were procured from a commercial beef processing facility at 24 h postmortem. These muscles, originating

from carcasses of comparable age and background, were collected on two occasions, representing two trials ($n = 5$ per trial). All muscles underwent wet aging in individual vacuum bags at 2°C until 14 days postmortem. Subsequently, the aged muscles were halved for easier manipulation and subjected to a decontamination protocol. This involved submerging them in boiling water for a specified duration. Specifically, PM muscles were immersed in boiling water for 1 min, removed for 30 s, and then re-submerged for an additional 1 min (Smith et al., 2024a). Internal muscle temperatures were monitored using a ThermoPen One thermometer (ThermoWorks, American Fork, UT), with probes inserted centrally and just beneath the surface, to confirm that the 4°C threshold was not surpassed during decontamination. Following this, the decontaminated muscles were aseptically trimmed, with the entire heat-exposed exterior excised. The trimmed muscles were then aseptically sliced into 0.5-inch (1.27 cm) thick steaks, placed on soaker pad-lined foam trays, and randomly allocated to either a decontaminated control (DCON) or inoculated (INOC) treatment group.

Inoculum preparation, inoculation, packaging, and retail display

The inoculum was prepared following the same procedure described in Chapter 3. Briefly, three strains of *Pseudomonas* and three strains of lactic acid bacteria were revived from our laboratory's culture collection in tryptic soy broth (TSB; Difco™, Becton, Dickinson, and Company, Sparks, MD). The isolates were plated onto tryptic soy agar (TSA; Neogen Culture Media, Lansing, MI), subcultured once onto TSA, and then a single colony forming unit was used to activate the isolates in TSB for 24 h at 25°C. The cultures were then washed twice, combined, and diluted to 6 log CFU/mL (Smith et al., 2024a). For the INOC treatment, the light exposed surface of the steaks

was inoculated with 0.15 mL of the spoilage bacteria inoculum with a micropipette and distributed across the steaks' surface with an L-shaped sterile spreader. Bacteria were allowed 15 min of undisturbed attachment time prior to packaging. An identical procedure was repeated with DCON steaks using sterile phosphate buffered saline (PBS; pH 7.4, Sigma-Aldrich, St. Louis, MO) instead of inoculum.

Following preparation, steaks were overwrapped with a film (Resinite Packaging Films, Borden, Inc., North Andover, MA; 72 gauge, O₂ transmission = 23,250 mL × m² × d⁻¹) and subsequently placed in a multideck retail display case at 3 ± 1°C for a maximum duration of 7 days. This case maintained a continuous lighting environment (2800 lx, 1810LX4000 LED fixture; Kason, Newnan, GA; color rendering index = 84, color temperature = 4,500 K). The first day of retail display was designated as day 0. Before initial color assessment and microbial analysis on day 0, steaks were allowed to bloom for 2 h after overwrapping. To mitigate potential effects of temperature and lighting variations within the retail display case, steaks were rotated daily. At approximately 24-h intervals, one steak per loin for each treatment (i.e., *n* = 10 for both INOC and DCON groups) was selected in a pre-established random order for comprehensive analysis. These analyses included instrumental color, visual color evaluation by panelists, microbial population levels, meat pH, TBARS, 16S rRNA sequencing, metatranscriptomics, and surface metabolite profiling.

Instrumental color evaluation

Instrumental color parameters, including lightness (*L*^{*}), redness (*a*^{*}), and yellowness (*b*^{*}), were determined using a HunterLab MiniScan LabScan EZ4500 colorimeter (Hunter Associates Laboratory, Reston, VA). The instrument was configured

with a 2.54-cm diameter aperture, a 12.5 mm measurement port, illuminant A, and a 10° standard observer, as described by King et al. (2023). For each INOC or DCON steak, the average of three measurements taken from random locations on the light-exposed surface was recorded. Daily calibration of the colorimeter was performed using black and white tiles before analysis.

Visual color evaluation

Five to eight panelists evaluated lean redness and percent surface discoloration using a randomized survey tool (Qualtrics, Provo, UT). This study, approved by the Colorado State University Institutional Review Board (IRB#5092), utilized a continuous lean redness color lexicon (adapted from King et al., 2023) with values ranging from 1 (extremely bright cherry red) to 8 (extremely dark red). Percent discoloration was assessed on a continuous scale from 0% to 100%. Results for both metrics are presented as estimated marginal means and standard error per treatment per day.

Microbiological analyses

For microbial analyses, a 4 × 4 cm (16 cm²) section of the steak surface was aseptically excised at approximately 1 mm deep using a sterile template and scalpel. Each sample was placed into a filter-separated sterile sample bag (710 mL; Whirl-Pak, Pleasant Prairie, WI), and 25 mL of maximum recovery diluent (MRD; Neogen Culture Media) was added. Samples were hand-massaged for 60 s and then vigorously shaken 60 times to detach bacteria (Smith et al., 2024b). The resulting rinsate was serially diluted tenfold, and appropriate dilutions were surface-plated in duplicate on tryptic soy agar (TSA) for aerobic plate counts (APC) and on *Pseudomonas* agar base (Oxoid Ltd.) supplemented with *Pseudomonas* CFC supplement (Oxoid Ltd.) for *Pseudomonas* spp.

counts. Additionally, a pour plate overlay method with Lactobacilli MRS agar (MRS; Difco™; Becton, Dickinson and Company) was used to determine lactic acid bacteria counts (LABC). All plates were incubated at 25°C for 72 h, followed by manual colony counting. Colony counts were converted to log CFU/cm², with a detection limit of 0.2 log CFU/cm². For molecular analysis, 15 mL of the remaining sample rinsate was collected into a sterile tube and centrifuged (Sorvall Legend X1R, Thermo Scientific, Germany) at 4,280 ×g for 20 min at 4°C. The supernatant was discarded, and the pellets were frozen at -70°C until DNA extraction for 16S rRNA sequencing and RNA extraction for metatranscriptomics analysis.

Bacterial growth kinetics

The growth kinetics of the bacterial populations recovered with the culture-dependent analysis were calculated using the DMFit software (available from <https://combase.errc.ars.usda.gov/>) based on the Baranyi and Roberts (1994) primary growth model. The software calculated lag phase duration (in days), maximum growth rate per 24 h (log CFU/cm²), and the goodness of fit (R²) for the model.

Meat pH

To measure pH, approximately 20 g of lean tissue (excluding connective tissue and external fat) from each sample was initially homogenized with a blender (Waring Laboratory Science, Stamford, CT). Duplicate 2.5 g portions of this homogenate were then re-homogenized with 15 mL of distilled water using an immersion blender (Pro Scientific, Oxford, CT). The pH was determined using an Orion Star A211 pH meter (Fisher Scientific, Pittsburg, PA) equipped with an Orion 8157BNUMD Ross Ultra pH/ATC triode electrode (Fisher Scientific).

Lipid oxidation - thiobarbituric acid reactive substances

Lipid oxidation was quantified via the *thiobarbituric acid reactive substances* (TBARS) method. Duplicate 2.5 g portions of homogenized sample was mixed with 11.25 mL of 11% trichloroacetic acid (TCA; Sigma-Aldrich, St. Louis, MO). This mixture was then filtered using Whatman #1 filter paper (Global Life Sciences Solutions, Buckinghamshire, UK). Two mL of the resulting filtrate was combined with 2 mL of 20 mM thiobarbituric acid (MP Biomedicals, Solon, OH). Samples were incubated at 25°C for 20 h, and absorbance was subsequently read at 532 nm on a UV-1800 Shimadzu spectrophotometer (UV-1800 Shimadzu, Canby, OR). A standard curve was constructed with 1,1,3,3-tetraethoxypropane (Sigma-Aldrich) to determine MDA concentration, which was ultimately expressed as mg MDA/kg of meat.

Bacterial DNA extraction, library preparation, and 16S rRNA gene sequencing and analysis

For 16S rRNA gene sequencing, bacterial DNA extraction, library preparation, and sequencing and analysis were performed in the same way as in Chapter 3. In summary, bacterial DNA was extracted from the pellets captured from the INOC steaks using the DNeasy PowerFood Microbial Kit (Qiagen, Germantown, MD). DNA amplification and sequencing were done in accordance with the Earth Microbiome Project guidelines. Resulting reads were processed in QIIME2, denoised with DADA2, and sequences were trimmed to 250 base pairs. Taxonomy was assigned with the SILVA database. Data analysis was performed in R. All controls, chloroplasts, eukaryota, and mitochondria were removed from the dataset prior to analysis. Alpha diversity metrics were analyzed using a pairwise Wilcoxon rank sum test, and beta

diversity was analyzed using the cumulative sum squares with a PERMANOVA with 9,999 permutations in the vegan package in R (version 2.6-6.1; Oksanen et al., 2024). For both diversity and relative abundance, the Benjamini-Hochberg multiple comparisons test adjustment was used. For all microbiome analyses, significance was set at $\alpha = 0.05$.

Metabolomic analysis

A subset of 32 samples was used for metabolite analysis via gas chromatography mass spectrometry. Sixteen samples were from the DCON treatment and 16 from the INOC treatment on days 2 through 5, when discoloration developed on the PM steak surface. Samples from these days were chosen to represent time points before surface discoloration occurred until discoloration was greater than 50% of the surface, which allowed for examination of metabolite and bacterial genetic changes during meat surface discoloration. Approximately 5 g of tissue from the surface of the steaks was collected and flash frozen in liquid nitrogen and stored at -70°C until analysis.

Samples for metabolomic analysis were prepared identically to the methods described in Chapter 3. Briefly, PM samples were lyophilized, extracted with a 4:4:2 methanol, acetonitrile, and water mixture, and derivatized with methoxyamine hydrochloride in pyridine and silylated with MSTFA +1% TMCS. Gas chromatography mass spectrometry instrument parameters, compound identification and analysis were performed in accordance with the methods described in Chapter 3.

Metatranscriptomics

For metatranscriptomic analysis, total RNA was extracted from the rinsate pellet of 16 INOC treatment samples, corresponding to the samples previously used in metabolomic analysis. Total RNA was isolated from stored cell samples using the RNeasy PowerFecal Pro Kit (Qiagen) according to the manufacturer's instructions. The eluted RNA was then frozen and shipped to Novogene (Novogene Corp. Inc., Sacramento, CA) for rRNA depletion, library preparation, and sequencing. Data processing involved quality assessment of paired-end sequences using FastQC (v0.12.0; Andrews, 2010), with 14 of 16 samples yielding acceptable quality. Adapter sequences were removed with Trimmomatic (v0.39; Bolger et al., 2014), and paired-end reads were merged using bbmerge (BBTools package; Bushnell et al., 2017). Merged reads were subsequently processed via the HuMaNn2.0 pipeline, converting genes to Kyoto Encyclopedia of Genes and Genomes (KEGG) orthologs (KO). Statistical analysis was conducted in R using the MaAsLin3.0 package. A linear model was constructed for metatranscriptomics analysis, with display day as the primary effect. Ordered comparisons were performed for day 2 vs. 3, day 3 vs. 4, and day 4 vs. 5. Significance was set at $P < 0.05$, with False Discovery Rate correction applied.

Statistical analysis

Statistical analysis for instrumental color, panelist visual color evaluation, microbial population levels, meat pH, TBARS, and comparisons of relative metabolite abundance was conducted in R (v4.2.2). Mixed models were fitted using the lme4 (v1.1.33) and lmerTest (v3.1.3) packages. Data were analyzed in a factorial model with display day and treatment type (DCON, INOC) as fixed effects, including their interaction. Loin served as a random variable, and trial served as a block. Relative

abundance values of metabolic signals were log-transformed prior to analysis and a False Discovery Rate correction was applied after analysis. Means were statistically separated using an Analysis of Variance (ANOVA) with Kenward-Roger degrees of freedom adjustment. Estimated marginal means were calculated using the emmeans package (v1.8.5) for post-hoc comparisons of both interactions and main effects. Tukey's multiple testing correction was applied, and significance was set at $\alpha=0.05$.

Results

Instrumental color

There was a display day effect ($P < 0.05$) for L^* values, where day 3 had the greatest ($P < 0.05$) L^* value compared with the other days (Figure 4.1), although it was only slightly numerically higher compared to the other days. There was a display day x treatment interaction ($P < 0.05$) for both a^* and b^* values of PM steaks. Both a^* and b^* values were similar ($P \geq 0.05$) between the treatments on days 0 through 4; however, on days 5 and 6, a^* and b^* values decreased ($P < 0.05$) for INOC PM steaks compared to DCON steaks (Table 4.1).

Visual color evaluation

There was a display day effect ($P < 0.05$) for visual lean color scores. Lean color scores of PM INOC and DCON steaks increased ($P < 0.05$) during the display period (Figure 4.2); however, no differences ($P \geq 0.05$) were observed between the treatments on the same day. Further, there was a display day x treatment interaction ($P < 0.05$) for percentage surface discoloration of PM steaks (Table 4.2). The INOC and DCON PM steaks had similar ($P \geq 0.05$) surface discoloration from days 0 to 3 of display. From display days 4 to 6, INOC steaks had greater ($P < 0.05$) percentage discoloration

compared with the DCON steaks, and by the end of display, DCON steaks had approximately 37% discoloration compared with 87% of the INOC steaks.

Culture-based analysis of microbial population levels

There was a display day x treatment interaction ($P < 0.05$) for the APC, LABC, and *Pseudomonas* spp. counts recovered from the PM steaks (Table 4.3). The day 0 APC, LABC, and *Pseudomonas* spp. counts of INOC steaks were 4.0, 3.8, and 3.6 log CFU/cm², respectively. Comparatively, bacterial counts of DCON steaks were <0.3 (APC), <0.2 (LABC), and <0.2 (*Pseudomonas* spp. counts) log CFU/cm² on day 0, with 70%, 90%, and 100%, respectively, of the samples having counts that were below the detection limit (0.2 log CFU/cm²). On the last day of retail display, day 6, bacterial counts of INOC steaks were >7.5 log CFU/cm² regardless of count type (Table 4.3), whereas the DCON steaks had counts of <1.7, <0.7, and <1.3 log CFU/cm² for APC, LABC, and *Pseudomonas* spp., respectively, with 50% (APC), 80% (LABC), and 80% (*Pseudomonas* spp. counts) of the samples having counts that were below the detection limit.

Bacterial growth kinetics

The lag phase duration was greater for bacteria recovered from LL for all count types compared to PM (Table 4.4). More specifically, there were 9.74, 9.77, and 40.15 hours longer lag phase duration for bacteria from LL for APC, *Pseudomonas* spp., and LABC, respectively compared to PM INOC steaks. Moreover, maximum growth rates were similar between bacteria on LL and PM for all count types (Table 4.4).

TBARS and pH

There was a display day main effect ($P < 0.05$) for TBARS values (mg MDA/kg). More specifically, mg MDA/Kg increased throughout the display period for the steaks, with initial levels at 0.03 mg MDA/kg and ending display with 0.34 mg MDA/kg (Figure 4.3). The pH values of DCON and INOC steaks were similar (5.83; $P \geq 0.05$) throughout the display period.

16S rRNA sequencing

For PM INOC steaks, the average number of ASVs per sample was 25,924, with a range of 5,698 to 127,096 ASVs, and 194 unique taxa were identified across 68 samples. Alpha diversity, as measured with Shannon's Index, Simpson's Index, and Inverse Simpson's index, showed that the evenness and richness of ASVs decreased ($P < 0.05$) from days 0 through 3, but were similar ($P \geq 0.05$) for days 3 to 6 (Figure 4.4). Beta diversity measured by weighted UniFrac distances was different ($P < 0.05$) between display days 0 and 1, and these days were different ($P < 0.05$) compared to all other display days (Figure 4.5). Beta diversity on display days 3, 5, and 6 was similar ($P \geq 0.05$) to each other; however, day 4 was similar ($P \geq 0.05$) to days 3 and 5, but different ($P < 0.05$) from day 6. *Pseudomonadaceae* was the most prominent taxon during the display period (Figure 4.6).

GC-MS metabolomics

For metabolomic analysis of PM, there was a display day x treatment interaction ($P < 0.05$) for the relative abundances of 12 metabolites. Phenylalanine was detected in lesser concentrations ($P < 0.05$) on day 4 for DCON steaks compared to INOC steaks (Table 4.5). The DCON steaks had a greater ($P < 0.05$) relative abundance of tyrosine on day 6 compared with INOC steaks. The metabolite xanthine was detected in greater

abundance ($P < 0.05$) on days 4 and 5 for INOC steaks compared with DCON steaks (Table 4.5). Lactic acid, idose, glucose, galactose, and galactose-6-phosphate were present in greater ($P < 0.05$) relative abundances for DCON steaks compared to INOC steaks on day 5, whereas mannose was lower ($P < 0.05$) in DCON steaks on day 4 compared with INOC steaks. Phosphoric acid was detected in greater ($P < 0.05$) abundance on day 5 for INOC steaks compared with DCON steaks. There was a treatment effect ($P < 0.05$) for xylose, with INOC samples having greater relative abundance of xylose (3.5×10^7 vs 3.4×10^7) compared with DCON samples.

Metatranscriptomic analysis

There was an average of 28,430,662 reads in the dataset, with an average sequence length of 150 base pairs. After sequence adapter trimming and quality filtering, there were 27,321,774 average reads per sample with an average sequence length of 148 base pairs. Further, 48% of reads did not belong to a known gene family, were uncharacterized, or had numerous homologs and could not be confidently assigned.

In the total data set, there were 5,689 unique KOs assigned which can be viewed in Figure 4.7. There were 32 KOs with changes ($P < 0.05$) in gene abundance during the retail display period (Supplemental Table 1). Of these, half were classified as signaling and cellular processes proteins. Others included metabolism and genetic information processing. Notably, a large section of microbial metabolism was captured, along with cellular processing, co-factor generation and regulation, and cellular communication to name a few.

Discussion

Meat color

Several studies have reported a lower color stability for PM steaks compared to other color stable muscles (Joseph et al., 2012; Najjar-Villarreal et al., 2021; Ramanathan et al., 2021). For example, Seyfert et al. (2006) showed a sharp decrease in a^* values for aerobically-packaged PM steaks on day 2 of retail display, which was slightly shorter than that observed in the current study. The color results in the current study suggest that bacteria have an impact on PM steak color stability, which aligns with previous findings (Smith et al., 2024a). However, there could be muscle-specific factors playing a role in the color stability of PM steaks, as the DCON steaks had an average 37% discoloration by the end of retail display (Table 4.2). Concurrently, DCON steaks had less than 2 log CFU/cm² of bacterial growth at the same time point, further suggesting there may also be a muscle specific factor influencing on color stability. In comparison, DCON beef LL muscles had only 0.7% discoloration and had less than 2 log CFU/cm² of bacterial growth by day 7 of display (Chapter 3).

Microbial enumeration and growth kinetics

In the current study, the APC for DCON steaks on day 0 was <0.3 CFU/cm² and for INOC steaks it was 4.0 CFU/cm², indicating that we achieved the intended initial microbial levels in both treatments. By day 4, the APC for INOC steaks increased to 7.4 CFU/cm², which coincided with the increase in discoloration on the PM steaks compared to DCON steaks (16.3% vs 46.4 % discoloration). Previous studies have suggested that approximately 7.0 log CFU is the spoilage threshold for aerobically packaged fresh beef (Nychas et al., 2008; Comi, 2017). Our results are in agreement

that at ~ 7 log CFU, the PM steaks were discolored beyond the 20% discoloration acceptance threshold of consumers (Hood and Riordan, 1973).

There was a difference between the increase of *Pseudomonas* spp. and LABC populations on INOC steaks during the display period, with *Pseudomonas* spp. exhibiting a larger increase in growth (1.3 log CFU/cm² vs 0.2 log CFU/cm²) between days 1 and 2 compared with LABC (Table 4.3). After day 2, however, both LABC and *Pseudomonas* spp. experienced a similar increase daily. Most likely, this was due to *Pseudomonas*'s competitive advantage in aerobic packaging, along with competitive advantages with iron assimilation and glucose to gluconate conversion (Wickramasinghe et al., 2019; Zhang et al., 2024).

Metabolomics

There were statistical differences in the relative abundances of amino acids glutamic acid, phenylalanine, and tyrosine between treatments during the display period (Table 4.5). The sharp decrease of glutamic acid in INOC versus DCON steaks on day 5 could have been because glutamic acid can be readily converted to alpha-ketoglutarate by bacterial glutamate dehydrogenase and then utilized in aerobic respiration. Further, bacteria commonly use and prefer glutamic acid as a source of nitrogen and carbon (Commichau et al., 2008). The increase in phenylalanine on day 4 for INOC compared to DCON may result from aromatic amino acid production via the pentose phosphate pathway, which bacteria use for energy production. Moreover, in a closed system such as fresh meat, the limited carbohydrate availability can instigate increases in usage of other compounds for carbon sequestration, and could help explain the decreases in phenylalanine and tyrosine in the INOC treatment compared to

DCON. However, the metatranscriptomic data did not demonstrate evidence that bacteria were increasing transcripts for these metabolic pathways.

Xanthine was found in higher concentrations in INOC samples on day 5, which is to be expected in spoiling meat (Devi et al., 2013; Fang et al., 2022). Xanthine accumulates due to the breakdown of adenosine triphosphate to inosine monophosphate and is part of the purine metabolism. In high enough quantities, xanthine and hypoxanthine (a common derivative of xanthine) can contribute to bitter flavors and have been used to monitor meat spoilage (Jones, 1969; Devi et al., 2013; Bekhit et al., 2021). Fang et al. (2022) reported that xanthine production was associated with the co-culture of *Brochothrix thermosphacta* and *Pseudomonas lundensis* in meat exudate and suggested that lactic acid bacteria are more responsible for xanthine formation compared with *Pseudomonas* spp. The spoilage cocktail used in the current study included three strains of *Pseudomonas* and three strains of lactic acid bacteria.

Pyruvic acid was detected in greater abundance in the INOC samples compared to the DCON samples across display days (Table 4.5). In Chapter 3, pyruvic acid was also higher in the INOC samples compared to DCON LL samples during retail display. However, the difference in pyruvic acid concentration between treatments was magnitudes less in LL compared to PM, which could be due to a difference in the rate at which bacteria are utilizing aromatic amino acids between muscles.

Breakdown of phenylalanine can yield tyrosine, and tyrosine degradation metabolites can be shuttled into the citrate cycle (Sáez et al., 1999). Therefore, combining the lack of differences in the aromatic amino acid abundances between treatments in LL steaks, and the decrease in phenylalanine and tyrosine in the INOC

PM samples, it might be reasonable to conclude the degradation of aromatic amino acids could be one of the key differences between these systems. Moreover, decreased concentrations of glucose for INOC PM samples by day 5 might be indicating that bacteria were utilizing glucose throughout the display period.

The decreased abundance of galactose and galactose-6-phosphate in the INOC samples on day 5 may be suggesting that bacteria are forming a substantial number of glycosylated compounds, which could be impacting cellular function (Benz and Schmidt, 2002; Szymanski, 2022). This hypothesis is supported by increased glycosylamine and lipoglycan synthesis KOs in the metatranscriptomic dataset. However, there is limited knowledge on bacterial glycosylation (Szymanski, 2022). Further, galactose can be used for energy production, yet the transcripts for the rate limiting enzyme that controls the pathway was detected in decreasing abundance across display days. This suggests that bacteria might be utilizing galactose for exopolysaccharide (EPS) formation or alternative purposes, such as being converted to glucose and used in glycolytic pathways (Chai et al., 2012).

Metatranscriptomics

The metatranscriptomic data showed minimal functional changes over the measurement period (day 2 through 5) on PM steaks compared to the changes in beef LL (Chapter 3). There were statistically significant transcript changes between days 2 and 3 (2 changes) and/or 3 and 4 (30 changes). The percentage discoloration and a^* values became lower for INOC compared with DCON on day 4, suggesting that the transcript changes happened close to the change in meat color.

There were increases in transcripts related to the pentose phosphate pathway in the INOC steaks, which provides alternative pathways for glucose utilization, produces reducing equivalents, and generates amino sugars for RNA and DNA synthesis (Stincone et al., 2015). Along the same lines, there were two increased KOs for alternative sugar utilization, including mannose and galactose. The metabolomic data indicated that, compared to DCON, INOC had higher mannose concentrations on day 4 and lower galactose concentrations on day 5, suggesting that bacteria may have been utilizing or synthesizing saccharides. However, these sugars are not typically preferred by meat spoilage bacteria, and may be suggestive that the often preferred glucose was not as available (Gill, 1976; Wickramasinghe et al., 2019).

The substrates available to microbes generally dictate their growth potential. Differences in the environment, such as nominal changes to pH, temperature, or even carbon source, can impact bacterial function. For most meat spoilage bacteria, glucose is a vital and often the preferred carbon source (Nychas et al., 1988; Lambropoulou et al., 1996; Wickramasinghe et al., 2019). To better understand how glucose availability may influence bacterial function, it may be imperative to review a phenomenon known as carbon catabolite repression (CCR). Carbon catabolite repression is a regulatory mechanism found in almost all bacteria, and it suppresses bacterial functions for accessing secondary carbon sources (i.e., amino acids, fatty acids, alternative saccharides) when the preferred carbon source is present (Görke and Stülke, 2008). However, the exact mechanisms behind CCR are not well understood, and current evidence suggests post translational changes to RNA may control CCR in

gammaproteobacteria, to which pseudomonads belong (Görke and Stülke, 2008). Thus, CCR would not have been captured with the techniques used in this study.

While carbon metabolism has received the greatest attention in relation to bacterial metabolism and growth, nitrogen assimilation and utilization are also important. Bacterially derived nitrogenous compounds, such as putrescine and xanthine, have been routinely used to denote and characterize microbial spoilage of meat (Casaburi et al., 2015; Bekhit et al., 2021). Further, bacterial carbon sequestration is co-dependent with nitrogen sequestration, and sources of either element can impact bacterial growth rate and metabolism (Touratier et al., 1999). It is possible that the combination of glucose and amino acid availability was impacting bacterial metabolism and carbon catabolite suppression. For example, the metabolomic data showed decreased concentrations of phenylalanine and tyrosine in the INOC samples by day 5 compared with DCON. The decrease in these amino acids could suggest that they provided more favorable ratios of nitrogen and carbon compared to other amino acid and saccharide combinations.

Other transcript changes between days 3 and 4 in the PM INOC steaks included increases in transcripts generating cellular components, including flagellar assembly, biofilm formation, and quorum sensing transcripts. These findings were not surprising considering that bacteria were in the logarithmic phase of growth. There was no transcriptomic evidence of increased oxidative stress, such as increased antioxidant formation pathways, suggesting bacteria were not experiencing high stress during this phase (Mols and Abee, 2011).

Comparison of LL and PM muscles

In our previous study (Chapter 3), beef LL steaks were examined using similar methods. The data analysis in these two studies revealed differences in bacterial functional roles during discoloration. The bacteria from the LL steaks showed numerous changes to metabolic functions during the display period, specifically concerning amino acid and fatty acid metabolism (Chapter 3). The same spoilage organisms on PM steaks did not have the same changes as in LL, nor did they have a large magnitude of functional changes during initiation of substantial surface discoloration. However, the color and microbiological count data in the PM steaks suggest a strong connection between microbial growth and discoloration, suggesting that the bacterial functional changes may be muscle specific.

Due to the shorter shelf-life and shorter lag phase of bacterial populations on beef PM steaks, the metabolomic and metatranscriptomic analyses for PM and LL steaks were conducted on different display days (days 2 to 5 for PM and days 3 to 6 for LL). However, bacterial concentration, surface discoloration, and changes to redness (a^* values) were similar between the muscles. For example, APC on LL INOC steaks on day 3 was 5.1 log CFU/cm² whereas APC for PM INOC steaks was 5.0 log CFU/cm² on day 2. On those days (day 3 for LL and day 2 for PM), surface discoloration was approximately 0% for LL INOC steaks and 1% for PM INOC steaks. In LL steaks, bacterial functional changes occurred right before the color changes to the steaks' surface, whereas in PM, the majority (93.75%) of bacterial transcript changes occurred on day 4 when a^* values decreased and surface discoloration greatly increased for PM INOC steaks.

The combination of findings from both Chapter 3 and the current study suggests that muscle specific characteristics might be driving bacterial function differences. The PM muscle, which is a color labile muscle, tends to possess a greater proportion of type 1 muscle fibers compared with color stable muscles such as LL (Hunt and Hedrick, 1977). The muscle fiber differences could be leading to significant differences in metabolites available for microbial growth. Type 1 fibers contain lower concentrations of glucose compared with other fiber types (Picard and Gagaoua, 2020). The PM also contains a higher mitochondrial content than the LL (Mohan et al., 2010; Ramanathan et al., 2015), which can substantially affect postmortem metabolite utilization. Moreover, previous studies by Abraham et al. (2017) demonstrated that there were differences in metabolites in beef LL and PM, which could be contributing to their different color stability during retail display.

There was also a slight difference in pH between LL and PM, with PM having 0.1 to 0.2 units higher pH than LL (Smith et al., 2024b). The difference in muscle pH could play a role in bacterial function (Abraham et al., 2018). The higher pH in PM could promote metabolic changes based on pH-related enzymatic feedback loops (Koutsoumanis et al., 2006). Another muscle-specific difference could be the iron availability. Iron concentrations in PM may be greater than LL (Valenzuela et al., 2009; Food Search | USDA FoodData Central), and iron is a vital cofactor for bacteria, especially pseudomonads (Ercolini et al., 2009; Cornelis, 2010; Zhang et al., 2024). Along the same lines, pseudomonads oxidize ferric to ferrous iron as the oxidized form is more accessible (Cornelis, 2010). Moreover, there is limited information concerning meat spoilage bacteria and iron utilization. Previous studies have shown that *L. sakei*

can use heme iron from myoglobin, which could influence meat color stability through similar redox reactions to pseudomonads (Verplaetse et al., 2020). Nonetheless, the data from the study provide evidence that in both muscles, bacterial growth impacts color stability, and thus shelf-life differences.

Conclusions

The results of this study showed that the growth of spoilage bacteria can impact the color stability of PM during retail display. The metabolomic and metatranscriptomic data suggest a decreased reliance on glucose derived energy metabolism with a general shift toward aromatic amino acid utilization by bacteria around the same time as discoloration is occurring on PM steaks. Moreover, there could be muscle-specific factors impacting microbial growth, substrate utilization, and function in PM steaks during retail display. These results imply that strategies to increase shelf-life of one muscle may not be as effective when applied to another, suggesting the need for targeted approaches to improve meat shelf-life for different beef muscles.

Table 4.1. Marginal means \pm standard error of CIE a^* (redness), and b^* (yellowness) of decontaminated (DCON) and inoculated (INOC) treatment groups of beef *psoas major* steaks during simulated retail display (3°C).

Day	a^* value		b^* value	
	DCON	INOC	DCON	INOC
0	28.26 \pm 0.62 ^{az}	28.28 \pm 0.37 ^{az}	22.77 \pm 0.58 ^{az}	22.64 \pm 0.44 ^{az}
1	24.81 \pm 0.74 ^{ay}	25.85 \pm 0.63 ^{az}	20.94 \pm 0.47 ^{azy}	21.46 \pm 0.45 ^{azy}
2	23.06 \pm 0.98 ^{ayx}	22.86 \pm 0.69 ^{ay}	20.51 \pm 0.68 ^{ay}	20.07 \pm 0.49 ^{ay}
3	21.44 \pm 0.77 ^{axw}	21.01 \pm 1.09 ^{ay}	19.95 \pm 0.44 ^{ayx}	19.83 \pm 0.65 ^{ay}
4	18.40 \pm 0.54 ^{av}	16.78 \pm 0.92 ^{ax}	17.64 \pm 0.42 ^{aw}	17.52 \pm 0.58 ^{ax}
5	17.90 \pm 0.75 ^{av}	13.33 \pm 0.91 ^{bw}	18.16 \pm 0.49 ^{axw}	16.36 \pm 0.49 ^{bx}
6	19.18 \pm 1.07 ^{awv}	13.97 \pm 0.76 ^{bw}	20.59 \pm 0.57 ^{ay}	17.28 \pm 0.47 ^{bx}

^{a-b}Marginal means within a row and measurement type without a common superscript letter are different ($P < 0.05$).

^{z-w}Marginal means within a column without a common superscript letter are different ($P < 0.05$).

Table 4.2. Marginal means \pm standard error of percentage discoloration of decontaminated (DCON) and inoculated (INOC) treatment groups of beef *psaos major* steaks during simulated retail display (3°C).

Day	% Discoloration ¹	
	DCON	INOC
0	0.0 \pm 0.0 ^{ay}	0.0 \pm 0.0 ^{ax}
1	0.0 \pm 0.0 ^{ay}	0.0 \pm 0.0 ^{ax}
2	1.0 \pm 0.6 ^{ay}	0.8 \pm 0.5 ^{ax}
3	5.6 \pm 2.7 ^{ay}	8.0 \pm 2.3 ^{ax}
4	16.3 \pm 5.5 ^{by}	46.4 \pm 8.8 ^{ay}
5	12.4 \pm 6.0 ^{by}	71.9 \pm 8.2 ^{az}
6	37.3 \pm 9.0 ^{bx}	87.1 \pm 2.8 ^{az}

^{a-b}Marginal means within a row without a common superscript letter are different ($P < 0.05$).

^{z-y}Marginal means within a column without a common superscript letter are different ($P < 0.05$).

¹Panelists scored each steak to assess lean color using a continuous 8-point scale (1 = extremely bright cherry-red, 2 = bright cherry-red, 3 = moderately bright cherry-red, 4 = slightly bright cherry-red, 5 = slightly dark cherry-red, 6 = moderately dark red, 7 = dark red, 8 = extremely dark red).

Table 3. Marginal mean \pm standard deviation (log CFU/cm²) of aerobic plate counts (APC), lactic acid bacteria counts (LABC), and *Pseudomonas* spp. counts recovered from decontaminated (DCON) and inoculated (INOC) treatment groups of beef *psaos major* steaks during simulated retail display (3°C).

Day	APC		LABC		<i>Pseudomonas</i> spp.	
	DCON	INOC	DCON	INOC	DCON	INOC
0	<0.3 \pm 0.1 ^{by*}	4.0 \pm 0.2 ^{aw}	<0.2 \pm 0.2 ^{bz}	3.8 \pm 0.2 ^{av}	<0.2 \pm 0.0 ^{by}	3.6 \pm 0.2 ^{av}
1	<0.5 \pm 0.6 ^{by}	4.5 \pm 0.2 ^{aw}	<0.4 \pm 0.7 ^{bz}	4.1 \pm 0.2 ^{av}	<0.3 \pm 0.5 ^{bzy}	4.2 \pm 0.3 ^{awv}
2	<0.3 \pm 0.3 ^{by}	5.0 \pm 0.2 ^{aw}	<0.2 \pm 0.0 ^{bz}	4.3 \pm 0.4 ^{awv}	<0.3 \pm 0.1 ^{by}	5.5 \pm 0.2 ^{aw}
3	<0.9 \pm 1.3 ^{bzy}	6.1 \pm 0.5 ^{ax}	<0.8 \pm 1.1 ^{bz}	5.1 \pm 0.6 ^{axw}	<0.6 \pm 1.3 ^{bzy}	6.3 \pm 0.5 ^{ax}
4	<0.5 \pm 0.7 ^{by}	7.4 \pm 0.5 ^{ay}	<0.3 \pm 0.3 ^{bz}	5.9 \pm 0.7 ^{ayx}	<0.4 \pm 0.8 ^{bzy}	7.5 \pm 0.5 ^{ay}
5	<1.2 \pm 1.5 ^{bzy}	8.1 \pm 0.4 ^{azy}	<0.5 \pm 0.9 ^{bz}	6.4 \pm 0.5 ^{ay}	<0.9 \pm 1.4 ^{bzy}	8.2 \pm 0.4 ^{azy}
6	<1.7 \pm 2.0 ^{bz}	8.7 \pm 0.4 ^{az}	<0.7 \pm 1.4 ^{bz}	7.4 \pm 0.4 ^{az}	<1.3 \pm 2.0 ^{bz}	8.7 \pm 0.4 ^{az}

^{a-b}Marginal means within a row and bacterial count type without a common superscript letter are different ($P < 0.05$).

^{z-u}Marginal means within a column without a common superscript letter are different ($P < 0.05$).

*Marginal means with a less than symbol (<) indicate one or more of the samples within the treatment had plate counts below the analysis detection limit (0.2 log CFU/cm²).

Table 4.4. Bacterial growth kinetics for the INOC treatment calculated from the bacterial population counts recovered from beef *longissimus lumborum* (LL) and *psoas major* (PM) steaks in aerobic packaging during simulated retail display at 3°C up to 8 days for LL and 7 days for PM.

Count Type	Muscle	Lag Duration ¹	Maximum Growth Rate ²	R ²	Standard Error of Fit
APC ³	LL	1.625±0.268	1.022±0.070	0.948	0.442
	PM	1.219±0.196	1.146±0.072	0.955	0.373
<i>Pseudomonas</i> spp. ⁴	LL	1.179±0.244	1.010±0.057	0.958	0.415
	PM	0.772±0.184	1.177±0.065	0.964	0.358
LABC ⁵	LL	3.109±0.218	0.786±0.050	0.903	0.361
	PM	1.436±0.316	0.764±0.053	0.884	0.448

¹Duration of the lag phase in 24 h increments.

²Maximum growth measured in log CFU/cm² bacteria could achieve in 24 h.

³Aerobic Plate Counts

⁴*Pseudomonas* spp. Plate Counts

⁵Lactic Acid Bacteria Plate Counts

Table 4.5. Marginal means of relative abundance of metabolites with treatment by display day interactions ($P < 0.05$) detected from decontaminated (DCON) and inoculated (INOC) treatment groups of beef *psoas major* steaks during simulated retail display (3°C).

Metabolite	Display Day							
	2		3		4		5	
	DCON	INOC	DCON	INOC	DCON	INOC	DCON	INOC
Phenylalanine	9.4×10^{6a}	9.4×10^{6a}	1.0×10^{7a}	1.0×10^{7a}	9.5×10^{6a}	1.4×10^{7b}	1.6×10^{7a}	1.3×10^{7a}
Tyrosine	2.1×10^{7a}	2.0×10^{7a}	2.2×10^{7a}	2.1×10^{7a}	2.2×10^{7a}	2.4×10^{7a}	2.7×10^{7a}	1.8×10^{7b}
Glutamic Acid	8.7×10^{6a}	9.0×10^{6a}	9.8×10^{6a}	6.1×10^{6a}	8.1×10^{6a}	6.4×10^{6a}	1.2×10^{7a}	2.5×10^{6b}
Xanthine	1.9×10^{7a}	1.8×10^{7a}	1.8×10^{7a}	1.9×10^{7a}	2.1×10^{7b}	3.7×10^{7a}	2.3×10^{7b}	4.0×10^{7a}
Lactic Acid	2.8×10^{8a}	2.8×10^{8a}	2.7×10^{8a}	2.8×10^{8a}	2.8×10^{8a}	2.6×10^{8a}	2.7×10^{8a}	2.5×10^{8b}
Pyruvic Acid	3.6×10^{5a}	4.1×10^{5a}	3.5×10^{5b}	2.4×10^{6a}	3.7×10^{5b}	1.4×10^{7a}	3.1×10^{5b}	2.0×10^{7a}
Idose	1.3×10^{8a}	1.3×10^{8a}	1.4×10^{8a}	1.3×10^{8a}	1.0×10^{8a}	1.1×10^{8a}	1.3×10^{8a}	4.9×10^{7b}
Mannose	4.0×10^{7a}	4.3×10^{7a}	4.8×10^{7a}	4.3×10^{7a}	3.0×10^{7b}	5.3×10^{7a}	4.2×10^{7a}	3.3×10^{7a}
Glucose	3.1×10^{7a}	3.1×10^{7a}	3.2×10^{7a}	2.9×10^{7a}	2.4×10^{7a}	2.6×10^{7a}	3.1×10^{7a}	1.3×10^{7b}
Galactose	9.3×10^{6a}	9.4×10^{6a}	1.1×10^{7a}	7.5×10^{6a}	8.2×10^{6a}	7.2×10^{6a}	8.8×10^{6a}	3.0×10^{6b}
Galactose-6-Phosphate	4.4×10^{6a}	5.5×10^{6a}	5.5×10^{6a}	4.1×10^{6a}	2.2×10^{6a}	5.2×10^{6a}	4.4×10^{6a}	1.8×10^{6b}
Phosphoric Acid	7.6×10^{8a}	7.4×10^{8a}	7.6×10^{8a}	7.6×10^{8a}	8.0×10^{8a}	7.6×10^{8a}	7.5×10^{8a}	8.4×10^{8b}

^{a-b}Marginal means within a row and display day without a common superscript letter are different ($P < 0.05$).

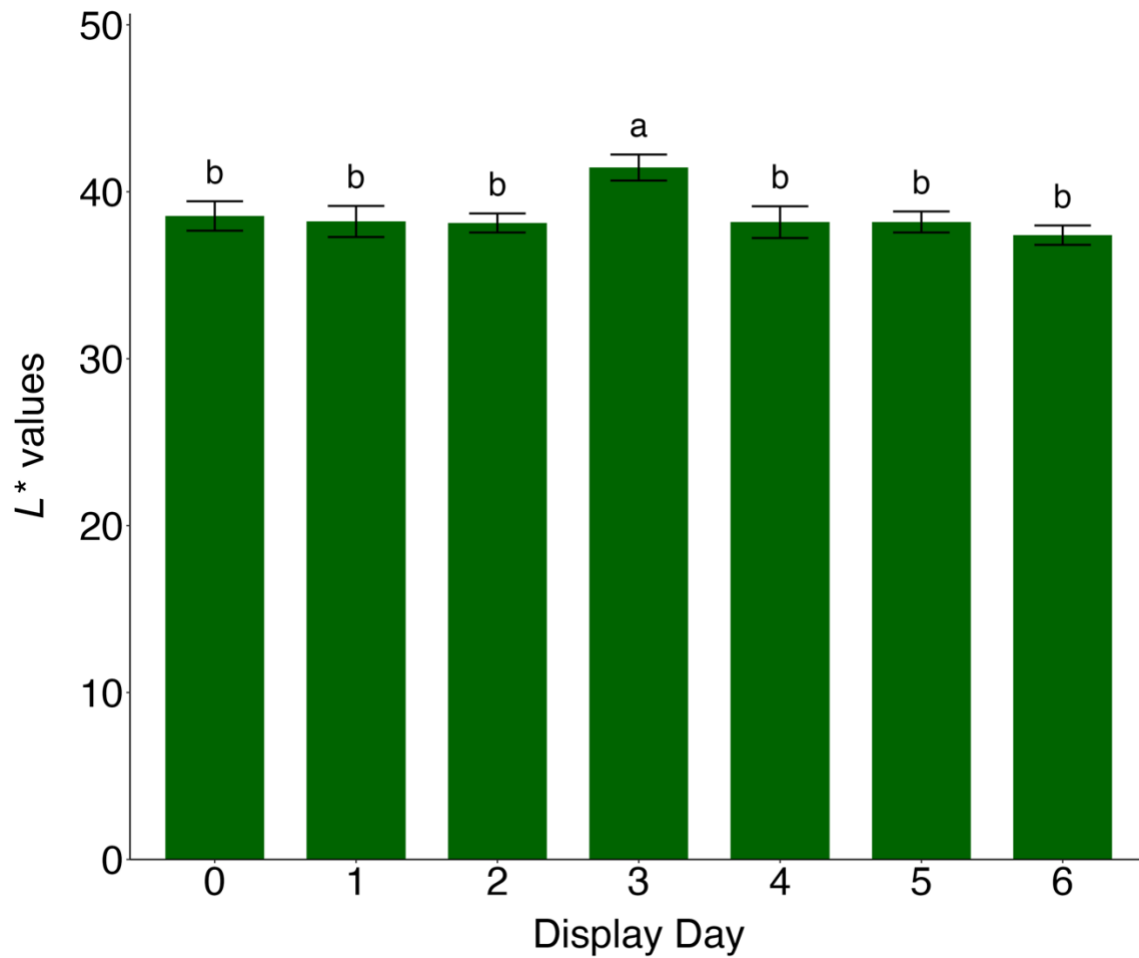


Figure 4.1. Marginal means \pm standard error of CIE L^* (lightness) of decontaminated (DCON) and inoculated (INOC) treatment groups of beef *psoas major* steaks during simulated retail display (3°C).

^{a-b}Bars without a common superscript letter are different ($P < 0.05$).

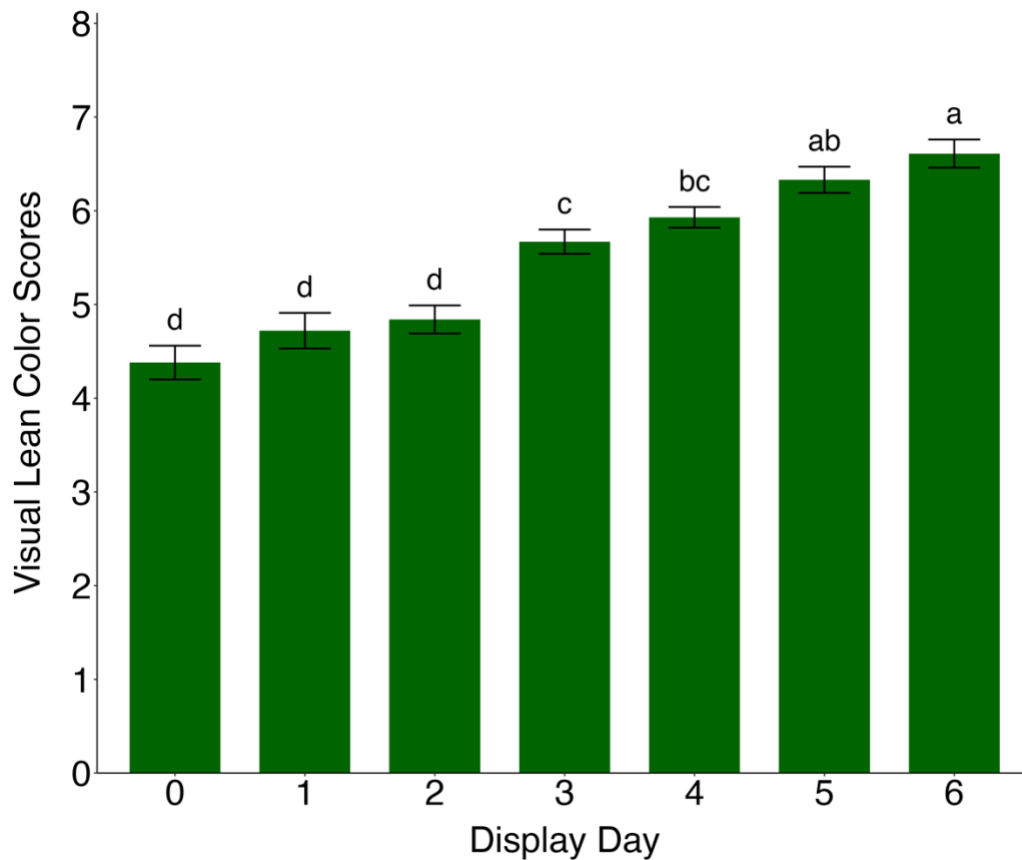


Figure 4.2. Marginal means \pm standard error of visual lean color scores of decontaminated (DCON) and inoculated (INOC) treatment groups of beef *psaos major* steaks during simulated retail display (3°C). Panelists scored each steak to assess lean color using a continuous 8-point scale (1 = extremely bright cherry-red, 2 = bright cherry-red, 3 = moderately bright cherry-red, 4 = slightly bright cherry-red, 5 = slightly dark cherry-red, 6 = moderately dark red, 7 = dark red, 8 = extremely dark red).
^{a-d}Bars without a common superscript letter are different ($P < 0.05$).

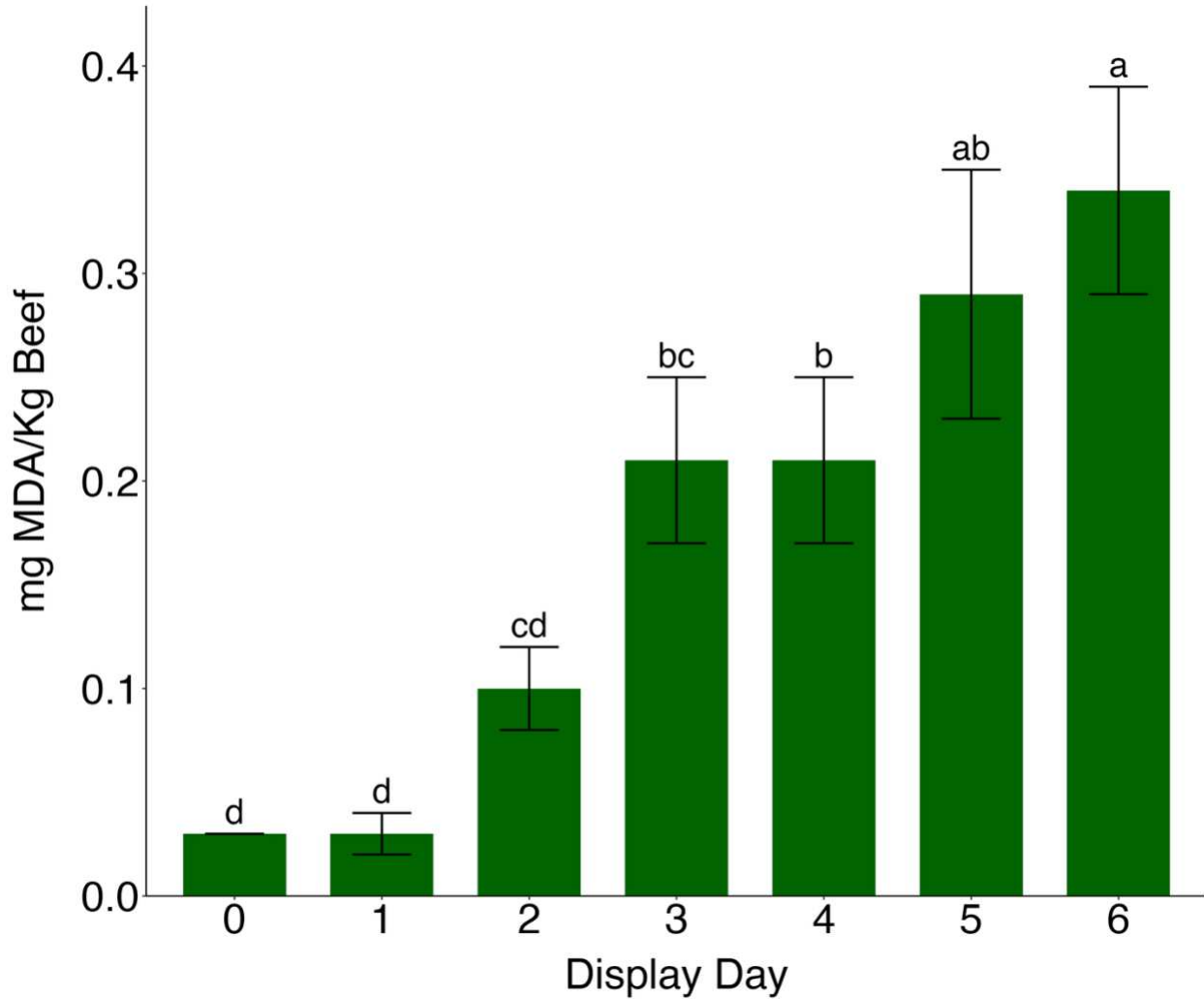


Figure 4.3. Marginal means \pm standard error of thiobarbituric reactive substances (TBARS) of decontaminated (DCON) and inoculated (INOC) treatment groups averaged across day of beef *psoas major* steaks during simulated retail display (3°C).
^{a-d}Bars without a common superscript letter are different ($P < 0.05$).

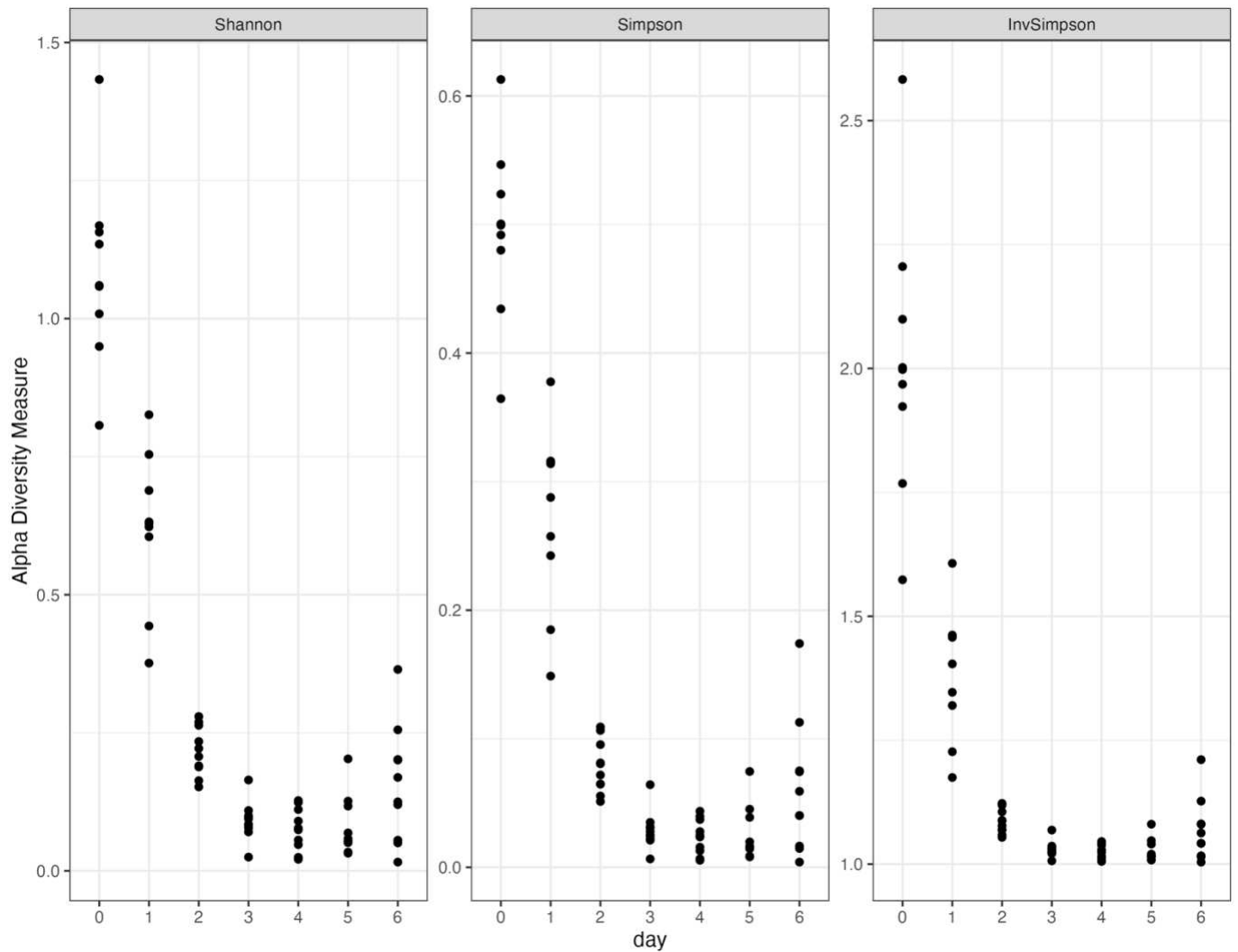


Figure 4.4. Alpha diversity metrics of Shannon, Simpson, and Inverse Simpson Indices as plotted for beef *psoas major* steaks inoculated with a 6-isolate spoilage bacteria mixture and subsequently placed into simulated retail display (3°C).

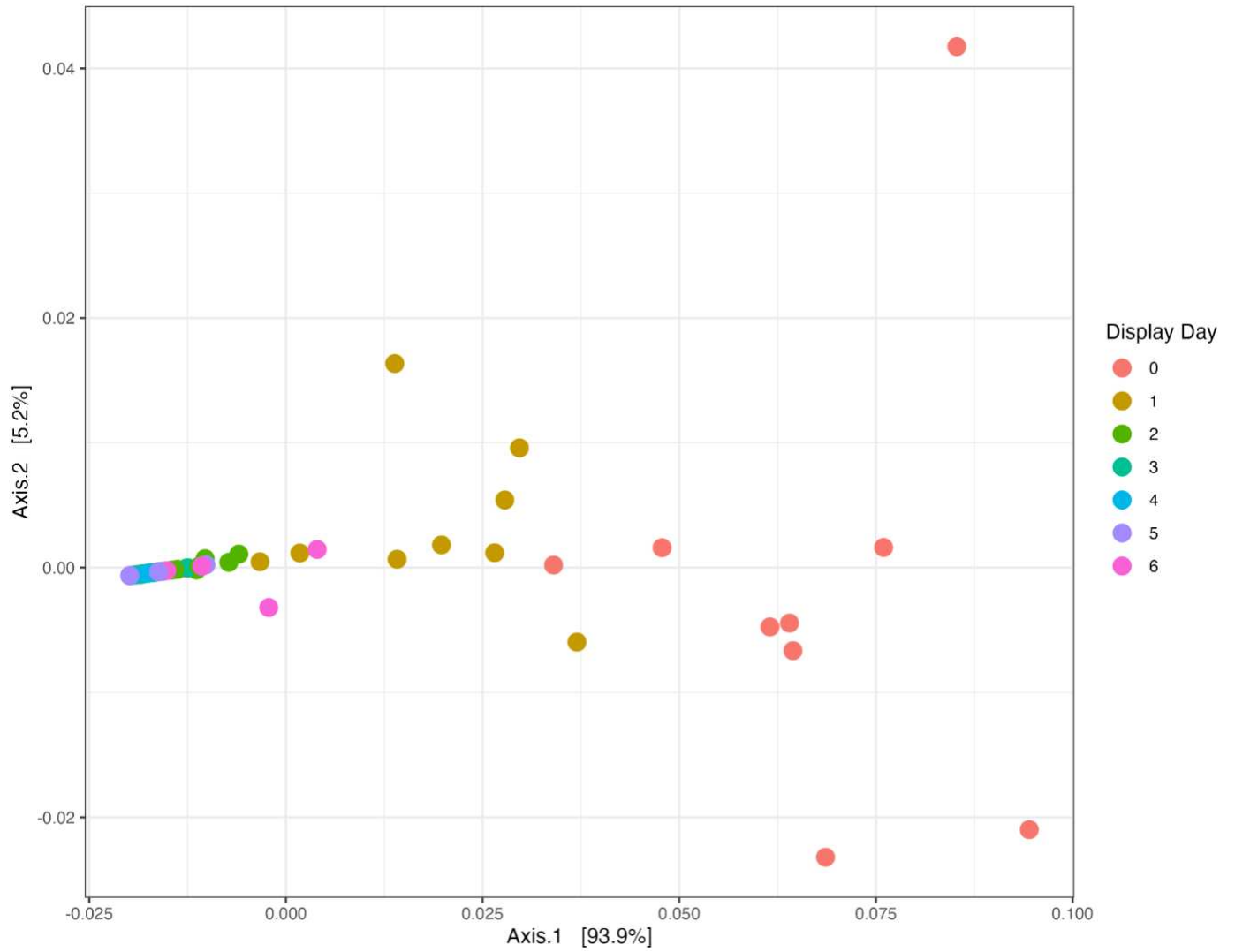


Figure 4.5. Beta diversity shown as a weighted UniFrac principle coordinates analysis (PCoA) for beef *psoas major* steaks inoculated with a 6-isolate spoilage bacteria mixture and subsequently placed into simulated retail display (3°C).

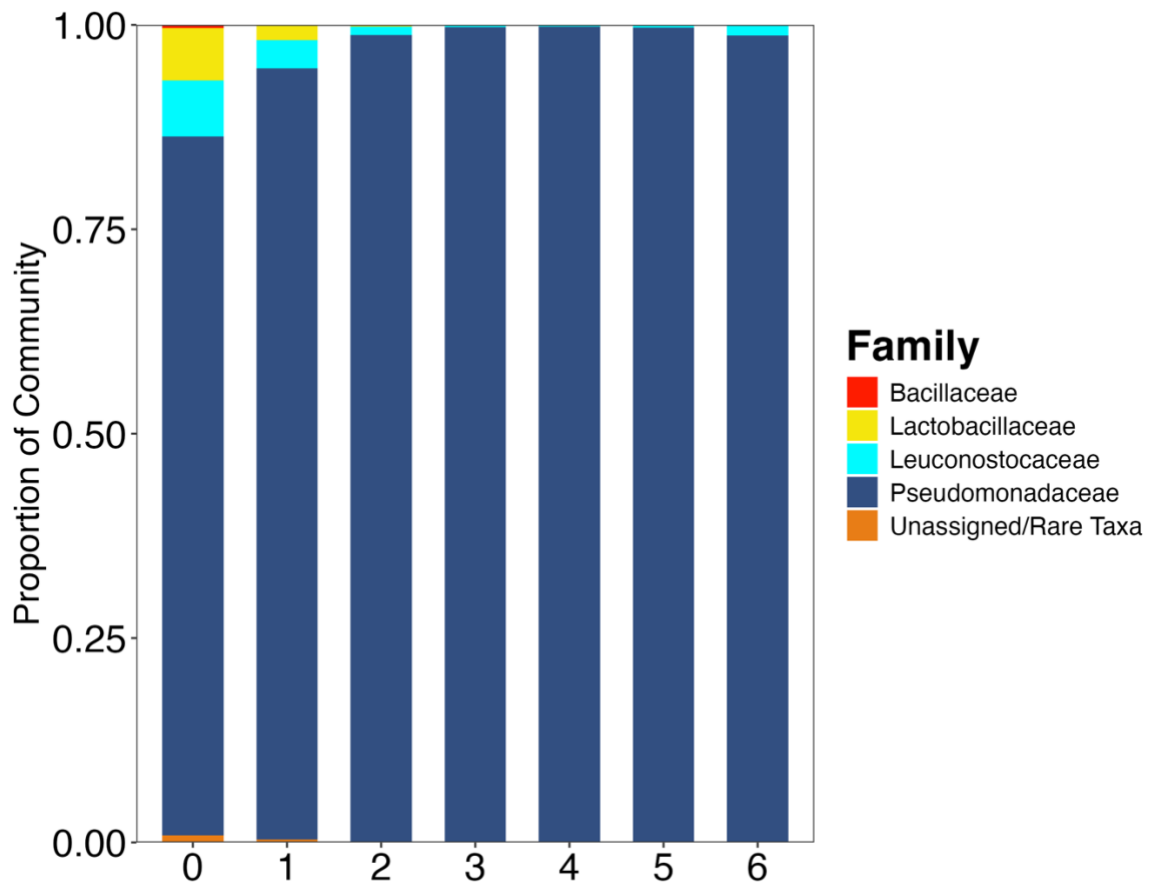


Figure 4.6. Relative abundance taxa bar plot organized at the family level for beef *psoas major* (PM) steaks inoculated with a 6-isolate spoilage bacteria mixture and subsequently placed into simulated retail display (3°C).

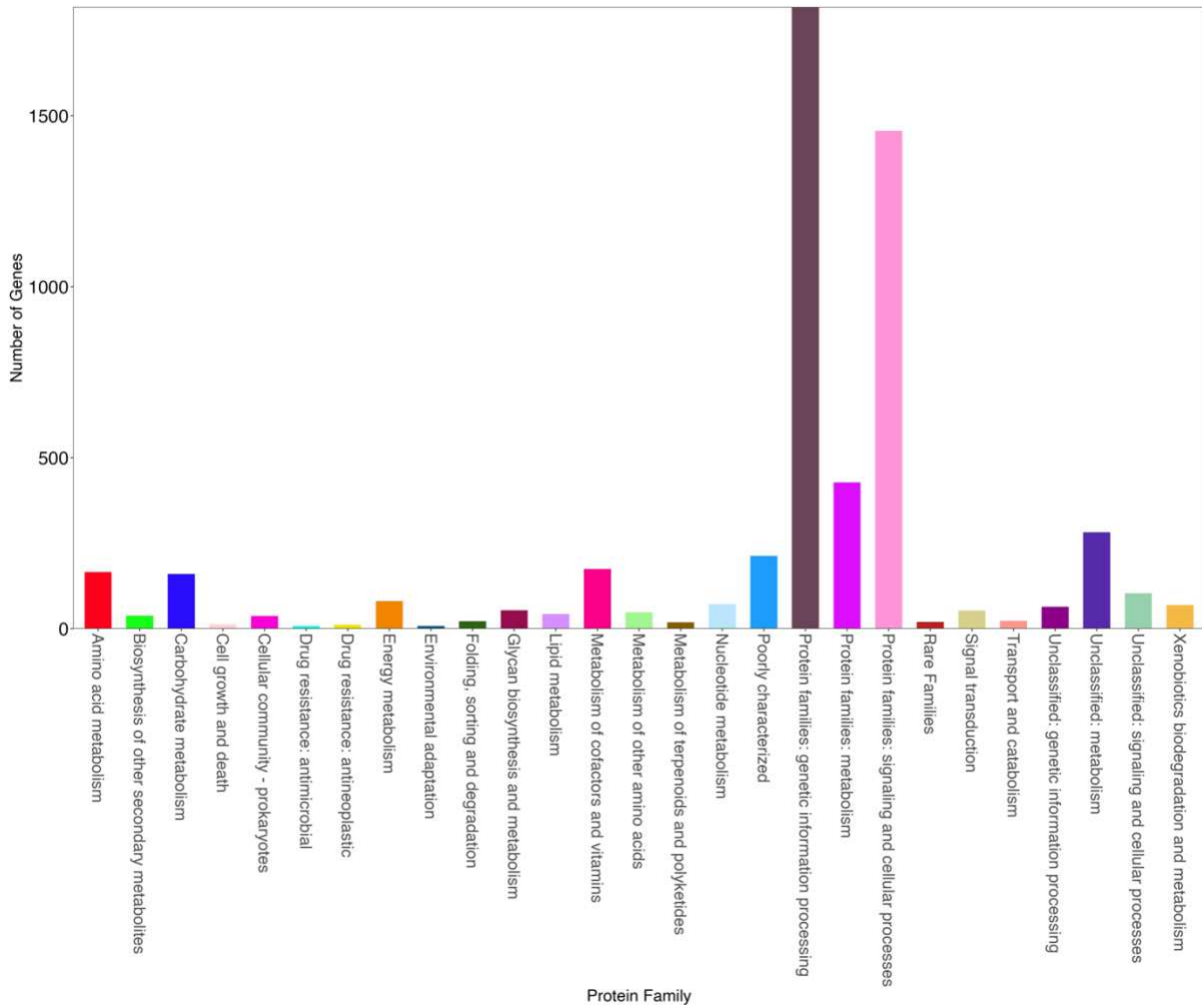


Figure 4.7. Total number of protein families detected in the metatranscriptomic dataset collected from bacterial populations growing on beef *psaos major* during retail display in aerobic packaging.

REFERENCES

- Amino Acid Catabolism. 2016. Biol. Libr. Available from:
[https://bio.libretexts.org/Bookshelves/Biochemistry/Book%3A_Biochemistry_Free_and_Easy_\(Ahern_and_Rajagopal\)/07%3A_Metabolism_II/7.08%3A_Amino_Acid_Catabolism](https://bio.libretexts.org/Bookshelves/Biochemistry/Book%3A_Biochemistry_Free_and_Easy_(Ahern_and_Rajagopal)/07%3A_Metabolism_II/7.08%3A_Amino_Acid_Catabolism)
- Abraham, A., J. W. Dillwith, D. L. VanOverbeke, G. G. Mafi, and R. Ramanathan. 2018. Analyzing Beef Color Stability Differences with Metabolomics. *Meat Muscle Biol.* 1. doi:10.221751/rmc2016.150. Available from:
<https://www.iastatedigitalpress.com/mmb/article/id/9245/>
- Ahn, S., J. Jung, I.-A. Jang, E. L. Madsen, and W. Park. 2016. Role of Glyoxylate Shunt in Oxidative Stress Response. *J. Biol. Chem.* 291:11928–11938. doi:10.1074/jbc.M115.708149.
- Alanís, E., P. Lara, and I. Guerrero. 1999. Proteolytic activity of four strains of *Pseudomonas* on crude extracts of contractile proteins. *Food Chem.* 67:45–51. doi:10.1016/S0308-8146(99)00108-9.
- Ardö, Y. 2006. Flavour formation by amino acid catabolism. *Biotechnol. Adv.* 24:238–242. doi:10.1016/j.biotechadv.2005.11.005.
- Argyri, A. A., A. Mallouchos, E. Z. Panagou, and G.-J. E. Nychas. 2015. The dynamics of the HS/SPME–GC/MS as a tool to assess the spoilage of minced beef stored under different packaging and temperature conditions. *Int. J. Food Microbiol.* 193:51–58. doi:10.1016/j.ijfoodmicro.2014.09.020.
- Atkinson, J. L., and M. J. Follett. 1973. Biochemical studies on the discoloration of fresh meat. *Int. J. Food Sci. Technol.* 8:51–58. doi:10.1111/j.1365-2621.1973.tb01688.x.
- Ayres, j. c. 1960. Temperature relationships and some other characteristics of the microbial flora developing on refrigerated beef a. *J. Food Sci.* 25:1–18. doi:10.1111/j.1365-2621.1960.tb17930.x.
- Bala, K., R. T. Marshall, W. C. Stringer, and H. D. Naumann. 1977. Effect of *Pseudomonas fragi* on the color of beef. *J. Food Sci.* 42:1176–1179. doi:10.1111/j.1365-2621.1977.tb14454.x.
- Baranyi, J., and T. A. Roberts. 1994. A dynamic approach to predicting bacterial growth in food. *Int. J. Food Microbiol.* 23(3-4):277-294. doi:10.1016/0168-1605(94)90157-0.
- Bekhit, A. E.-D. A., B. W. B. Holman, S. G. Giteru, and D. L. Hopkins. 2021. Total volatile basic nitrogen (TVB-N) and its role in meat spoilage: A review. *Trends Food Sci. Technol.* 109:280–302. doi:10.1016/j.tifs.2021.01.006.
- Benz, I., and M. A. Schmidt. 2002. Never say never again: protein glycosylation in pathogenic bacteria. *Mol. Microbiol.* 45:267–276. doi:10.1046/j.1365-2958.2002.03030.x.
- Bhat, Z. F., J. D. Morton, S. L. Mason, and A. E.-D. A. Bekhit. 2018. Role of calpain system in meat tenderness: A review. *Food Sci. Hum. Wellness.* 7:196–204. doi:10.1016/j.fshw.2018.08.002.

- Bren, A., J. O. Park, B. D. Towbin, E. Dekel, J. D. Rabinowitz, and U. Alon. 2016. Glucose becomes one of the worst carbon sources for E.coli on poor nitrogen sources due to suboptimal levels of cAMP. *Sci. Rep.* 6:24834. doi:10.1038/srep24834.
- Cabos, A., and O. Diaz. 2015. Chapter 16: Chemical composition of meat and meat products. P. C. K. Cheung and B. M. Mehta (eds.). in *Handbook of Food Chemistry*. doi:10.1007/978-3-642-36605-5_6
- Capouya, R., T. Mitchell, D. I. Clark, D. L. Clark, and P. Bass. 2020. A Survey of Microbial Communities on Dry-Aged Beef in Commercial Meat Processing Facilities. *Meat Muscle Biol.* 4. doi:10.22175/mmb.10373.
- Carpenter, C. E., D. P. Cornforth, and D. Whittier. 2001. Consumer preferences for beef color and packaging did not affect eating satisfaction. *Meat Sci.* 57:359–363. doi:10.1016/S0309-1740(00)00111-X.
- Casaburi, A., P. Piombino, G.-J. Nychas, F. Villani, and D. Ercolini. 2015. Bacterial populations and the volatilome associated to meat spoilage. *Food Microbiol.* 45:83–102. doi:10.1016/j.fm.2014.02.002.
- Cassens, R. G. 2008. *Meat preservation: Preventing losses and assuring safety*. John Wiley & Sons.
- Chai, C., S.-Y. Lee, and S.-W. Oh. 2017. Shelf-life charts of beef according to level of bacterial contamination and storage temperature. *LWT - Food Sci. Technol.* 81:50–57. doi:10.1016/j.lwt.2017.03.023.
- Chai, Y., P. B. Beauregard, H. Vlamakis, R. Losick, and R. Kolter. 2012. Galactose Metabolism Plays a Crucial Role in Biofilm Formation by *Bacillus subtilis*. *mBio.* 3:10.1128/mbio.00184-12. doi:10.1128/mbio.00184-12.
- Chan, W. K. M., S.-T. Joo, C. Faustman, Q. Sun, and R. Vieth. 1998. Effect of *Pseudomonas fluorescens* on beef discoloration and oxymyoglobin oxidation in vitro. *J. Food Prot.* 61:1341–1346. doi:10.4315/0362-028X-61.10.1341.
- Chen, J., J. Zhang, N. Wang, B. Xiao, X. Sun, J. Li, K. Zhong, L. Yang, X. Pang, F. Huang, and A. Chen. 2024. Critical review and recent advances of emerging real-time and non-destructive strategies for meat spoilage monitoring. *Food Chem.* 445:138755. doi:10.1016/j.foodchem.2024.138755.
- Chen, Y., F. Ma, Y. Wu, S. Tan, A. Niu, W. Qiu, and G. Wang. 2023. Biosurfactant from *Pseudomonas fragi* enhances the competitive advantage of *Pseudomonas* but reduces the overall spoilage ability of the microbial community in chilled meat. *Food Microbiol.* 115:104311. doi:10.1016/j.fm.2023.104311.
- Clark, D. S., and C. P. Lentz. 1969. The effect of carbon dioxide on the growth of slime producing bacteria on fresh beef. *Can. Inst. Food Technol. J.* 2:72–75. doi:10.1016/S0008-3860(69)74365-3.
- Comi, G. 2017. Chapter 8 - Spoilage of meat and fish. In: A. Bevilacqua, M. R. Corbo, and M. Sinigaglia, editors. *The Microbiological Quality of Food*. Woodhead Publishing. p. 179–210.
- Commichau, F. M., K. Gunka, J. J. Landmann, and J. Stülke. 2008. Glutamate Metabolism in *Bacillus subtilis*: Gene Expression and Enzyme Activities Evolved To Avoid Futile Cycles and To Allow Rapid Responses to Perturbations of the System. *J. Bacteriol.* 190:3557–3564. doi:10.1128/JB.00099-08.

- Cornelis, P. 2010. Iron uptake and metabolism in pseudomonads. *Appl. Microbiol. Biotechnol.* 86:1637–1645. doi:10.1007/s00253-010-2550-2.
- Couchet, M., C. Breuillard, C. Corne, J. Rendu, B. Morio, U. Schlattner, and C. Moinard. 2021. Ornithine Transcarbamylase – From Structure to Metabolism: An Update. *Front. Physiol.* 12:748249. doi:10.3389/fphys.2021.748249.
- Cross, H.R., P. R. Durland, S. C. Seideman. 1986. Sensory qualities of meat. In: Bechtel, P.J. (Ed.), *Muscle as Food*. Academic Press, Orlando, pp. 284–285.
- Dainty, R. H., and B. M. Mackey. 1992. The relationship between the phenotypic properties of bacteria from chill-stored meat and spoilage processes. *J. Appl. Bacteriol.* 73:103s–114s. doi:10.1111/j.1365-2672.1992.tb03630.x.
- Dainty, R. H., R. A. Edwards, and C. M. Hibbard. 1985. Time course of volatile compound formation during refrigerated storage of naturally contaminated beef in air. *J. Appl. Bacteriol.* 59:303–309. doi:10.1111/j.1365-2672.1985.tb03324.x.
- Dainty, R. H., R. A. Edwards, C. M. Hibbard, and J. J. Marnewick. 1989. Volatile compounds associated with microbial growth on normal and high pH beef stored at chill temperatures. *J. Appl. Bacteriol.* 66:281–289. doi:10.1111/j.1365-2672.1989.tb02480.x.
- De Filippis, F. D., A. L. Storia, F. Villani, and D. Ercolini. 2013. Exploring the sources of bacterial spoilers in beefsteaks by culture-independent high-throughput sequencing. *PLOS ONE.* 8:e70222. doi:10.1371/journal.pone.0070222.
- Degeest, B., B. Janssens, and L. De Vuyst. 2001. Exopolysaccharide (EPS) biosynthesis by *Lactobacillus sakei* 0–1: production kinetics, enzyme activities and EPS yields. *J. Appl. Microbiol.* 91:470–477. doi:10.1046/j.1365-2672.2001.01404.x.
- Devi, R., B. Batra, S. Lata, S. Yadav, and C. S. Pundir. 2013. A method for determination of xanthine in meat by amperometric biosensor based on silver nanoparticles/cysteine modified Au electrode. *Process Biochem.* 48:242–249. doi:10.1016/j.procbio.2012.12.009.
- Domínguez, R., M. Pateiro, M. Gagaoua, F. J. Barba, W. Zhang, and J. M. Lorenzo. 2019. A comprehensive review on lipid oxidation in meat and meat products. *Antioxidants.* 8:429. doi:10.3390/antiox8100429.
- Doster, E., K. M. Thomas, M. D. Weinroth, J. K. Parker, K. K. Crone, T. M. Arthur, J. W. Schmidt, T. L. Wheeler, K. E. Belk, and P. S. Morley. 2020. Metagenomic characterization of the microbiome and resistome of retail ground beef products. *Front. Microbiol.* 11. doi:10.3389/fmicb.2020.541972.
- Doulgeraki, A. I., D. Ercolini, F. Villani, and G.-J. E. Nychas. 2012. Spoilage microbiota associated to the storage of raw meat in different conditions. *Int. J. Food Microbiol.* 157:130–141. doi:10.1016/j.ijfoodmicro.2012.05.020.
- Dourou, D., A. I. Doulgeraki, S. Vitsou-Anastasiou, A. A. Argyri, N. G. Chorianopoulos, G.-J. E. Nychas, and C. C. Tassou. 2023. Deciphering the growth responses and genotypic diversity of bioluminescent *Photobacterium phosphoreum* on chicken meat during aerobic refrigerated storage. *Int. J. Food Microbiol.* 405:110334. doi:10.1016/j.ijfoodmicro.2023.110334.
- Downard, K. 2007. *Mass Spectrometry: A Foundation Course*. Royal Society of Chemistry.

- Ederer, P., I. Baltenweck, J. N. Blignaut, C. Moretti, and S. Tarawali. 2023. Affordability of meat for global consumers and the need to sustain investment capacity for livestock farmers. *Anim. Front.* 13:45–60. doi:10.1093/af/vfad004.
- Eisenreich, W., A. Bacher, D. Arigoni, and F. Rohdich. 2004. Biosynthesis of isoprenoids via the non-mevalonate pathway. *Cell. Mol. Life Sci. CMLS.* 61:1401–1426. doi:10.1007/s00018-004-3381-z.
- Ercolini, D., A. Casaburi, A. Nasi, I. Ferrocino, R. Di Monaco, P. Ferranti, G. Mauriello, and F. Villani. 2010. Different molecular types of *Pseudomonas fragi* have the same overall behaviour as meat spoilers. *Int. J. Food Microbiol.* 142:120–131. doi:10.1016/j.ijfoodmicro.2010.06.012.
- Ercolini, D., F. Russo, A. Nasi, P. Ferranti, and F. Villani. 2009. Mesophilic and Psychrotrophic Bacteria from Meat and Their Spoilage Potential In Vitro and in Beef. *Appl. Environ. Microbiol.* 75:1990–2001. doi:10.1128/AEM.02762-08.
- Fang, J., L. Feng, H. Lu, and J. Zhu. 2022. Metabolomics reveals spoilage characteristics and interaction of *Pseudomonas lundensis* and *Brochothrix thermosphacta* in refrigerated beef. *Food Res. Int.* 156:111139. doi:10.1016/j.foodres.2022.111139.
- Faustman, C., Q. Sun, R. Mancini, and S. P. Suman. 2010. Myoglobin and lipid oxidation interactions: Mechanistic bases and control. *Meat Sci.* 86:86–94. doi:10.1016/j.meatsci.2010.04.025.
- Faustman, C., R. G. Cassens. 1990. Influence of aerobic metmyoglobin reducing capacity on color stability of beef. *J. Food Sci.* 55:1201-1484. doi:10.1111/j.1365-2621.1990.tb03915.x
- Feuz, R., F. B. Norwood, and R. Ramanathan. 2020. Do consumers have an appetite for discolored beef? *Agribusiness.* 36:631–652. doi:10.1002/agr.21651.
- Flint, A., A. Cooper, M. Rao, K. Weedmark, C. Carrillo, and S. Tamber. 2023. Targeted metagenomics using bait-capture to detect antibiotic resistance genes in retail meat and seafood. *Front. Microbiol.* 14. doi:10.3389/fmicb.2023.1188872.
- Font-i-Furnols, M., and L. Guerrero. 2014. Consumer preference, behavior and perception about meat and meat products: An overview. *Meat Sci.* 98:361–371. doi:10.1016/j.meatsci.2014.06.025.
- Food Search | USDA FoodData Central. Available from: <https://fdc.nal.usda.gov/food-search?type=Branded&query=beef%20tenderloin>
- Franco, D., L. González, E. Bispo, A. Latorre, T. Moreno, J. Sineiro, M. Sánchez, and M. J. Núñez. 2012. Effects of calf diet, antioxidants, packaging type and storage time on beef steak storage. *Meat Sci.* 90:871–880. doi:10.1016/j.meatsci.2011.10.008.
- Frank, D., J. Hughes, U. Piyasiri, Y. Zhang, M. Kaur, Y. Li, G. Mellor, and J. Stark. 2020. Volatile and non-volatile metabolite changes in 140-day stored vacuum packaged chilled beef and potential shelf life markers. *Meat Sci.* 161:108016. doi:10.1016/j.meatsci.2019.108016.
- Fu, Y., S. Cao, L. Yang, and Z. Li. 2022. Flavor formation based on lipid in meat and meat products: A review. *J. Food Biochem.* 46:e14439. doi:10.1111/jfbc.14439.
- Fuertes-Perez, S., P. Hauschild, M. Hilgarth, and R. F. Vogel. 2019. Biodiversity of *Photobacterium* spp. isolated from meats. *Front. Microbiol.* 10. doi:10.3389/fmicb.2019.02399.

- Fung, D. Y. C., C. Liang, and N. A. Cox. 1990. Critical review of isolation, detection, and identification of yeasts from meat products. *Crit. Rev. Food Sci. Nutr.* doi:10.1080/10408399009527532. Available from:
- Galloway-Peña, J., and B. Hanson. 2020. Tools for analysis of the microbiome. *Dig. Dis. Sci.* 65:674–685. doi:10.1007/s10620-020-06091-y.
- Gänzle, M. G. 2015. Lactic metabolism revisited: metabolism of lactic acid bacteria in food fermentations and food spoilage. *Curr. Opin. Food Sci.* 2:106–117. doi:10.1016/j.cofs.2015.03.001.
- GILL, C. O. 1976. Substrate Limitation of Bacterial Growth at Meat Surfaces. *J. Appl. Bacteriol.* 41:401–410. doi:10.1111/j.1365-2672.1976.tb00652.x.
- Gill, C. O. 1983. Meat Spoilage and Evaluation of the Potential Storage Life of Fresh Meat. *J. Food Prot.* 46:444–452. doi:10.4315/0362-028X-46.5.444.
- Gill, C. O. 1996. Extending the storage life of raw chilled meats. *Meat Sci.* 43:99–109. doi:10.1016/0309-1740(96)00058-7.
- Gill, C. O., and K. G. Newton. 1978. The ecology of bacterial spoilage of fresh meat at chill temperatures. *Meat Sci.* 2:207–217. doi:10.1016/0309-1740(78)90006-2.
- Gill, C. O., and K. G. Newton. 1979. Spoilage of vacuum-packaged dark, firm, dry meat at chill temperatures. *Appl. Environ. Microbiol.* 37:362–364. doi:10.1128/aem.37.3.362-364.1979.
- Gill, C. O., and N. Penney. 1977. Penetration of bacteria into meat. doi:10.1128/aem.33.6.1284-1286.1977.
- Giménez, A., F. Ares, and G. Ares. 2012. Sensory shelf-life estimation: A review of current methodological approaches. *Food Res. Int.* 49:311–325. doi:10.1016/j.foodres.2012.07.008.
- Glitsch, K. 2000. Consumer perceptions of fresh meat quality: cross-national comparison. *Br. Food J.* 102:177–194. doi:10.1108/00070700010332278.
- Godfray, H. C. J., P. Aveyard, T. Garnett, J. W. Hall, T. J. Key, J. Lorimer, R. T. Pierrehumbert, P. Scarborough, M. Springmann, and S. A. Jebb. 2018. Meat consumption, health, and the environment. *Science.* 361:eaam5324. doi:10.1126/science.aam5324.
- Görke, B., and J. Stülke. 2008. Carbon catabolite repression in bacteria: many ways to make the most out of nutrients. *Nat. Rev. Microbiol.* 6:613–624. doi:10.1038/nrmicro1932.
- Grada, A., and K. Weinbrecht. 2013. Next-Generation Sequencing: Methodology and Application. *J. Invest. Dermatol.* 133:1–4. doi:10.1038/jid.2013.248.
- Grebitus, C., H. H. Jensen, and J. Roosen. 2013a. US and German consumer preferences for ground beef packaged under a modified atmosphere – Different regulations, different behaviour? *Food Policy.* 40:109–118. doi:10.1016/j.foodpol.2013.02.005.
- Grebitus, C., H. H. Jensen, J. Roosen, and J. G. Sebranek. 2013b. Fresh meat packaging: consumer acceptance of modified atmosphere packaging including carbon monoxide. *J. Food Prot.* 76:99–107. doi:10.4315/0362-028X.JFP-12-045.
- Gunders, D. 2012. Wasted: How America is losing up to 40 percent of its food from farm to fork to landfill. Natural Resources Defense Council. Available from: <https://www.nrdc.org/sites/default/files/wasted-food-IP.pdf>

- Hammond, S. T., J. H. Brown, J. R. Burger, T. P. Flanagan, T. S. Fristoe, N. Mercado-Silva, J. C. Nekola, and J. G. Okie. 2015. Food spoilage, storage, and transport: implications for a sustainable future. *BioScience*. 65:758–768. doi:10.1093/biosci/biv081.
- Hauschild, P., R. F. Vogel, and M. Hilgarth. 2022. Transcriptomic analysis of the response of *Photobacterium phosphoreum* and *Photobacterium carnosum* to co-contaminants on chicken meat. *Arch. Microbiol.* 204:467. doi:10.1007/s00203-022-03059-6.
- Hierro, E., L. de la Hoz, and J. A. Ordóñez. 1997. Contribution of microbial and meat endogenous enzymes to the lipolysis of dry fermented sausages. *J. Agric. Food Chem.* 45:2989–2995. doi:10.1021/jf970127g.
- Hilgarth, M., S. Fuertes, M. Ehrmann, and R. F. Vogel. 2018. *Photobacterium carnosum* sp. nov., isolated from spoiled modified atmosphere packaged poultry meat. *Syst. Appl. Microbiol.* 41:44–50. doi:10.1016/j.syapm.2017.11.002.
- Höll, L., M. Hilgarth, A. J. Geissler, J. Behr, and R. F. Vogel. 2020. Metatranscriptomic analysis of modified atmosphere packaged poultry meat enables prediction of *Brochothrix thermosphacta* and *Carnobacterium divergens* in situ metabolism. *Arch. Microbiol.* 202:1945–1955. doi:10.1007/s00203-020-01914-y.
- Holman, B. W. B., R. J. van de Ven, Y. Mao, C. E. O. Coombs, and D. L. Hopkins. 2017. Using instrumental (CIE and reflectance) measures to predict consumers' acceptance of beef colour. *Meat Sci.* 127:57–62. doi:10.1016/j.meatsci.2017.01.005.
- Hood, D. E. 1980. Factors affecting the rate of metmyoglobin accumulation in pre-packaged beef. *Meat Sci.* 4:247–265. doi:10.1016/0309-1740(80)90026-1.
- Hood, D. E., and E. B. Riordan 1973. Discolouration in pre-packaged beef: measurement by reflectance spectrophotometry and shopper discrimination. *Int. J. Food Sci. Technol.* 8:333–343. doi:10.1111/j.1365-2621.1973.tb01721.x.
- Huergo, L. F., and R. Dixon. 2015. The Emergence of 2-Oxoglutarate as a Master Regulator Metabolite. *Microbiol. Mol. Biol. Rev. MMBR.* 79:419–435. doi:10.1128/MMBR.00038-15.
- Hultman, J., P. Johansson, and J. Björkroth. 2020. Longitudinal Metatranscriptomic Analysis of a Meat Spoilage Microbiome Detects Abundant Continued Fermentation and Environmental Stress Responses during Shelf Life and Beyond. *Appl. Environ. Microbiol.* 86:e01575-20. doi:10.1128/AEM.01575-20.
- Hunt, M. C., and H. B. Hedrick. 1977. Profile of Fiber Types and Related Properties of Five Bovine Muscles. *J. Food Sci.* 42:513–517. doi:10.1111/j.1365-2621.1977.tb01535.x.
- Hwang, B. K., H. Choi, S. H. Choi, and B.-S. Kim. 2020. Analysis of microbiota structure and potential functions influencing spoilage of fresh beef meat. *Front. Microbiol.* 11. doi:10.3389/fmicb.2020.01657.
- Indio, V., C. Oliveri, A. Lucchi, F. Savini, U. Gonzales-Barron, P. Skandamis, F. Achemchem, G. Manfreda, A. Serraino, and A. D. Cesare. 2024. Shotgun metagenomic investigation of foodborne pathogens and antimicrobial resistance genes in artisanal fermented meat products from the Mediterranean area. *Ital. J. Food Saf.* 13:12210. doi:10.4081/ijfs.2024.12210.

- Iulietto, M. F., P. Sechi, E. Borgogni, and B. T. Cenci-Goga. 2015. Meat Spoilage: A Critical Review of a Neglected Alteration Due to Ropy Slime Producing Bacteria. *Ital. J. Anim. Sci.* 14:4011. doi:10.4081/ijas.2015.4011.
- Jackson, T. C., G. R. Acuff, C. Vanderzant, T. R. Sharp, and J. W. Savell. 1992. Identification and evaluation of volatile compounds of vacuum and modified atmosphere packaged beef strip loins. *Meat Sci.* 31:175–190. doi:10.1016/0309-1740(92)90037-5.
- Jacques, B., M. Coinçon, and J. Sygusch. 2018. Active site remodeling during the catalytic cycle in metal-dependent fructose-1,6-bisphosphate aldolases. *J. Biol. Chem.* 293:7737–7753. doi:10.1074/jbc.RA117.001098.
- Jo, J.-H., E. A. Kennedy, and H. H. Kong. 2016. Research Techniques Made Simple: Bacterial 16S Ribosomal RNA Gene Sequencing in Cutaneous Research. *J. Invest. Dermatol.* 136:e23–e27. doi:10.1016/j.jid.2016.01.005.
- Johansson, P., E. Jääskeläinen, T. Nieminen, J. Hultman, P. Auvinen, and K. J. Björkroth. 2020. Microbiomes in the context of refrigerated raw meat spoilage. *Meat Muscle Biol.* 4. doi:10.22175/mmb.10369.
- Jones, N. R. 1969. Meat and fish flavors; significance of ribomononucleotides and their metabolites. *J. Agric. Food Chem.* 17:712–716. doi:10.1021/jf60164a017.
- Jones, R. J. 2004. Observations on the succession dynamics of lactic acid bacteria populations in chill-stored vacuum-packaged beef. *Int. J. Food Microbiol.* 90:273–282. doi:10.1016/S0168-1605(03)00310-6.
- Jørgensen, L. V., H. H. Huss, and P. Dalgaard. 2000. The effect of biogenic amine production by single bacterial cultures and metabiosis on cold-smoked salmon. *J. Appl. Microbiol.* 89:920–934. doi:10.1046/j.1365-2672.2000.01196.x.
- Joseph, P., S. P. Suman, G. Rentfrow, S. Li, and C. M. Beach. 2012. Proteomics of muscle-specific beef color stability. *J. Agric. Food Chem.* 60:3196–3203. doi:10.1021/jf204188v.
- Kanner, J. 1994. Oxidative processes in meat and meat products: Quality implications. *Meat Sci.* 36:169–189. doi:10.1016/0309-1740(94)90040-X.
- Killinger, K. M., C. R. Calkins, W. J. Umberger, D. M. Feuz, and K. M. Eskridge. 2004. Consumer visual preference and value for beef steaks differing in marbling level and color. *J. Anim. Sci.* 82(11):3288-3293. doi:10.2527/2004/82113288x.
- Kim, H.-J., S.-H. Park, T.-H. Lee, B.-H. Nahm, Y.-R. Kim, and H.-Y. Kim. 2008. Microarray detection of food-borne pathogens using specific probes prepared by comparative genomics. *Biosens. Bioelectron.* 24:238–246. doi:10.1016/j.bios.2008.03.019.
- King, D. A., M. C. Hunt, S. Barbut, J. R. Claus, D. P. Cornforth, P. Joseph, Y. H. B. Kim, G. Lindahl, R. A. Mancini, M. N. Nair, K. J. Merok, A. Milkowski, A. Mohan, F. Pohlman, R. Ramanathan, C. R. Raines, M. Seyfert, O. Sørheim, S. P. Suman, and M. Weber. 2023. American Meat Science Association Guidelines for Meat Color Measurement. *Meat Muscle Biol.* 6. doi:10.22175/mmb.12473.
- King, D. A., S. D. Shackelford, and T. L. Wheeler. 2011. Relative contributions of animal and muscle effects to variation in beef lean color stability. *J. Anim. Sci.* 89:1434–1451. doi:10.2527/jas.2010-3595.
- Klont, R. E., L. Brocks, and G. Eikelenboom. 1998. Muscle fibre type and meat quality. *Meat Sci.* 49:S219–S229. doi:10.1016/S0309-1740(98)90050-X.

- Kolbeck, S., M. Abele, M. Hilgarth, and R. F. Vogel. 2021. Comparative proteomics reveals the anaerobic lifestyle of meat-spoiling pseudomonas species. *Front. Microbiol.* 12. doi:10.3389/fmicb.2021.664061.
- Koutsoumanis, K., A. Stamatiou, P. Skandamis, and G.-J. E. Nychas. 2006. Development of a microbial model for the combined effect of temperature and pH on spoilage of ground meat, and validation of the model under dynamic temperature conditions. *Appl. Environ. Microbiol.* 72:124–134. doi:10.1128/AEM.72.1.124-134.2006.
- Labadie, J. 1999. Consequences of packaging on bacterial growth. Meat is an ecological niche. *Meat Sci.* 52:299–305. doi:10.1016/S0309-1740(99)00006-6.
- Lambropoulou, K. A., E. H. Drosinos, and G. J. E. Nychas. 1996. The effect of glucose supplementation on the spoilage microflora and chemical composition of minced beef stored aerobically or under a modified atmosphere at 4 °C. *Int. J. Food Microbiol.* 30:281–291. doi:10.1016/0168-1605(96)00954-3.
- Laursen, M. F., M. D. Dalgaard, and M. I. Bahl. 2017. Genomic GC-Content Affects the Accuracy of 16S rRNA Gene Sequencing Based Microbial Profiling due to PCR Bias. *Front. Microbiol.* 8. doi:10.3389/fmicb.2017.01934. Available from: <https://www.frontiersin.org/journals/microbiology/articles/10.3389/fmicb.2017.01934/full>
- Ledward, D. A. 1992. Haemoproteins in meat and meat products. In: B. J. F. Hudson, editor. *Biochemistry of Food Proteins*. Springer US, Boston, MA. p. 197–234.
- Legako, J. F., J. C. Brooks, T. G. O'Quinn, T. D. J. Hagan, R. Polkinghorne, L. J. Farmer, and M. F. Miller. 2015. Consumer palatability scores and volatile beef flavor compounds of five USDA quality grades and four muscles. *Meat Sci.* 100:291–300. doi:10.1016/j.meatsci.2014.10.026.
- Lepper, E., and C. J. Martin. 1930. The oxidation-reduction potential of cooked-meat media following the inoculation of bacteria. *Br. J. Exp. Pathol.* 11:140.
- Leroy, F., and L. De Vuyst. 2004. Lactic acid bacteria as functional starter cultures for the food fermentation industry. *Trends Food Sci. Technol.* 15:67–78. doi:10.1016/j.tifs.2003.09.004.
- Lipinski, B. 2020. Why does animal-based food loss and waste matter? *Anim. Front.* 10:48–52. doi:10.1093/af/vfaa039.
- Lowe, R., N. Shirley, M. Bleackley, S. Dolan, and T. Shafee. 2017. Transcriptomics technologies. *PLoS Comput. Biol.* 13:e1005457. doi:10.1371/journal.pcbi.1005457.
- Lu, X., Y. Zhang, B. Xu, L. Zhu, and X. Luo. 2020. Protein degradation and structure changes of beef muscle during superchilled storage. *Meat Sci.* 168:108180. doi:10.1016/j.meatsci.2020.108180.
- Luong, N.-D. M., L. Coroller, M. Zagorec, J.-M. Membré, and S. Guillou. 2020. spoilage of chilled fresh meat products during storage: A quantitative analysis of literature data. *Microorganisms.* 8:1198. doi:10.3390/microorganisms8081198.
- Malheiros, J. M., C. P. Braga, R. A. Grove, F. A. Ribeiro, C. R. Calkins, J. Adamec, and L. A. L. Chardulo. 2019. Influence of oxidative damage to proteins on meat tenderness using a proteomics approach. *Meat Sci.* 148:64–71. doi:10.1016/j.meatsci.2018.08.016.

- Mancini, R. A., and M. C. Hunt. 2005. Current research in meat color. *Meat Sci.* 71:100–121. doi:10.1016/j.meatsci.2005.03.003.
- Mancini, R. A., K. Belskie, S. P. Suman, and R. Ramanathan. 2018. Muscle-specific mitochondrial functionality and its influence on fresh beef color stability. *J. Food Sci.* 83:2077–2082. doi:10.1111/1750-3841.14219.
- Mansur, A. R., E.-J. Song, Y.-S. Cho, Y.-D. Nam, Y.-S. Choi, D.-O. Kim, D.-H. Seo, and T. G. Nam. 2019. Comparative evaluation of spoilage-related bacterial diversity and metabolite profiles in chilled beef stored under air and vacuum packaging. *Food Microbiol.* 77:166–172. doi:10.1016/j.fm.2018.09.006.
- Martín, A., M. J. Benito, E. Aranda, S. Ruiz-Moyano, J. J. Córdoba, and M. G. Córdoba. 2010. characterization by volatile compounds of microbial deep spoilage in iberian dry-cured ham. *J. Food Sci.* 75:M360–M365. doi:10.1111/j.1750-3841.2010.01674.x.
- Matarneh, S. K., E. M. England, T. L. Scheffler, and D. E. Gerrard. 2017. Chapter 5 - The Conversion of Muscle to Meat. In: F. Toldra´, editor. *Lawrie´s Meat Science (Eighth Edition)*. Woodhead Publishing. p. 159–185.
- McKeith, R. O., D. A. King, A. L. Grayson, S. D. Shackelford, K. B. Gehring, J. W. Savell, and T. L. Wheeler. 2016. Mitochondrial abundance and efficiency contribute to lean color of dark cutting beef. *Meat Sci.* 116:165–173. doi:10.1016/j.meatsci.2016.01.016.
- McKenna, D. R., P. D. Mies, B. E. Baird, K. D. Pfeiffer, J. W. Ellebracht, and J. W. Savell. 2005. Biochemical and physical factors affecting discoloration characteristics of 19 bovine muscles. *Meat Sci.* 70:665–682. doi:10.1016/j.meatsci.2005.02.016.
- Mellor, G. E., J. A. Bentley, and G. A. Dykes. 2011. Evidence for a role of biosurfactants produced by *Pseudomonas fluorescens* in the spoilage of fresh aerobically stored chicken meat. *Food Microbiol.* 28:1101–1104. doi:10.1016/j.fm.2011.02.003.
- Mills, B. I. 2021. 2015 and 2018 National Meat Case Studies: Packaging type, marketing claims, and allocation in the self-service meat case. Available from: <https://hdl.handle.net/2346/87855>
- Molin, G., and A. Ternström. 1982. Numerical taxonomy of psychrotrophic pseudomonads. *Microbiology.* 128:1249–1264. doi:10.1099/00221287-128-6-1249.
- Molly, K., D. Demeyer, T. Civera, and A. Verplaetse. 1996. Lipolysis in a Belgian sausage: Relative importance of endogenous and bacterial enzymes. *Meat Sci.* 43:235–244. doi:10.1016/S0309-1740(96)00018-6.
- Mols, M., and T. Abee. 2011. Primary and secondary oxidative stress in *Bacillus*. *Environ. Microbiol.* 13:1387–1394. doi:10.1111/j.1462-2920.2011.02433.x.
- Motoyama, M., M. Kobayashi, K. Sasaki, M. Nomura, and M. Mitsumoto. 2010. *Pseudomonas* spp. convert metmyoglobin into deoxymyoglobin. *Meat Sci.* 84:202–207. doi:10.1016/j.meatsci.2009.08.050.
- Munekata, P. E. S., S. Finardi, C. K. de Souza, C. Meinert, M. Pateiro, T. G. Hoffmann, R. Domínguez, S. L. Bertoli, M. Kumar, and J. M. Lorenzo. 2023. Applications of electronic nose, electronic eye and electronic tongue in quality, safety and shelf

- life of meat and meat products: A review. *Sensors*. 23:672. doi:10.3390/s23020672.
- Muriel, E., T. Antequera, M. J. Petró, A. I. Andrés, and J. Ruiz. 2004. Volatile compounds in Iberian dry-cured loin. *Meat Sci*. 68:391–400. doi:10.1016/j.meatsci.2004.04.006.
- Nair, M. N., S. Li, C. M. Beach, G. Rentfrow, S. P. Suman. 2018. Changes in the sarcoplasmic proteome of beef muscles with differential color stability during postmortem aging. *Meat Muscle Biol*. 2(1). doi:10.22175/mmb2017.07.0037.
- Najar-Villarreal, F., E. A. E. Boyle, C. I. Vahl, Q. Kang, J. J. Kastner, J. Amamcharla, and M. C. Hunt. 2021. Determining the Longissimus lumborum and Psoas major Beef Steak Color Life Threshold and Effect of Postmortem Aging Time Using Meta-analysis. *Meat Muscle Biol*. 5. doi:10.22175/mmb.12526. Available from: <https://www.iastatedigitalpress.com/mmb/article/id/12526/>
- Nicol, D., M. Shaw, and D. Ledward. 1970. Hydrogen sulfide production by bacteria and sulfmyoglobin formation in prepacked chilled beef. doi:10.1128/am.19.6.937-939.1970.
- Nieminen, T. T., P. Dalgaard, and J. Björkroth. 2016. Volatile organic compounds and *Photobacterium phosphoreum* associated with spoilage of modified-atmosphere-packaged raw pork. *Int. J. Food Microbiol*. 218:86–95. doi:10.1016/j.ijfoodmicro.2015.11.003.
- Nychas, G.-J. E., P. N. Skandamis, C. C. Tassou, and K. P. Koutsoumanis. 2008. Meat spoilage during distribution. *Meat Sci*. 78:77–89. doi:10.1016/j.meatsci.2007.06.020.
- Nychas, G., V. Dillon, and R. Board. 1988. Glucose, the key substrate in the microbiological changes occurring in meat and certain meat products. *Biotechnol. Appl. Biochem*. 10:203–231. doi:10.1111/j.1470-8744.1988.tb00014.x.
- O'Quinn, T. G., J. C. Brooks, and M. F. Miller. 2015. Consumer Assessment of Beef Tenderloin Steaks from Various USDA Quality Grades at 3 Degrees of Doneness. *J. Food Sci*. 80:S444–S449. doi:10.1111/1750-3841.12775.
- Odeyemi, O. A., O. O. Alegbeleye, M. Strateva, and D. Stratev. 2020. Understanding spoilage microbial community and spoilage mechanisms in foods of animal origin. *Compr. Rev. Food Sci. Food Saf*. 19:311–331. doi:10.1111/1541-4337.12526.
- Olivera, D. F., R. Bambicha, G. Laporte, F. C. Cárdenas, and N. Mestorino. 2013. Kinetics of colour and texture changes of beef during storage. *J. Food Sci. Technol*. 50:821–825. doi:10.1007/s13197-012-0885-7.
- Papadopoulou, O. S., V. Iliopoulos, A. Mallouchos, E. Z. Panagou, N. Chorianopoulos, C. C. Tassou, and G.-J. E. Nychas. 2020. Spoilage potential of *Pseudomonas* (*P. fragi*, *P. putida*) and LAB (*Leuconostoc mesenteroides*, *Lactobacillus sakei*) strains and their volatilome profile during storage of sterile pork meat using GC/MS and data analytics. *Foods*. 9:633. doi:10.3390/foods9050633.
- Papon, M., and R. Talon. 1988. Factors affecting growth and lipase production by meat *Lactobacilli* strains and *Brochothrix thermosphacta*. *J. Appl. Bacteriol*. 64:107–115. doi:10.1111/j.1365-2672.1988.tb02729.x.

- Paramithiotis, S., P. N. Skandamis, and G.-J. E. Nychas. 2009. Insights into Fresh Meat Spoilage. In: F. Toldrá, editor. *Safety of Meat and Processed Meat*. Springer, New York, NY. p. 55–82.
- Pellissery, A. J., P. G. Vinayamohan, M. A. R. Amalaradjou, and K. Venkitanarayanan. 2020. Chapter 17 - Spoilage bacteria and meat quality. In: A. K. Biswas and P. K. Mandal, editors. *Meat Quality Analysis*. Academic Press. p. 307–334.
- Pessione, A., C. Lamberti, and E. Pessione. 2010. Proteomics as a tool for studying energy metabolism in lactic acid bacteria. *Mol. Biosyst.* 6:1419–1430. doi:10.1039/C001948H.
- Picard, B., and M. Gagaoua. 2020. Muscle Fiber Properties in Cattle and Their Relationships with Meat Qualities: An Overview. *J. Agric. Food Chem.* 68:6021–6039. doi:10.1021/acs.jafc.0c02086.
- Poirier, S., N.-D. M. Luong, V. Anthoine, S. Guillou, J.-M. Membré, N. Moriceau, S. Rezé, M. Zagorec, C. Feurer, B. Frémaux, S. Jeuge, E. Robieu, M. Champomier-Vergès, G. Coeuret, E. Cauchie, G. Daube, N. Korsak, L. Coroller, N. Desriac, M.-H. Desmots, R. Gohier, D. Werner, V. Loux, O. Rué, M.-H. Dohollou, T. Defosse, and S. Chaillou. 2020. Large-scale multivariate dataset on the characterization of microbiota diversity, microbial growth dynamics, metabolic spoilage volatiles and sensorial profiles of two industrially produced meat products subjected to changes in lactate concentration and packaging atmosphere. *Data Brief.* 30:105453. doi:10.1016/j.dib.2020.105453.
- Pothakos, V., F. Devlieghere, F. Villani, J. Björkroth, and D. Ercolini. 2015. Lactic acid bacteria and their controversial role in fresh meat spoilage. *Meat Sci.* 109:66–74. doi:10.1016/j.meatsci.2015.04.014.
- Puttamreddy, S., M. D. Carruthers, M. L. Madsen, and F. C. Minion. 2008. Transcriptome Analysis of Organisms with Food Safety Relevance. *Foodborne Pathog. Dis.* 5:517–529. doi:10.1089/fpd.2008.0112.
- Rajpurohit, H., and M. A. Eiteman. 2024. Citrate synthase variants improve yield of acetyl-CoA derived 3-hydroxybutyrate in *Escherichia coli*. *Microb. Cell Factories.* 23:173. doi:10.1186/s12934-024-02444-8.
- Ramanathan, R., L. H. Lambert, M. N. Nair, B. Morgan, R. Feuz, G. Mafi, and M. Pfeiffer. 2022. Economic loss, amount of beef discarded, natural resources wastage, and environmental impact due to beef discoloration. *Meat Muscle Biol.* 6. doi:10.22175/mmb.13218.
- Ramanathan, R., M. N. Nair, M. C. Hunt, and S. P. Suman. 2019. Mitochondrial functionality and beef colour: A review of recent research. *South Afr. J. Anim. Sci.* 49:9–19. doi:10.4314/sajas.v49i1.2.
- Ramanathan, R., M. N. Nair, Y. Wang, S. Li, C. M. Beach, R. A. Mancini, K. Belskie, and S. P. Suman. 2021. Differential Abundance of Mitochondrial Proteome Influences the Color Stability of Beef Longissimus Lumborum and Psoas Major Muscles. *Meat Muscle Biol.* 5. doi:10.22175/mmb.11705. Available from: <https://www.iastatedigitalpress.com/mmb/article/id/11705/>
- Ramírez, H. L., A. Soriano, S. Gómez, J. U. Iranzo, and A. I. Briones. 2018. Evaluation of the Food Sniffer electronic nose for assessing the shelf life of fresh pork meat compared to physicochemical measurements of meat quality. *Eur. Food Res. Technol.* 244:1047–1055. doi:10.1007/s00217-017-3021-0.

- Robach, D. L., and R. N. Costilow. 1961. Role of bacteria in the oxidation of myoglobin. *Appl. Microbiol.* 9:529–533. doi:10.1128/am.9.6.529-533.1961.
- Robbins, K., J. Jensen, K. J. Ryan, C. Homco-Ryan, F. K. McKeith, and M. S. Brewer. 2003. Consumer attitudes towards beef and acceptability of enhanced beef. *Meat Sci.* 65:721–729. doi:10.1016/S0309-1740(02)00274-7.
- Romano, A. H., S. J. Eberhard, S. L. Dingle, and T. D. McDowell. 1970. Distribution of the phosphoenolpyruvate: glucose phosphotransferase system in bacteria. *J. Bacteriol.* 104:808–813. doi:10.1128/jb.104.2.808-813.1970.
- Rood, L., J. P. Bowman, T. Ross, R. Corkrey, J. Pagnon, S. W. T. Yang, and C. Kocharunchitt. 2022. The effects of glucose on microbial spoilage of vacuum-packed lamb. *Meat Sci.* 188:108781. doi:10.1016/j.meatsci.2022.108781.
- Saenz-García, C. E., P. Castañeda-Serrano, E. M. Mercado Silva, C. Z. Alvarado, and G. M. Nava. 2020. insights into the identification of the specific spoilage organisms in chicken meat. *Foods.* 9:225. doi:10.3390/foods9020225.
- Sáez, L. P., F. Castillo, and F. J. Caballero. 1999. Metabolism of L-phenylalanine and L-tyrosine by the phototrophic bacterium *Rhodobacter capsulatus*. *Curr. Microbiol.* 38:51–56. doi:10.1007/pl00006772.
- Savijoki, K., H. Ingmer, and P. Varmanen. 2006. Proteolytic systems of lactic acid bacteria. *Appl. Microbiol. Biotechnol.* 71:394–406. doi:10.1007/s00253-006-0427-1.
- Senaratne, L. 2012. Mechanism and control of beef toughening during retail display in high oxygen modified atmosphere packages. *Dep. Anim. Sci. Diss. Theses Stud. Res.* Available from: <https://digitalcommons.unl.edu/animalscidiss/54>
- Seyfert, M., R. A. Mancini, M. C. Hunt, J. Tang, C. Faustman, and M. Garcia. 2006. Color stability, reducing activity, and cytochrome c oxidase activity of five bovine muscles. *J. Agric. Food Chem.* 54:8919–8925. doi:10.1021/jf061657s.
- Shelef, L. A. 1977. Effect of glucose on the bacterial spoilage of beef. *J. Food Sci.* 42:1172–1175. doi:10.1111/j.1365-2621.1977.tb14453.x.
- Shishani, E. (Isaac), S. C. Chai, S. Jamokha, G. Aznar, and M. K. Hoffman. 2003. Determination of ractopamine in animal tissues by liquid chromatography-fluorescence and liquid chromatography/tandem mass spectrometry. *Anal. Chim. Acta.* 483:137–145. doi:10.1016/S0003-2670(03)00120-X.
- Signorini, M. I., E. Ponce-Alquicira, and I. Guerrero-Legarreta. 2006. Effect of lactic acid and lactic acid bacteria on growth of spoilage microorganisms in vacuum-packaged beef. *J. Muscle Foods.* 17:277–290. doi:10.1111/j.1745-4573.2006.00050.x.
- Smit, B. A., W. J. M. Engels, and G. Smit. 2009. Branched chain aldehydes: production and breakdown pathways and relevance for flavour in foods. *Appl. Microbiol. Biotechnol.* 81:987–999. doi:10.1007/s00253-008-1758-x.
- Smith, C. L., I. Geornaras, and M. N. Nair. 2024a. Impact of spoilage bacterial populations on discoloration of beef steaks. *Meat Muscle Biol.* 8. doi:10.22175/mmb.17796.
- Smith, C. L., S. V. Gonzalez, J. L. Metcalf, I. Geornaras, and M. N. Nair. 2024b. Differences in spoilage microflora growth kinetics could be contributing to beef muscle-specific color stability. *Meat Muscle Biol.* 8. doi:10.22175/mmb.16915.

- Spence, C. 2015. Just how much of what we taste derives from the sense of smell? *Flavour*. 4:30. doi:10.1186/s13411-015-0040-2.
- Stead, D. 1986. Microbial lipases: their characteristics, role in food spoilage and industrial uses. *J. Dairy Res.* 53:481–505. doi:10.1017/S0022029900025103.
- Stead, D. 1987. Production of extracellular lipases and proteinases during prolonged growth of strains of psychrotrophic bacteria in whole milk. *J. Dairy Res.* 54:535–543. doi:10.1017/s0022029900025735.
- Stellato, G., A. La Storia, F. De Filippis, G. Borriello, F. Villani, and D. Ercolini. 2016. Overlap of spoilage-associated microbiota between meat and the meat processing environment in small-scale and large-scale retail distributions. *Appl. Environ. Microbiol.* 82:4045–4054. doi:10.1128/AEM.00793-16.
- Stincone, A., A. Prigione, T. Cramer, M. M. C. Wamelink, K. Campbell, E. Cheung, V. Olin-Sandoval, N.-M. Grüning, A. Krüger, M. Tauqeer Alam, M. A. Keller, M. Breitenbach, K. M. Brindle, J. D. Rabinowitz, and M. Ralser. 2015. The return of metabolism: biochemistry and physiology of the pentose phosphate pathway. *Biol. Rev.* 90:927–963. doi:10.1111/brv.12140.
- Szymanski, C. M. 2022. Bacterial glycosylation, it's complicated. *Front. Mol. Biosci.* 9. doi:10.3389/fmolb.2022.1015771. Available from: <https://www.frontiersin.org/journals/molecular-biosciences/articles/10.3389/fmolb.2022.1015771/full>
- Thies, A. J., B. A. Altmann, A. M. Countryman, C. Smith, and M. N. Nair. 2024. Consumer willingness to pay (WTP) for beef based on color and price discounts. *Meat Sci.* 217:109597. doi:10.1016/j.meatsci.2024.109597.
- Touratier, F., L. Legendre, and A. Vézina. 1999. Model of bacterial growth influenced by substrate C:N ratio and concentration. *Aquat. Microb. Ecol.* 19:105–118. doi:10.3354/ame019105.
- Ullrich, M. 2009. *Bacterial polysaccharides: Current innovations and future trends.* Norfolk Publishing.
- Upton, A. M., and J. D. McKinney. 2007. Role of the methylcitrate cycle in propionate metabolism and detoxification in *Mycobacterium smegmatis*. *Microbiol. Read. Engl.* 153:3973–3982. doi:10.1099/mic.0.2007/011726-0.
- USDA ERS - Statistics & Information. 2023. Available from: <https://www.ers.usda.gov/topics/animal-products/cattle-beef/statistics-information/>
- Valenzuela, C., D. López de Romaña, M. Olivares, M. S. Morales, and F. Pizarro. 2009. Total Iron and Heme Iron Content and their Distribution in Beef Meat and Viscera. *Biol. Trace Elem. Res.* 132:103–111. doi:10.1007/s12011-009-8400-3.
- Verplaetse, E., G. André-Leroux, P. Duhutrel, G. Coeuret, S. Chaillou, C. Nielsen-Leroux, and M.-C. Champomier-Vergès. 2020. Heme Uptake in *Lactobacillus sakei* Evidenced by a New Energy Coupling Factor (ECF)-Like Transport System. *Appl. Environ. Microbiol.* 86:e02847-19. doi:10.1128/AEM.02847-19.
- Viana, E. S., L. A. M. Gomide, and M. C. D. Vanetti. 2005. Effect of modified atmospheres on microbiological, color and sensory properties of refrigerated pork. *Meat Sci.* 71:696–705. doi:10.1016/j.meatsci.2005.05.013.
- Vitha, M. F. 2018. *Spectroscopy: Principles and Instrumentation.* John Wiley & Sons.

- Wagner, M., L. Shen, A. Albersmeier, N. van der Kolk, S. Kim, J. Cha, C. Bräsen, J. Kalinowski, B. Siebers, and S.-V. Albers. 2018. *Sulfolobus acidocaldarius* Transports Pentoses via a Carbohydrate Uptake Transporter 2 (CUT2)-Type ABC Transporter and Metabolizes Them through the Aldolase-Independent Weimberg Pathway. *Appl. Environ. Microbiol.* 84:e01273-17. doi:10.1128/AEM.01273-17.
- Wang, G., F. Ma, L. Zeng, Y. Bai, H. Wang, X. Xu, and G. Zhou. 2018. Modified atmosphere packaging decreased *Pseudomonas fragi* cell metabolism and extracellular proteolytic activities on meat. *Food Microbiol.* 76:443–449. doi:10.1016/j.fm.2018.07.007.
- Wickramasinghe, N. N., J. Ravensdale, R. Coorey, S. P. Chandry, and G. A. Dykes. 2019. The predominance of psychrotrophic pseudomonads on aerobically stored chilled red meat. *Compr. Rev. Food Sci. Food Saf.* 18:1622–1635. doi:10.1111/1541-4337.12483.
- Wood, J. D., R. I. Richardson, G. R. Nute, A. V. Fisher, M. M. Campo, E. Kasapidou, P. R. Sheard, and M. Enser. 2004. Effects of fatty acids on meat quality: a review. *Meat Sci.* 66:21–32. doi:10.1016/S0309-1740(03)00022-6.
- Yang, X., N. R. Noyes, E. Doster, J. N. Martin, L. M. Linke, R. J. Magnuson, H. Yang, I. Geornaras, D. R. Woerner, K. L. Jones, J. Ruiz, C. Boucher, P. S. Morley, and K. E. Belk. 2016. Use of metagenomic shotgun sequencing technology to detect foodborne pathogens within the microbiome of the beef production chain. *Appl. Environ. Microbiol.* 82:2433–2443. doi:10.1128/AEM.00078-16.
- Yang, X., Y. Zhang, L. Zhu, M. Han, S. Gao, and X. Luo. 2016. Effect of packaging atmospheres on storage quality characteristics of heavily marbled beef longissimus steaks. *Meat Sci.* 117:50–56. doi:10.1016/j.meatsci.2016.02.030.
- Ye, P., X. Li, B. Cui, S. Song, F. Shen, X. Chen, G. Wang, X. Zhou, and Y. Deng. 2022. Proline utilization A controls bacterial pathogenicity by sensing its substrate and cofactors. *Commun. Biol.* 5:1–9. doi:10.1038/s42003-022-03451-4.
- Yi, Z., X. Xiao, W. Cai, Z. Ding, J. Ma, W. Lv, H. Yang, Y. Xiao, and W. Wang. 2024. Unraveling the spoilage characteristics of refrigerated pork using high-throughput sequencing coupled with UHPLC-MS/MS-based non-targeted metabolomics. *Food Chem.* 460:140797. doi:10.1016/j.foodchem.2024.140797.
- Yu, Q., W. Wu, X. Tian, F. Jia, L. Xu, R. Dai, and X. Li. 2017. Comparative proteomics to reveal muscle-specific beef color stability of Holstein cattle during post-mortem storage. *Food Chem.* 229:769–778. doi:10.1016/j.foodchem.2017.03.004
- Yu, Q., X. Tian, L. Shao, X. Li, and R. Dai. 2019. Targeted metabolomics to reveal muscle-specific energy metabolism between bovine longissimus lumborum and psoas major during early postmortem periods. *Meat Sci.* 156:166–173. doi:10.1016/j.meatsci.2019.05.029.
- Zhang, W., Y. Ni, Y. Ma, Y. Xie, X. min Li, L. Tan, J. Zhao, C. Li, and B. Xu. 2024. *Pseudomonas weihenstephanensis* through the iron metabolism pathway promotes in situ spoilage capacity of prepared beef steaks during cold storage. *Food Microbiol.* 120:104466. doi:10.1016/j.fm.2024.104466.
- Zhao, F., Z. Wei, Y. Bai, C. Li, G. Zhou, K. Kristiansen, and C. Wang. 2022. Proteomics and metabolomics profiling of pork exudate reveals meat spoilage during storage. *Metabolites.* 12:570. doi:10.3390/metabo12070570.

Zhao, Z., M. Xian, M. Liu, and G. Zhao. 2020. Biochemical routes for uptake and conversion of xylose by microorganisms. *Biotechnol. Biofuels.* 13:21. doi:10.1186/s13068-020-1662-x.

SUPPLEMENTAL TABLE 1. List of Kyoto Encyclopedia of Genes and Genomes Orthologs (KO) with changes ($P < 0.05$) collected from bacteria grown on beef *psaos major* in aerobic simulated retail display between display days 2 to 5.

¹Number of transcripts increased on Display Day listed compared to day prior.

²Coefficient of Model represents the modeled change in the number of transcripts for a KO. Positive Coefficient of Model indicates increased number, negative indicates decreased number

KO	Display Day ¹	Coefficient of Model ²	Protein Family	Function	Enzyme Identity
K00748	4	0.57	Protein families: metabolism	Lipopolysaccharide biosynthesis proteins	lipid-A-disaccharide synthase [EC:2.4.1.182]
K00979	4	0.76	Protein families: metabolism	Lipopolysaccharide biosynthesis proteins	3-deoxy-manno-octulosonate cytidyltransferase (CMP-KDO synthetase) [EC:2.7.7.38]
K01625	4	0.46	Carbohydrate metabolism	Glyoxylate and dicarboxylate metabolism	2-dehydro-3-deoxyphosphogluconate aldolase / (4S)-4-hydroxy-2-oxoglutarate aldolase [EC:4.1.2.14 4.1.3.42]
K01784	4	1.33	Glycan biosynthesis and metabolism	Amino sugar and nucleotide sugar metabolism	UDP-glucose 4-epimerase [EC:5.1.3.2]
K02065	3	4.81	Protein families: signaling and cellular processes	Transporters	phospholipid/cholesterol/gamma-HCH transport system ATP-binding protein
K02065	4	-5.20	Protein families: signaling and cellular processes	Transporters	phospholipid/cholesterol/gamma-HCH transport system ATP-binding protein
K02388	4	1.03	Protein families: signaling and cellular processes	Bacterial motility proteins	flagellar basal-body rod protein FlgC
K02419	4	1.71	Protein families: signaling and cellular processes	Bacterial motility proteins	flagellar biosynthesis protein FljP
K02657	4	0.31	Protein families: signaling and cellular processes	Bacterial motility proteins	twitching motility two-component system response regulator PilG
K03186	4	1.05	Xenobiotics biodegradation and metabolism	Aminobenzoate degradation	flavin prenyltransferase [EC:2.5.1.129]
K03272	4	-0.09	Protein families: metabolism	Lipopolysaccharide biosynthesis proteins	D-beta-D-heptose 7-phosphate kinase / D-beta-D-heptose 1-phosphate adenosyltransferase [EC:2.7.1.167 2.7.7.70]

K03406	4	0.13	Protein families: signaling and cellular processes	Bacterial motility proteins	methyl-accepting chemotaxis protein
K03442	4	0.80	Protein families: signaling and cellular processes	Transporters	small conductance mechanosensitive channel
K03640	3	12.09	Protein families: signaling and cellular processes	Transporters	peptidoglycan-associated lipoprotein
K03640	4	-12.02	Protein families: signaling and cellular processes	Transporters	peptidoglycan-associated lipoprotein
K06148	4	1.48	Protein families: signaling and cellular processes	Transporters	ATP-binding cassette, subfamily C, bacterial
K06176	4	1.88	Protein families: genetic information processing	Transfer RNA biogenesis	tRNA pseudouridine13 synthase [EC:5.4.99.27]
K06867	4	1.25	Poorly characterized	Function unknown	uncharacterized protein
K07137	4	0.06	Poorly characterized	Function unknown	uncharacterized protein
K07263	4	0.06	Protein families: metabolism	Peptidases and inhibitors	zinc protease [EC:3.4.24.-]
K09926	4	3.55	Poorly characterized	Function unknown	uncharacterized protein
K10024	4	2.23	Protein families: signaling and cellular processes	Transporters	arginine/ornithine transport system permease protein
K10111	4	0.99	Protein families: signaling and cellular processes	Transporters	multiple sugar transport system ATP-binding protein [EC:7.5.2.-]
K10126	4	0.96	Protein families: signaling and cellular processes	Two-component system	two-component system, NtrC family, C4-dicarboxylate transport response regulator DctD
K10763	4	0.61	Protein families: genetic information processing	DNA replication proteins	DnaA-homolog protein

K10816	4	3.44	Protein families: signaling and cellular processes	Bacterial toxins	hydrogen cyanide synthase HcnC [EC:1.4.99.5]
K11752	3	-0.37	Cellular community - prokaryotes	Quorum sensing	diaminohydroxyphosphoribosylaminopyrimidine deaminase / 5-amino-6-(5-phosphoribosylamino)uracil reductase [EC:3.5.4.26 1.1.1.193]
K11752	4	0.48	Cellular community - prokaryotes	Quorum sensing	diaminohydroxyphosphoribosylaminopyrimidine deaminase / 5-amino-6-(5-phosphoribosylamino)uracil reductase [EC:3.5.4.26 1.1.1.193]
K12254	4	1.70	Amino acid metabolism	Arginine and proline metabolism	4-guanidinobutyraldehyde dehydrogenase / NAD- dependent aldehyde dehydrogenase [EC:1.2.1.54 1.2.1.-]
K13038	4	-0.11	Metabolism of cofactors and vitamins	Pantothenate and CoA biosynthesis	phosphopantothencysteine decarboxylase / phosphopantothenate--cysteine ligase [EC:4.1.1.36 6.3.2.5]
K13893	4	1.70	Protein families: signaling and cellular processes	Transporters	microcin C transport system substrate-binding protein
K18297	4	2.02	Protein families: signaling and cellular processes	Antimicrobial resistance genes	LysR family transcriptional regulator, mexEF-oprN operon transcriptional activator
K21825	4	-0.01	Protein families: genetic information processing	Transcription factors	AraC family transcriptional regulator, L-arginine- responsive activator
